Conversion of biomass derived carbohydrate to value added chemicals by liquid-phase thermochemical and biochemical processing

by

Tapas Chandra Acharjee

A dissertation submitted to the Graduate Faculty of
Auburn University
in partial fulfillment of the
requirements for the Degree of
Doctor of Philosophy

Auburn, Alabama
August 05, 2017

Keywords: Levulinic acid, lactic acid, glucose, paper mill sludge, chlorine dioxide, fermentation

Approved by

Yoon Y Lee, Chair, Professor of Department of Chemical Engineering
Zhihua Jiang, Co-Chair, Assistant Professor of Department of Chemical Engineering
Thomas Hanley, Professor of Department of Chemical Engineering
Alan E David, Assistant Professor of Department of Chemical Engineering
Maobing Tu, Associate Professor of Department of Biomedical, Chemical, and Environmental Engineering, University of Cincinnati

Abstract

Levulinic and lactic acid are considered as highly versatile chemicals with a potential to be building-block for the synthesis of various upgraded chemicals. The main objective of this study is to develop novel strategies for efficient production of these two chemicals by liquid-phase processing of biomass-derived carbohydrates. In that event, the kinetic aspect of homogeneous acid catalyzed levulinic acid (LA) production from glucose in aqueous media was investigated at first. The experimental data collected from batch reactor over the following range of conditions: 150-200 °C, sulfuric acid concentrations of 1-5 (wt. %) and initial glucose concentrations of 5-15 (wt. %) were fitted to a kinetic model. The model has shown a good agreement with experimental data. The kinetic model derived here was further used to model continuous reactor system. The model suggests that high temperature and shorter reaction times are required to maximize hydroxymethylfurfural (HMF), an intermediate in the process. It also predicts low temperature and longer reaction times are essential to maximize LA yield. We also developed an optimum temperature profile for the levulinic acid production from glucose. This study thus can serve as a useful tool for optimal design and operation of acid catalyzed LA production from glucose.

Literature information suggests catalytic conversion of glucose to LA involves multi-step complex reaction sequence. The known reaction pathway includes glucose→fructose→ HMF→LA and various side-reactions. Each of these reactions are independent, thus behave differently depending on the type of acid catalyst. Specifically, Lewis-acid has much higher

selectivity for the first reaction (glucose→fructose) whereas Brønsted-acid favors the latter reactions. For this reason, we have prepared a series of solid Lewis acid catalysts by Solid State Ion Exchange method (SSIE) and tested them for glucose to fructose isomerization. We also tested these catalysts together with a commercial solid acid catalyst (Amberlyst-15) to produce LA from glucose as Amberlyst-15 was found to be very effective for the production of LA from fructose in aqueous media. Among the Lewis solid acid catalysts tested, a large-pore zeolite that contains tin (Sn-Beta) is able to isomerize glucose to fructose in aqueous media with high activity and selectivity. The dual-catalyst system, Sn-beta and Amberlyst -15, has improved the yield of LA due to enhanced isomerization of glucose to fructose by Sn-Beta. Although, Sn-beta zeolite catalyst loses its activity during the course of the reaction, it can be fully regenerated by calcination. Ambelyst-15 also suffers from deactivation. The deactivation is primarily due to humin deposit on the surface of the catalyst.

The 2nd part of the dissertation deals with the bioconversion of lignocellulosic biomass. The one of the main objective of this task is to investigate the technical feasibility of one-step bioconversion of cellulosic mixed feedstock into lactic acid through simultaneous saccharification and co-fermentation (SSCF). On that ground, hemp hurd, an industrial byproduct, was investigated as a complementary feedstock to paper mill sludge for lactic acid production via SSCF. The feedstock mixture was processed by Cellic C-Tec2 enzyme and *Lactobacillus pentosus* (ATCC-8041). The mixing ratio plays an important role in the production of lactic acid as the pH of the product titer depends on the sufficient supply of sludge to maintain at optimum level. Calcium carbonate, which retain as a fraction of ash in sludge react with lactic acid producing calcium lactate as final product. The final lactic acid concentration was obtained

66 g/L, which corresponds lactic acid yield 0.82 g/g-sugar, under 12 % solid loading at mixing ratio of sludge: hemp hurd =80:20.

In the final section, the efficacy of chlorine dioxide (ClO_2) as a secondary pretreatment reagent was investigated. Lignin is believed to be a major hindrance to bioconversion as it surrounds carbohydrates (cellulose and hemicellulose) making it highly recalcitrant to enzymes and microorganisms. ClO_2, a selective bleaching agent, have been used in pulp and paper industry to remove lignin very effectively. Here, two different types of two-step pretreatment process, alkaline followed by ClO_2 and dilute acid followed by ClO_2 were evaluated as a measure of enzymatic deconstruction of biomass to monomeric sugars. The effectiveness of the secondary treatment (ClO_2) is highly sensitive to the primary treatment reagent whether it is alkali or acidic. Thus, alkaline followed by ClO_2 improve glucan digestibility significantly and in some cases, xylan digestibility as well. On the contrary, dilute acid followed by ClO_2 has shown negative effect on enzymatic hydrolysis. Lignin quantity, lignin distribution, lignin structure of the treated feedstocks and lignin, which depend on the primary treatment reactions mechanism, were found to be the major parameters affecting the overall efficiency of the process.

In summary, the work of this dissertation provides first-hand knowledge regarding the technical feasibility for the acid catalyzed production of LA from glucose and biochemical production of lactic acid from mixed feedstocks.

Acknowledgments

I would like to express my thanks to the people who helped me in my journey in Auburn University. First of all, I would like to express my sincere gratitude to Dr. Yoon Y. Lee, my advisor, for his guidance, patience, enthusiasm, encouragement and total support that continually inspired me to reach out to new fields. I would like to thank Dr. Zhihua Jiang, my co-adviser, for providing the invaluable guidance and support throughout my research. I would also like to thank Dr. Thomas Hanley, Dr. Aland David, and Dr. Maobing Tu for their valuable guidance during the course of this investigation. I would like to thank Dr. Yi Wang for agreeing to be an external reader. Special thanks to Dr.Venkata Ramesh Pallapolu, Dr. Suan Shi and Dr. Wenjian Guan for their constant helps, supports and suggestions. I would like to thanks Tae Hyun Kim for providing LMMA and ELLA treated corn stover. I would also like to thanks Dr. Shaima Nahreen, Dr. Joyanta Goswami, Dr. Alexander Haywood, Dr. Shahadat Hussain, Dr. MariAnne Sullivan, David Roe, Mahesh Parit, Shounak Dutta and Nirmal Mitra for their help during experiment. I want to thank Novozymes, North America, Franklinton, NC for providing C-Tec2 enzyme, Boise Paper Company, Jackson, AL for providing the paper mill sludges and Pure Vision Technology Inc., Fort Lupton, CO for providing hemp hurd.

Finally, I gratefully acknowledge the financial support provided by Alabama Center for Paper and Renewable Resources Engineering, AkzoNobel Pulp & Performance chemicals, and Georgia-Pacific, Atlanta.

To my late Father and

Mother, Brothers & Sisters

Table of Contents

List of Tables

List of Figures

List of Scheme

Chapter 1

Introduction

1.1 Background

The production of fuels and chemicals from biomass is not a new concept. Apart from providing food, feed and energy, biomass was an important source of valuable products such as medicinal drugs and flavors and fragrances throughout recorded history (Gallezot, 2012). In this context, cellulose, ethanol, methanol and other biomass-derived chemicals have been in use since 1800 to make paint, glue adhesive and solvents (Demirbas, 2006). In the 19th century, the discovery of fossil petroleum created an inexpensive liquid fuel source that helped industrialize the world and improved living standards (Huber et al., 2006). Thus bio-based chemicals have been suffered a severe economic competition from much cheaper products synthesized by conventional routes from hydrocarbons for more than 100 years (Gallezot, 2012). Today, fossil fuels such as coal, oil, and natural gas provide more than three quarters of the world's energy. However, the worldwide reserves of petroleum are estimated to be depleted in less than 50 years at the present rate of consumption (Demirbas, 2007). Moreover, it is projected that the world energy consumption and petroleum demand will increase more than 30% over the next two decades due to the rapidly expanding worldwide population, particularly in emerging countries (Wang et al., 2014). A serious drawback of energy production from petroleum-derived fuels is significant carbon dioxide emission, which is a principle contributor to global warming and the problems related to climate change (Yu et al., 2008b). In addition, "World energy markets continue to be vulnerable to

disruptions precipitated by events ranging from geo-political strife to natural disasters" according to the World Energy Outlook (2014). Currently, the growing demand for petroleum resource combined with declining petroleum supplies by emerging economies, and political and environmental concerns about fossil fuels have stimulated a worldwide initiative to develop economical and energy-efficient processes for the sustainable production of fuels and chemicals. Therefore, renewable energy have been recognized as an important part of any strategy to address the environmental issues related to fossil fuels, to reduce our reliance on unstable countries to supply oil, and to increase sustainable development(Yu et al., 2008b). In addition, some other factors push the current move of the chemical industry to substitute a growing part of fossil feedstock by renewable carbon.

Instead of duplicating existing petroleum derived commodity, the chemistry of renewable sources opens an opportunity to develop a new portfolio of products that have no equivalence among those presently manufactured by classical synthesis routes from hydrocarbons (Gallezot, 2012). Organization like Europe's SusChem or U.S. Department of Energy (US DOE) have actively promoted the usage of renewable resources to produce new products to uphold the competition among the chemical industries in global market due to market potentiality of bio based bulk chemicals (Gallezot, 2012). Taking all these considerations into account, biomass exists as a unique and promising candidate, with potential for improved sustainability and biodegradability relative to its petroleum counterpart (Wang et al., 2014). Hence, experts have predicted that 20% of transportation fuel and 25% of chemicals will be produced from biomass by 2030 (US DOE, 2002).

To achieve these goals, the U.S. Department of Agriculture (USDA) and the U.S. Department of Energy (US DOE) estimated that the U.S. could sustainably produce 1.3 billion dry tons of biomass

per year using its agricultural (72% of total) and forest (28% of total) resources and still meet its food, feed, and export demands (Huber et al., 2006). Currently the fermentation of starches (primarily from corn grain or sugar cane) to ethanol and the transesterification of fatty acids from soy, canola, and other natural oils to biodiesel are the two major chemical pathways to produce biofuels commercially (Acharjee, 2010). These processes have limited capacity to fulfill these goals; technology development for processing more abundant lignocellulosic biomass for fuels and materials will be critical.

1.2 Biomass as a renewable source of carbon

Lignocellulosic material such as agricultural residues (e.g., wheat straw, sugarcane bagasse, corn stover), forest products (hardwood and softwood), and dedicated energy crops (switch grass, salix) can be used for the production of alternative transportation fuels and chemicals. The three main components of lignocellulose are cellulose, hemicellulose and lignin (Figure 1-1), with the relative proportions of the three dependent their species of origin. The cell wall of lignocellulosic biomass is a composite material of crystalline cellulose fibrils bound by non-crystalline hemicellulose and surrounded by a matrix of hemicellulose and lignin (Rubin, 2008). All three components can be used to produce different value-added products depending on their end use.

1.2.1 Cellulose

Cellulose, the major structural components of lignocellulosic biomass, acts as the natural framework in the form of cellulose microfibrils. It is the polymer of glucose monomer bonded with β (1→4) glycosidic linkages and the degree of polymerization (DP) of higher plants lies in the range of 7,000-14,000 in the secondary wall and 500-6000 in the primary wall approximately (Gupta, 2010). Indeed, long glucose polymer chains are stuck together with inter and intra

hydrogen bonds and van der Waals interactions, creating a resistant microfibrils network (Rubin, 2008).

1.2.2 Hemicellulose

Hemicellulose, the second most abundant component of lignocellulose, is a polymer of several simple sugars such as five carbon sugars (usually xylose and arabinose) and six carbon sugars (galactose, glucose, and mannose) (Rubin, 2008). Softwood hemicellulose is composed of a backbone of β-1, 4 linked mannose and glucose units in roughly a 3:1 ratio (Lai, 2010). Acetyl groups occur on the C_2 or C_3 carbon of roughly every third backbone unit. In contrast, hardwood hemicellulose is primarily consisted of xylans (15-30%), where many of its xylose units are acetylated at their C_2 or C_3 carbons (Lai, 2010). Due to its branched nature, hemicellulose is amorphous and thus relatively easy to hydrolyze to its monomer compared to cellulose.

1.2.3 Lignin

Lignin is a three-dimensional, highly branched, polyphenolic substance which plays a critical role in giving structural rigidity to hold plant fibers together. It is composed of three major phenolic components, namely p-coumaryl alcohol (H), coniferyl alcohol (G) and sinapyl alcohol (S) (Rubin, 2008). Lignin is synthesized by polymerization of these components and their ratio within the polymer varies between different plants, wood tissues and cell wall layers. In general, softwood lignin is formed from coniferyl alcohol where as hardwood lignin has both coniferyl and sinapyl alcohol as monomer units (Huber et al., 2006).

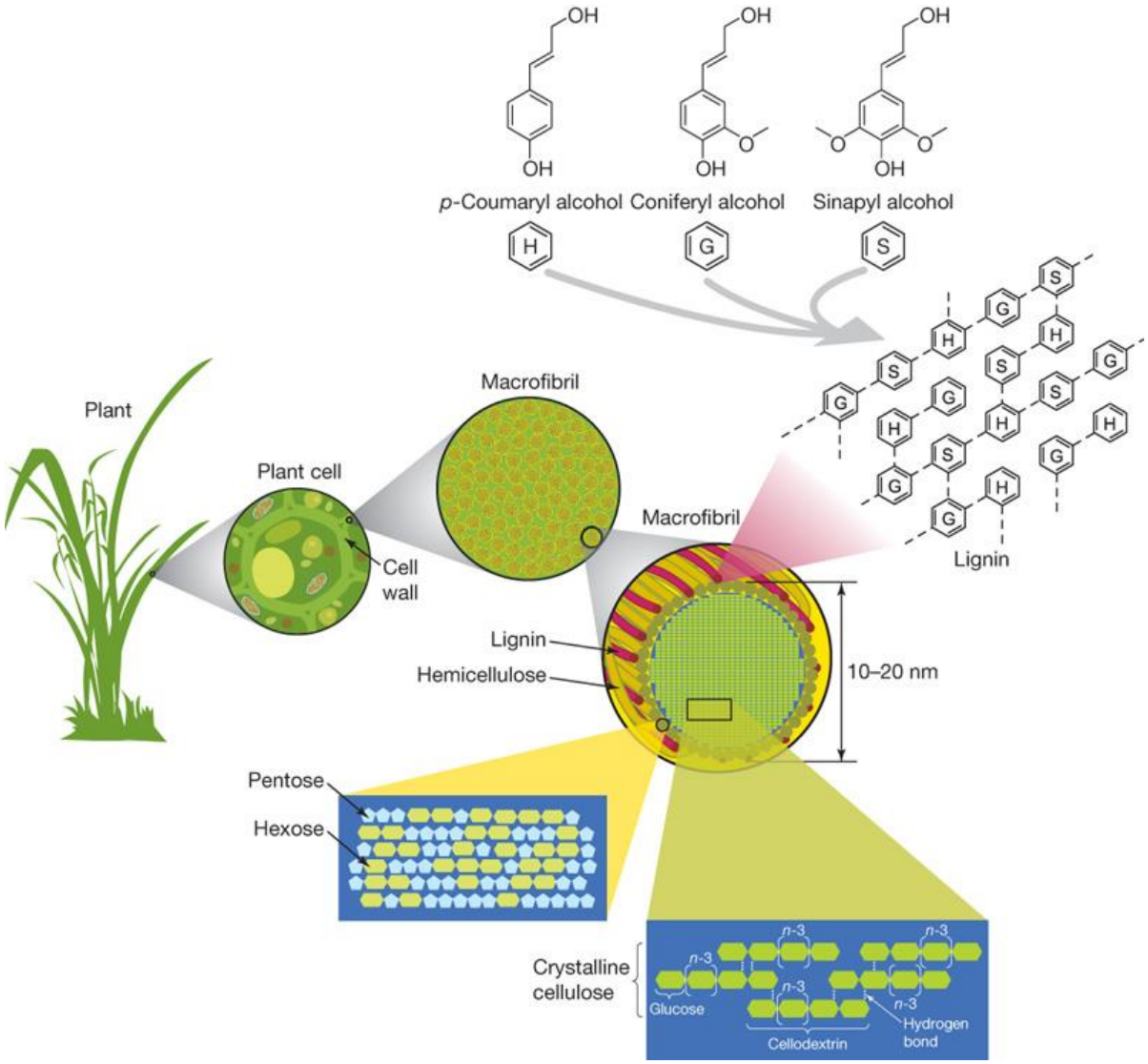

Figure 1-1 Structure of lignocellulose taken from (Rubin, 2008).

1.3 Strategies of biomass conversion

To steer the research and development activities of renewable resources to produce new products by utilizing biomass for the production of non-food products, a novel concept was introduced: bio refining. According to IEA Bioenergy Task ‘‘Biorefining is the sustainable processing of biomass into a spectrum of marketable products and energy’’ (Cherubini, 2010). The biorefinery concept grasp a broad range of technologies capable of separating biomass resources (wood, grasses, corn

etc.) into their building blocks (carbohydrates, proteins, triglycerides etc.) that can be converted to value added products, biofuels and chemicals (Cherubini, 2010). This concept is analogous to today's petroleum refinery, which produces multiple fuels and products from petroleum. Based on biomass feedstock source, different type of potential large-scale industrial biorefinery schemes is existed. Of these, the lignocellulosic feedstock (LCF) biorefinery scheme is very promising due to its potential to deal with a wide range of low-cost feedstocks (straw, reeds, grass, wood, paper-waste, etc.) conversion into values added chemicals in both the existing petrochemical-dominated market and the future biobased product market (Kamm & Kamm, 2004).

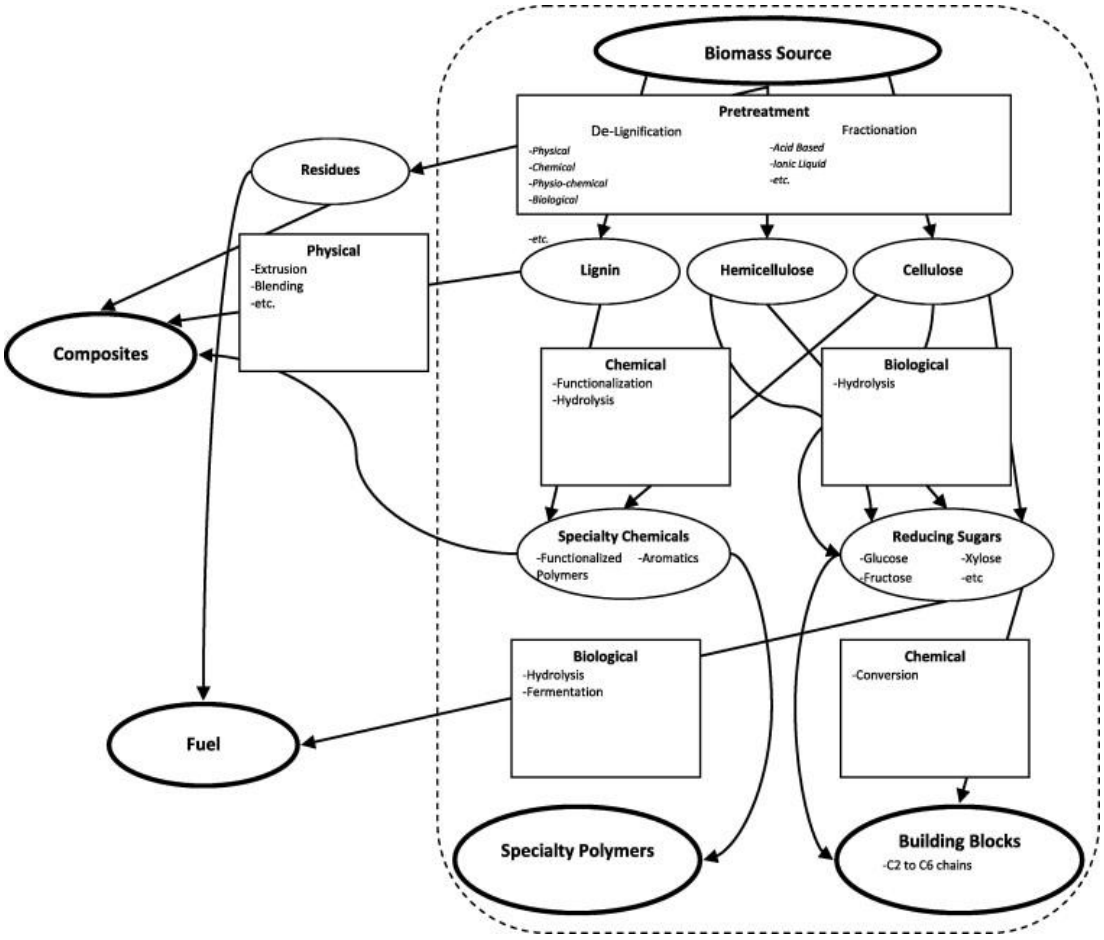

Figure 1-2 Overview of the processing of crude feedstocks to refined products in a sustainable biorefinery taken from (FitzPatrick et al., 2010).

Figure 1-2 illustrates the conversion of biomass into bioproducts and/or energy which involves a series of interconnected feed streams, processes, and chemical. The future success of biorefineries will require fundamental understanding of underlying process mechanism as well as understanding of the types of processes best suited for converting the various chemical moieties into biomass-derived constituents (Gallezot, 2012). There are two kinds of strategies on this regard. The target-driven approach considers searching of the most efficient synthetic routes to produce a given chemical starting from well-identified platform molecules by process analysis methodology. In contrast, process-driven approach deals biomass conversion by one or more catalytic processes (hydrogenation, hydrogenolysis, oxidation, etc.) yielding a variety of fuels and chemical intermediates (Gallezot, 2012; Bozell & Petersen, 2010)**.**

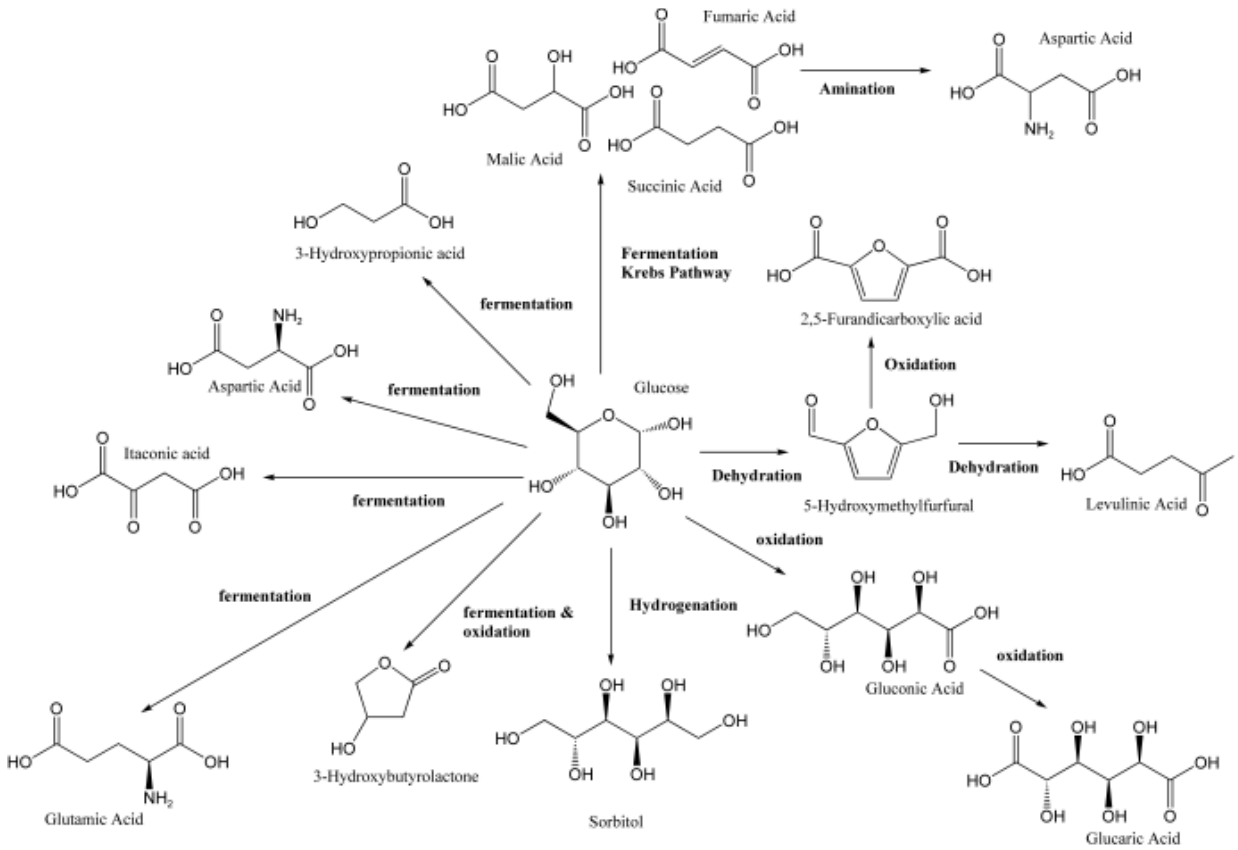

Figure 1-3 Top value-added chemicals from glucose taken from (Chheda et al., 2007).

In general, several type of reactions such as hydrolysis, dehydration, isomerization, aldol condensation, reforming, hydrogenation, and oxidation have been employed to synthesis a family of valuable products from carbohydrate (glucose) as shown in Figure 1-3. These conversion processes can be carried out in a wide range of condition; from low temperature isomerization of carbohydrates to high-temperature gasification of biomass (Figure 1-4). In this respect, liquid phase processing of carbohydrate feeds is typically carried out in the aqueous phase or under biphasic conditions employing an aqueous and an organic phase due to their low volatile and high reactive nature (Chheda et al., 2007).

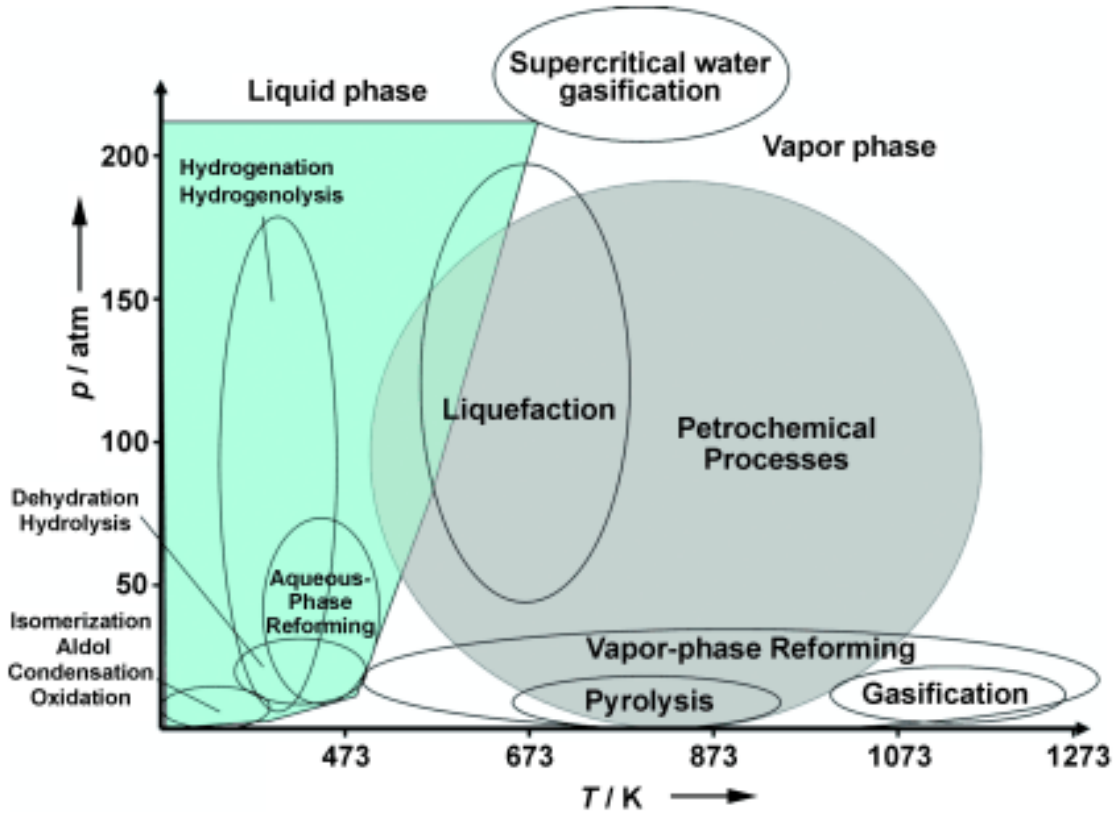

Figure 1-4 Diagram of approximate reaction conditions for the catalytic processing of petroleum versus biomass-derived carbohydrates taken from (Chheda et al., 2007).

1.4 Conversion via platform molecules

In 2004, National Renewable energy Laboratory (NREL) and Pacific Northwest National Laboratory (PNNL) conducted a detailed study to identify valuable sugar-based building blocks for lignocellulosic biomass (Werpy and Petersen, 2004). The aim of the research was to figure out those green intermediate that could best substitute for the eight fundamental petroleum- based building blocks still meeting the existing demand of chemical products but shifting reliance from oil to biomass (Roman-Leshkov, 2008). A list of chemicals was obtained by evaluating the potential markets of the building blocks and their derivatives and the complexity of the synthetic pathways. Lactic acid and levulinic acid (LA) were one of the top-thirty green building blocks; both can be produced from lignocellulosic biomass (Werpy and Petersen, 2004). In addition, HMF, an intermediate in the process of LA production, also ranked as one of the thirty chemicals. In this study we focus mainly selective conversions of biomass or biomass-derived feedstocks (especially sugars) at low temperatures (typically lower than 600 K) and in the liquid phase.

1.5 Conversion of biomass to HMF

HMF consists of a furan ring, containing both aldehyde and alcohol functional groups which makes it very reactive. The thermal dehydration of hexoses in acid media leads to the formation of two important basic nonpetroleum chemicals: HMF arising from dehydration of hexoses, and LA arising from hydration of HMF as seen in Figure 1-5. The dehydration process is more efficient and selective to HMF when started from ketohexoses than from aldohexoses (Corma et al., 2007).

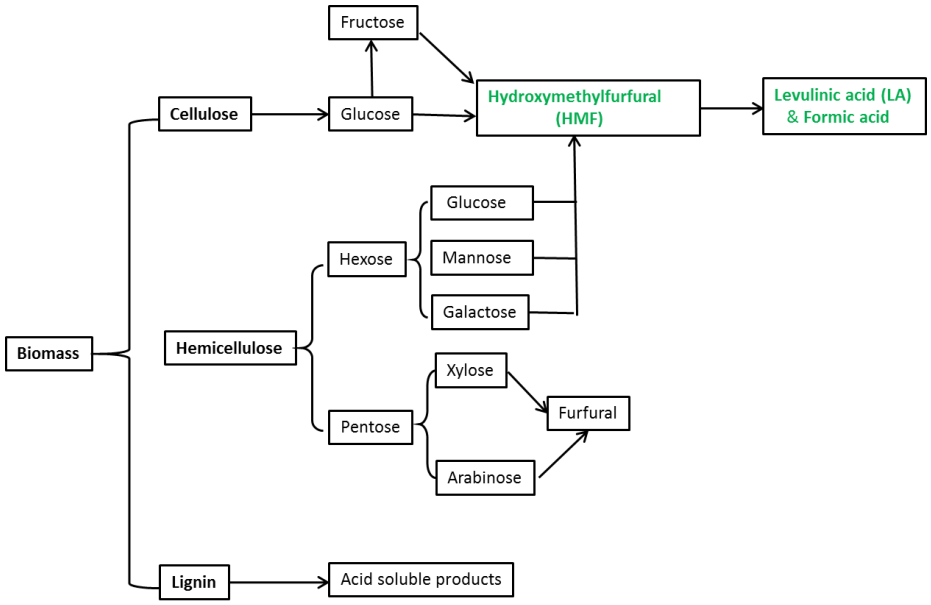

Figure 1-5 Simplified reaction scheme for the conversion of lignocellulosic biomass to LA.

1.5.1 Catalytic conversions in aqueous media

The dehydration of fructose in aqueous phase results into low yields of HMF in the absence of acid catalysts. The addition of mineral acids such as hydrochloric, sulfuric, and phosphoric acids enhance the yield of HMF in water (Asghari & Yoshida, 2006). In their study, Kuster et al. (1977) performed in-depth studies of all parameters that might influence the dehydration of fructose in water under homogeneous catalysis. Under optimal conditions of 95 °C, ambient pressure, and acid concentration of 2 M HCl, HMF yield was approximately 30% from fructose.

The homogeneous acid catalyst plays a key role in the improvement of HMF formation. However, the difficult recovery of the homogeneous catalyst and environmental pollution along with the equipment corrosion issues makes heterogeneous catalyst as a viable alternative due to their high selectivity and easy to handle nature. Watanabe et al. (2005) studied the effects of heterogeneous catalysts (TiO_2 and ZrO_2) on fructose dehydration in hot compressed water (473 K) by a batch-type reactor. They found HMF yield was ~20% with TiO_2 and ~15% with ZrO_2, with conversions

being 90–100% for each case from fructose at 200 °C, 25 bar Ar, and a 5 minute reaction. Although aqueous processes are very convenient from an ecological point of view, low HMF selectivity due to LA and humins formation limit the practical application of simple aqueous system.

1.5.2 Combined glucose to fructose isomerization and fructose to HMF strategy

It is obvious that the dehydration process is more efficient and selective to HMF when started from ketohexoses (fructose) than from aldohexoses (glucose). The aldohexose (glucose) enolyzes to a very low degree and the enolization is a determining step of the HMF formation from glucose. In this respect, glucose isomerization is a crucial step in the efficient production of valuable chemical intermediates, such as HMF and LA, from biomass. Therefore, combination of glucose isomerization catalyst with a fructose dehydration catalyst in either a "one-pot" or "two step" configuration could be promising approach.

1.5.3 Combined base and Brønsted acid systems

Glucose–fructose isomerization, known as the Lobry-deBruyn–van Ekenstein transformation, catalyzed by a base. Takagaki et al. (2009) designed a strategy for the selective HMF formation from glucose over solid acid and base catalysts via a one-pot reaction under mild conditions. Their strategy involves separating HMF synthesis from glucose into two reactions, (1) isomerization of glucose into fructose catalyzed by solid base and (2) dehydration of fructose into HMF by solid acid. After initial catalyst screening for the activity of the two individual steps, Mg–Al hydrotalcite and Amberlyst-15 were chosen as the solid base and acid, respectively. To minimize the mutual interaction of an acid–base pair, DMF, an organic aprotic solvent was selected as the media for this "one-pot" transformation. The combination of the base and acid catalysts was demonstrated to be effective, achieving glucose conversion of 73% with selectivity towards HMF of 58%.

1.5.4 Combined enzymatic and Brønsted acid catalysts systems

The preferred industrial isomerization method involves the use of an immobilized enzyme (xylose isomerase) at 333 K that produces an equilibrium mixture of 42% (wt⁄wt) fructose, 50% (wt⁄wt) glucose, and 8% (wt⁄wt) other saccharides (Moliner et al., 2010). Huang et al. (2010) used borate-assisted isomerase to shift equilibrium, which leads to higher fructose yield (87.8%). Once fructose was separated from the isomerase, the resulting sugar mixtures were dehydrated in water–butanol media by dilute HCl to produce HMF (63.3% yield). Simeonov et al. (2013) developed a new catalytic system featuring the integration of enzymatic and acid catalysis for the selective conversion of glucose into HMF. In their process, they used sweetzyme® for the isomerization reaction and HNO_3 for the subsequent dehydration in wet tetraethylammonium bromide (TEAB) media. They were able to increase HMF yield up to 90 %. Since the enzymatic isomerization requires a significantly longer time and chemo-catalytic dehydration is a relatively rapid reaction, the throughput difference can represent a challenge in integrating the two steps in spite of the effectiveness of this approach in obtaining the highest reported HMF yields.

1.5.5 Combined Lewis acid and Brønsted acid systems

The combined Lewis and Brønsted acid catalyst systems have several advantages over combined chemo-enzymatic approach and acid-base approach. The Lewis and Brønsted acid catalyst system can be easily integrated into “one-step” process in an aqueous media while the chemo-enzymatic approach requires two-step process. Moreover, this process doesn’t have “mutual interaction” which creates a problem for acid-base approach. It is known that Lewis acid has much higher selectivity for the glucose to fructose isomerization and Brønsted acid favors the dehydration of fructose in aqueous media. Recently, Moliner et al. (2010) reported on a tin-containing zeolite (tin in the framework of a pure-silica analog of zeolite beta, denoted Sn-beta) that was shown to be

active material over a wide temperature range (343– 413 K) for the isomerization. In another study, the same group reported that the combination of Sn-Beta with acid catalysts gave high yield of HMF from carbohydrates such as glucose, cellobiose, and starch in their "one-pot" biphasic reactor system. They were able to enhance HMF selectivity as high as 72 mol % at 79% glucose conversion with reaction conditions of: water– tetrahydrofuran (THF) biphasic system, catalysis by a combination of Sn-beta and HCl, reaction temperature of 180 °C, and reaction time of 70 min (Nikolla et al., 2011).

Amongst all the catalyst/reaction systems reviewed, a combined Lewis acid-catalyzed isomerization and subsequent Brønsted acid-catalyzed dehydration that converts glucose to HMF in an aqueous–organic biphasic system seems particularly promising.

1.6 Conversion of biomass to LA

LA (gamma-ketovaleric acid), a short-chain fatty acid, is one of the top-twelve building blocks which can be produced from lignocellulosic biomass using an acid catalyst. The conversion of a typical lignocellulosic biomass to LA is shown in Figure 1-5.

1.6.1 Homogeneous acid catalysts

The most common method to produce LA is the acid catalyzed hydrolysis of hexose sugars or carbohydrates. Traditionally, strong inorganic acids such as HCl and H_2SO_4 have been used as catalysts to produce LA from glucose (Girisuta et al., 2006b). Other carbohydrate-containing feedstocks including cellulose (Girisuta et al., 2007b) , corn starch (Cha & Hanna, 2002), water hyacinth plant (Girisuta et al., 2008), sugarcane bagasse (Girisuta et al., 2013), and pine (Rivas et al., 2013) have also been used. Table 1-1 gives an overview of LA synthesis using various types of feedstock and acid catalysts.

Table 1-1 Overview of acid catalyzed production method for LA

Feedstock	C_0 (wt %) [a]	Acid	C_{acid} (wt %)	T (°C)	t (h)	Y_{LA} (mol %) [b]	References
Glucose	1.8-18	H_2SO_4	0.5-9.8	140-200	f(T)[c]	~60	(Girisuta et al., 2006b)
Glucose	10	HCl	0.36	140-180	f(T)[c]	~60	(Weingarten et al., 2012)
Cellulose	0.8-2.4	HCl	1.1-3.4	160-200	f(T)[c]	~60	(Shen & Wyman, 2012)
Sucrose	6	H_2SO_4	9	125	16	~46	(Wiggins, 1949)
Sucrose	6	HCl	9.7	125	16	~66	(Wiggins, 1949)
Sucrose	6	HBr	9	125	16	~72	(Wiggins, 1949)
Cellulose	1.7-14	H_2SO_4	0.5-9.8	150-200	f(T)[c]	~60	(Girisuta et al., 2007a)
Fructose	4.5-18	HCl	2-7.5	100	24	~77	(Kuster & Vanderbaan, 1977)
Cellulose	10	H_2SO_4	5	150-250	2-7	~39	(Efremov et al., 1997)
Cellulose	10	HCl	1-5	150-250	2-7	~44	(Efremov et al., 1997)
Cellulose	10	HBr	1-5	150-250	2-7	~43	(Efremov et al., 1997)
Aspen wood	10	H_2SO_4	5	150-250	2-7	~24	(Efremov et al., 1997)
Aspen wood	10	HCl	1-5	150-250	2-7	~19	(Efremov et al., 1997)
Aspen wood	10	HBr	1-5	150-250	2-7	~13	(Efremov et al., 1997)
Wheat straw	6.4	H_2SO_4	3.5	210	0.63	~21	(Chang et al., 2009)
Sorghum grain	10	H_2SO_4	8	200	0.67	~46	(Fang & Hanna, 2002)
Bagasse	10	HCl	4.5	220	f(T)[c]	~63	(Girisuta et al., 2013)
Water hyacinth	1	H_2SO_4	10	175	0.5	~53	(Girisuta et al., 2008)

[a] C_o is the initial concentration of feedstock and defined as the ratio between the mass of feedstock and the total mass ; [b] Y_{LA} is defined as the ratio between the mole of LA and the mole of hexose; [c] time is a function of temperature.

1.6.2 Heterogeneous acid catalysts

A wealth of research have been conducted on conversion of lignocellulosic biomass to LA using homogeneous catalysts , but relatively few address heterogeneous catalyst in the process of LA production from soluble sugars. The difficulty in recovery of the homogeneous catalyst and disposal problem along with equipment corrosion issues make heterogeneous catalyst a viable option.

Heterogeneous acid catalysts such as faujasite (LZY and HY) and mordenite (MFI) type zeolites have been used previously for the synthesis of LA from fructose, glucose and cellulose (Jow et al., 1987; Lourvanij & Rorrer, 1993; Zeng et al., 2010). Recently, chromium chloride was found to be effective for the conversion of cellulose to LA, affording yield of 67 mol % (Peng et al., 2010). However, catalyst stability was found to be a concern, as atomic absorption spectrometry data show that significant amounts of chromium ions were found in the liquid product due to the leaching of metal ions from the solid to the solution or to partial dissolution of the solid. Acidic ion-exchange resins such as perfluorosulfonic acid-based catalysts (Nafion) and styrene-based sulfonic acids (Amberlyst) have been found to be effective for a wide range of acid-catalyzed reactions. Lucht and co-workers used Nafion SAC-13 to produce LA from cellulose and obtained a relatively low yield of LA (Hegner et al., 2010; Potvin et al., 2011). However, they were able to increase the yield of LA five-fold from 14% in aqueous medium to 72% in 25% NaCl solution. Weingarten et al. used Amberlyst-70 to produce LA from glucose and found the maximum yield to be 33% in aqueous media (Weingarten et al., 2012).

1.6.3 Industrial production of LA from biomass

The most promising technology proposed for the industrial production of LA, patented by the Biofine Corporation. Figure 1-6 shows the Biofine technology for the continuous production of

LA (Fitzpatrick, 2006). The carbohydrate feedstock is initially shredded to appropriate particle size (ca 0.5 to 1 cm) to ensure efficient hydrolysis and optimum yields.

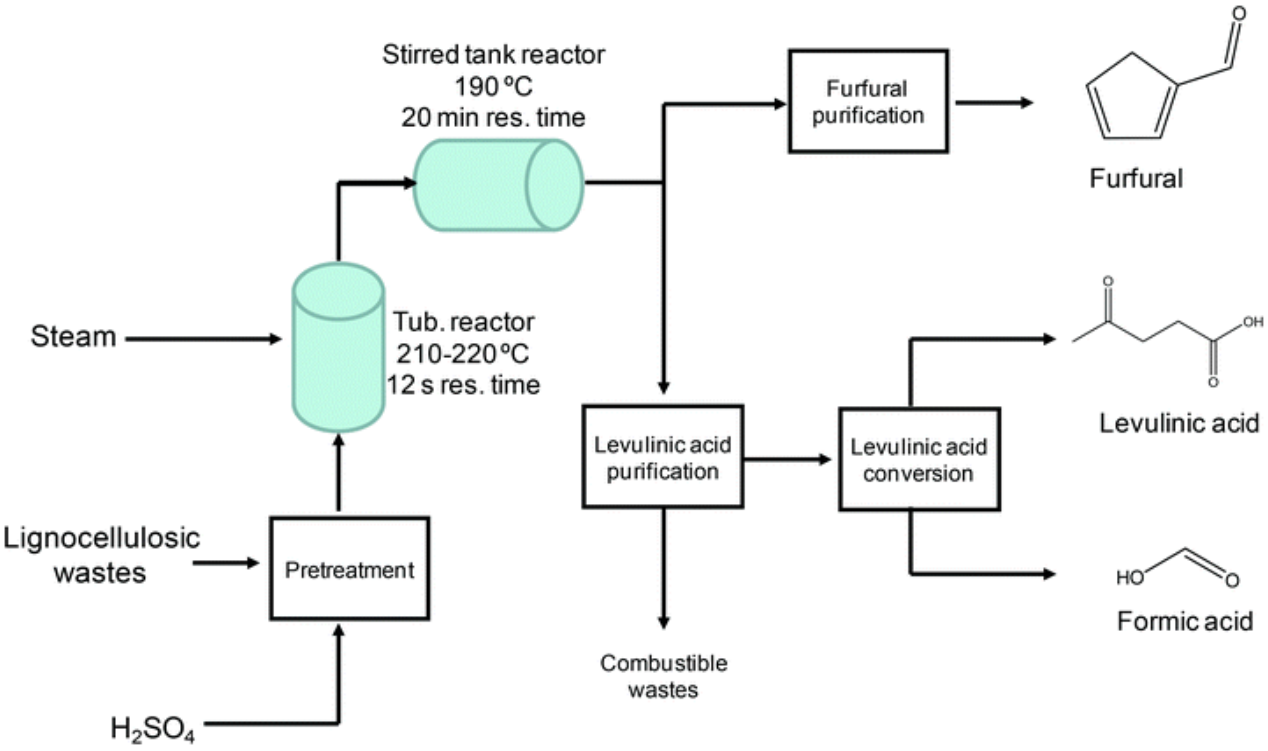

Figure 1-6 Continuous production of LA by the Biofine technology taken from (de Souza et al., 2014).

Then the shredded feedstock is mixed with dilute sulfuric acid (1.5-3%) and the slurry is supplied continuously to a plug flow reactor (1st reactor, preferable smaller diameter) which is operated a temperature of 210-220 °C, a pressure of 25 bar and a residence time of only 12 s. The reason of this short contact time is to ensure optimum production of soluble intermediates (e.g. HMF) by the acid hydrolysis of the carbohydrate polysaccharides. This initial hydrolysis product which is continuously removed and fed to a continuously stirred tank reactor (2nd reactor, larger diameter) operated at less severe condition (190-200 °C, 14 bar) but with a longer residence time of 20 min. The reaction conditions in the second reactor are adjusted to remove furfural and other volatile

products while the tarry mixture of LA and residues are passed to a gravity separator. After passing the dehydration unit, solid byproducts are removed from the LA solution in a filter-press unit and collected as combustible wastes. Then the crude 75% LA product can be purified up to a purity of 98%. This commercial process claims to achieve LA yields of 70-80% of the theoretical maximum from cellulosic feedstock in its two-reactor system by the conversion of approximately 50% hexose sugars to LA, with 20% being converted to formic acid and 30% to tars (Fitzpatrick, 1997; Hayes et al., 2006).

1.6.4 Mechanistic studies of LA production

The acid catalyzed degradation of hexoses into LA has been extensively studied. However, only a limited amount of information is available on the underlying reaction mechanism. The aqueous phase production of LA from hexoses involves isomerization, dehydration, fragmentation, reversion, and condensation steps. The available information implies that hexose sugars initially dehydrate to form the intermediate product HMF, which is subsequently hydrated to give the final product LA. Two schools of thought were proposed with regard to the HMF formation from C_6 carbohydrate in literature (Scheme 1-1). One pathway postulates that the isomerization of glucose into fructose is the primary reaction pathway together with a small amount of mannose (Choudhary et al., 2013; Moliner et al., 2010). Then fructose is converted to HMF by dehydration and subsequently hydrolyzes to form levulinic and formic acids. The Other theory suggests that the dehydration of glucose does not involve the isomerization of glucose to fructose as the first step of the reaction. According to this theory, glucose can be converted into HMF through cyclization of 3-deoxyglucosone (3-DG) intermediate formed from the open-ring form of glucose (Chidambaram & Bell, 2010; Locas & Yaylayan, 2008). The relatively low conversion of glucose to HMF is observed due to low propensity of glucose to exists in open ring form as well as many

other side reactions of 3-DG. The conversion of HMF into LA is the result of water addition to the $C_2 – C_3$ bond of the furan ring to give the final products LA and formic acid (see Scheme 1-2).

Scheme 1-1 Dehydration reactions of hexose sugars to HMF taken from (Corma et al., 2007).

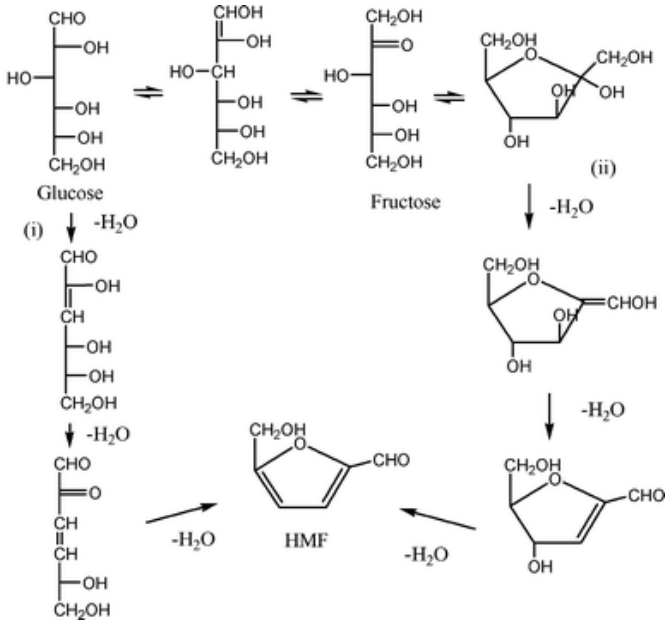

Scheme 1-2 Reaction mechanism for the conversion of HMF to LA (Horvat et al., 1985).1=LA. 2= HMF

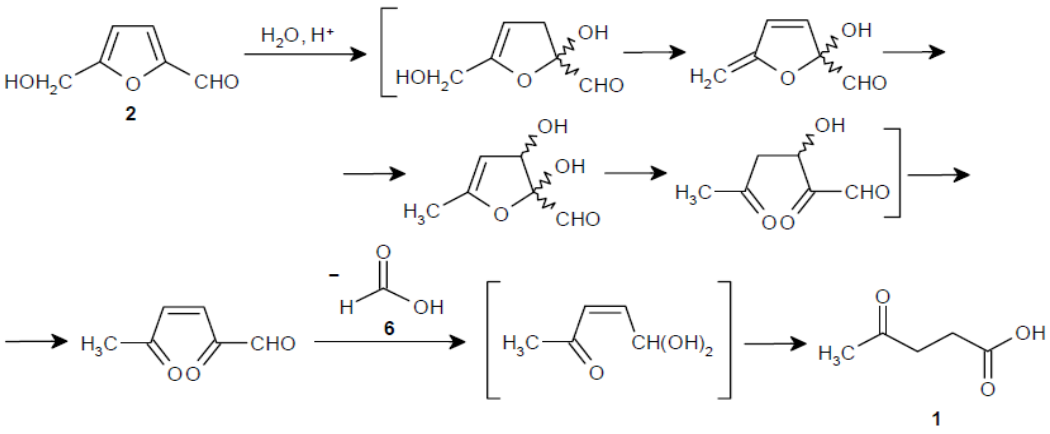

1.6.5 LA derivatives

The unique feature of LA is its ketone and a carboxylic acid groups. These two functional groups make LA a potentially very versatile building block for the synthesis of various organic chemicals. Figure 1-7 shows the transformations of LA.

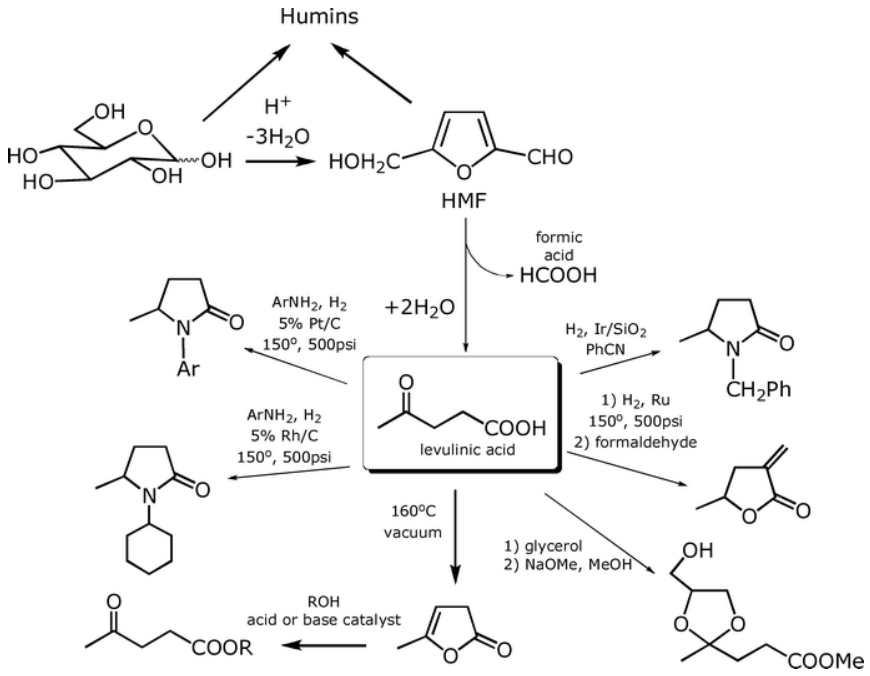

Figure 1-7 Transformation of LA taken from (Bozell et al., 2000).

1.7 Conversion of biomass to lactic acid

Lactic Acid is an important industrial commodity with large and fast growing market due to its widespread applications, mainly in food, chemical, cosmetic, and pharmaceutical industries (Xu et al., 2006). Its most dominant application is biodegradable and biocompatible polylactic acid (PLA) polymers that drive the current market expansion for lactic acid from 86,000 tons/year in 2001 to 260,000 tons in 2008, and expected to reach 1,000,000 tons in 2020 (Shi et al., 2015). Lactic acid production can be achieved either by chemical synthesis routes or fermentation

routes (Abdel-Rahman et al., 2013). Currently, most lactic acid is produced by microbial fermentation of carbohydrates due to low temperature, low energy consumption, and high product specificity as it produces a desired stereoisomer, optically pure L-(+)- or D-(−)-lactic acid when the appropriate microorganism is selected as the lactic acid producer (John et al., 2007). The fermentative production cost of lactic acid is dependent on many factors such as the nutrients, nitrogen sources, downstream recovery and purification process, and raw material cost (Garde et al., 2002; Parajo et al., 1997; Rhee et al., 2016; van der Pol et al., 2016). Most of the fermentation relies on starch-derived glucose or sucrose as feedstock (Shi et al., 2015) and the main obstacle for the fermentative production of lactic acid is the high cost of feedstocks (Abdel-Rahman et al., 2013). Therefore, lignocellulosic feedstocks are promising for lactic acid production. However, the biochemical conversion of lignocellulosic feedstock requires several processing steps to convert structural carbohydrates to monomeric sugars, e.g., glucose, xylose, arabinose, and mannose. These monomeric sugars can be fermented to lactic acid through different types of microorganisms (Abdel-Rahman et al., 2013).

Simultaneous saccharification and fermentation (SSF) has been considered as an efficient bioconversion strategy in lactic acid production due to reduced reactor volume, rapid processing time, less enzyme loading, reduced feedback inhibition, enhanced rate of hydrolysis, and increased productivity and higher lactic acid yields (Abdel-Rahman et al., 2011; Sun & Cheng, 2002; Tsai & Moon, 1998). In order to maximize yield and productivity, a large number of studies have investigated lactic acid fermentation by *Lactobacillus* (LAB) from lignocellulosic feedstocks in the field of microbial technology (Abdel-Rahman et al., 2011; Bustos et al., 2005; Monteagudo et al., 1997; Zhu et al., 2007). Under anaerobic conditions, *Lactobacillus pentosus* produce lactic acid by metabolizing hexose (glucose) via Embden–Meryerhof–Parnas (EMP)

pathway . It also ferments pentoses (xylose and arabinose) through the phosphoketolase (PK) pathway generating equal moles of lactic acid and acetic acid (Okano et al., 2009; Zhu et al., 2007).

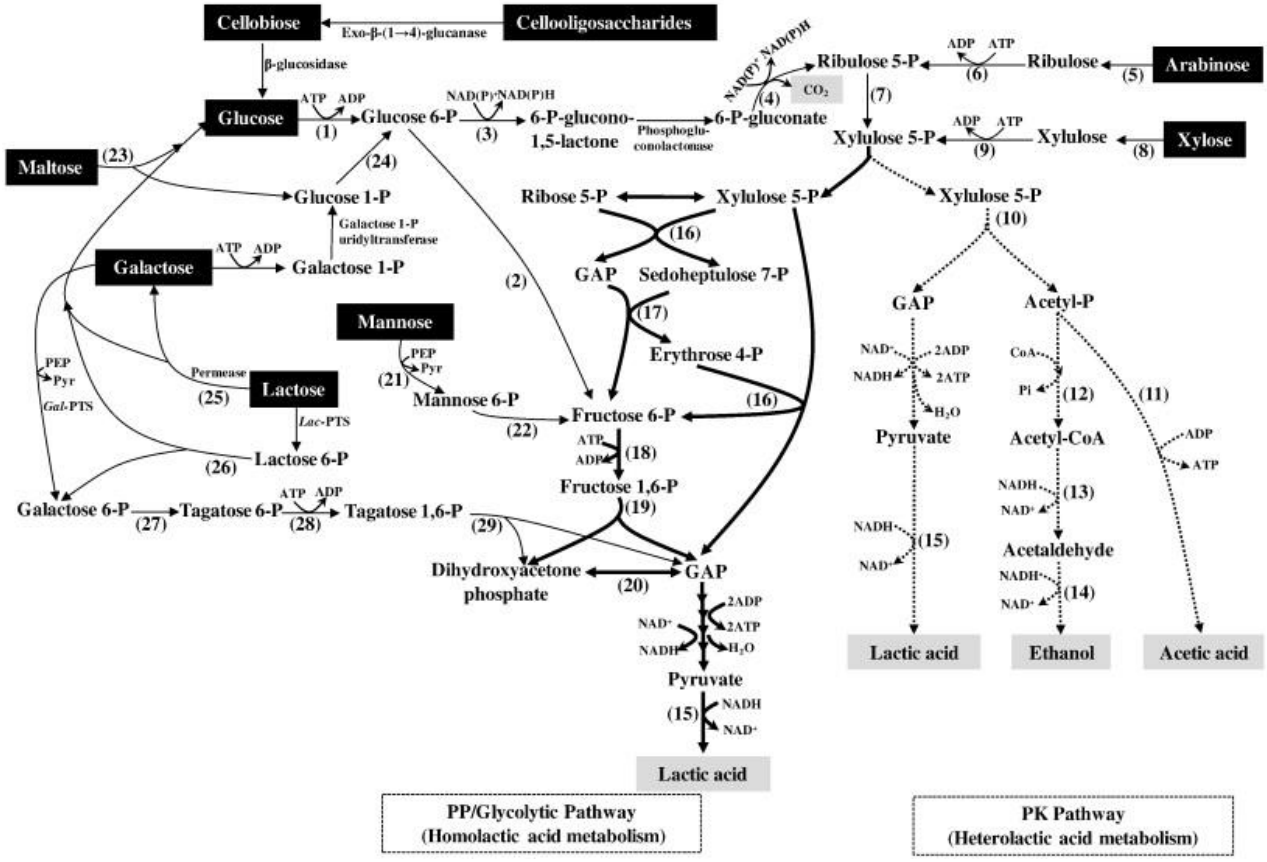

Figure 1-8 Metabolic pathways for lactic acid production from various sugars by LAB. Solid lines indicate the homofermentative pathway. Thick-solid lines and dashed lines indicate PP/glycolytic pathway and PK pathway, respectively. Lac-PTS: phosphoenolpyruvate-lactose phosphotransferase system (Abdel-Rahman et al., 2013).

Table 1-2 gives an overview of lactic acid synthesis using various types of feedstock and fermentation procedure.

Table 1-2 Overview of SSF production method for lactic acid

Feedstocks	Culture	Fermentation	Lactic acid (g/L)	Lactic acid yield (g/g)	Reference
Xylose	*E. mundtii QU 25*	Batch	86.7	0.84	Abdel-Rahman et al. (2013)
Glucose/cellobiose	*E. mundtii QU 25*	Batch	35.1	0.91	Abdel-Rahman et al. (2011)
Wheat straw hemicellulose	*Lb. brevis and Lb. pentosus*	Batch	7.1	0.95	Garde et al. (2002)
Cassava bagasse	*Lb. casei NCIMB 3254*	Batch SSF	83.8	0.96	John et al. (2006)
Pretreated cardboard	*Lb. coryniformis spp. torquens ATCC*	Batch SSF	23.4	0.56	Yanez et al. (2005)
Defatted rice bran	*Lb. delbrueckii IFO 3202*	SSF	28	0.28	Tanaka et al. (2006)
Brewer's spent grain	*Lb. delbrueckii UFV H2B20*	Batch	35.5	0.99	Mussatto et al. (2008)
Vine shoots	*Lb. pentosus*	Batch	24	0.76	Moldes et al. (2006)
Barley bran husks hydrolysates	*Lb. pentosus*	Batch	33	0.57	Moldes et al. (2006)
Corncob	*Lb. pentosus*	Batch	26	0.53	Moldes et al. (2006)
Vine-trimming wastes	*Lb. pentosus ATCC 8041*	Batch		0.77	Bustos et al. (2004)
Corn stover	*Lb. pentosus ATCC 8042*	Fed-batch SSF	74.8	0.65	Zhu et al. (2007)
Corn stover	*Lb. rhamnosus and Lb. brevis*	SSF	20.95	0.7	Cui et al. (2011)
Paper sludge	*Lb. rhamnosus ATCC 7469*	Batch SSF	73	0.97	Marques et al. (2008)
Apple pomace	*Lb. rhamnosus ATCC 9595 (CECT288)*	Batch	32.5	0.88	Gullon et al. (2008)

1.8 Pretreatment

To achieve high yields of glucose by hydrolysis, or to produce more favorable feedstock for downstream processing, lignocellulosic biomass must first be pretreated. During pretreatment, the crystallinity of cellulose decreases, biomass surface area increases, hemicellulose is removed, and the lignin seal breaks (Acharjee, 2010). Thus, biomass structure is altered and downstream processing is improved. Most pretreatments are done through physical, physicochemical, thermochemical, solvent extraction methods, and biological.

1.8.1 Thermochemical pretreatment

Thermo-chemical pretreatment employs the use of a wide variety of chemical agents such as acid, alkaline, organosolv, hot water, oxidizing reagent, ionic liquid and supercritical fluids to increase surface area and pore volume, and swelling of cellulose by breaking down specific components of the biomass (Gupta, 2008). Thermo-chemical pretreatments methods include acid, alkaline, organosolv, hot water, oxidizing reagent, ionic liquid and supercritical fluids etc. Some of the most commonly used thermochemical pretreatment methods are discussed below.

1.8.2 Acidic pretreatment

Different acidic reagents such as dilute sulfuric acid dilute nitric acid dilute hydrochloric acid, and dilute phosphoric acid have been used for the pretreatment process for a long time (Pallapolu, 2014). The method fractionates majority of hemicelluloses (75-90%). Two approaches for dilute acid pretreatment are followed. In one approach, high temperature (more than 160 °C) in a continuous flow reactor with low solid loading is used; while in another approach, low temperature batch process is used with high solids loading. Among the dilute acids, dilute sulfuric acid (0.5-1.5%) above 160 °C was found to be most suitable for the industrial application due to the dilute acid pretreatment process solubilizes the hemicellulose component of biomass into liquid stream, while leaving most of the cellulose fraction intact in the solid part (Gupta, 2008; Kothari, 2012). The major disadvantage of the process is the removal of acids or neutralization which yields a large amount of gypsum before next step of enzymatic hydrolysis. The disadvantages of the dilute acid process include high investment in equipment associated with acid corrosion, and high inhibitor content which makes fermentation very difficult.

1.8.3 Alkaline pretreatment

Among the various thermochemical pretreatments, alkali pretreatment is most widely used to enhance enzymatic hydrolysis of lignocellulose. During alkaline pretreatment, the lignin is degraded predominantly by cleavage of lignin-hemicellulose bonds, and delignification brings about changes in the structure of cellulose, whose DP and crystallinity decrease and accessible surface area increases, thus making the biomass more susceptible to enzymatic hydrolysis (Gupta, 2008; Kothari, 2012; Pallapolu, 2014; Kang, 2011). The main reagents used for alkali pretreatment are sodium hydroxide, ammonia, ethylene diamine and calcium hydroxide.

1.8.4 Hydrothermal pretreatment

In this pretreatment, biomass is treated in hot compressed water, resulting in three products, including gases, aqueous chemicals, and a solid fuel (Acharjee, 2010). The temperature is in the range of 200–260°C, and the pressures are up at least the water saturation pressure. It is considered as an environmentally benign, nontoxic and inexpensive reagent.

1.8.5 Oxidizing reagents pretreatment

Lignin is believed to be a major hindrance as it surrounds carbohydrates (cellulose and hemicellulose) making it highly recalcitrant especially for bioconversion. Therefore, delignification is an important step for successful liquid phase processing of carbohydrate feeds. Oxidative delignification has primarily been applied for pulping and bleaching. Its application in biomass pretreatment is relatively new. Oxidation increases the positive valance state of a molecule by removal of one or more electrons from an atom or ion. Oxidizing agents, including ozone, hydrogen peroxide, hypochlorite, chlorine dioxide, sodium chloride, and peracetic acid have been used for the chemical treatment of biomass (Chapman, 2003). A recent laboratory investigation by Siqueira et al. (2013) explored use of an aqueous solution of acetic acid and sodium chlorite for delignification of biomass and reported that more than 90% delignification was achieved for corn stover and other feedstocks. Yu et al. (2011) applied alkaline pretreatment followed by sodium chlorite or ozone delignification for softwood and hardwood. They observed both delignification methods improved enzymatic hydrolysis especially for softwood, while pretreatment alone was effective for hardwood (da Costa Correia et al., 2013; Yu et al., 2011).They reported 87% enzymatic hydrolysis yield after treating cashew apple bagasse with alkaline hydrogen peroxide. A recent laboratory investigation by Sannigrahi et al. (2012) explored the use of an aqueous solution of ethanol and chlorine dioxide mixture for ethanol production from sweet

gum. They achieved 87% ethanol yield with sweet gum treated using 60% ethanol solution with 1.1% chlorine dioxide, liquid/solid ratio 7, 75 °C, 3 hours.

In the process of chlorine dioxide based bleaching of pulp, most of the chlorine dioxide is reduced to chloride ion (Cl-). Rest of them is either reduced to organically linked chlorine or oxidized to chlorate (Kolar et al., 1983). Initially, chlorine dioxide reacts with phenolic and non-phenolic compounds through one-electron transfer reaction to form chlorite ion and a radical phenolic or non-phenolic intermediate. Then the radical intermediate is further oxidized by chlorine dioxide that results in the formation of variety of oxidation products and hypochlorous acid (HOCl). The hypochlorous acid and its equilibrium partner, chlorine, are the initiators of several side reactions along with chlorite. These side reactions eventually generate different type of free radicals which cause chlorate formation, chlorite oxidation and finally produce chloride ion and organic chlorine by chlorination (Svenson et al., 2006). As evidenced in literature, most of the pretreatment studies were done using sodium chlorite under acidic conditions.

1.9 Enzymatic hydrolysis

The main advantages of enzymatic degradation of lignocellulose into fermentable sugars are higher sugar yields, lower energy input and lower level of inhibitory products (Guan, 2016). Due to complex nature of heterogeneous system, enzymatic hydrolysis is known to be affected by both enzyme and substrate related factors. The factors that affect the enzymatic hydrolysis of lignocellulosic biomass include substrate characteristics such as chemical composition, porosity, pore size, degree of crystallinity and polymerization, accessible surface area, surface charge, etc. and enzyme-related factors including specific activity, nonspecific binding, end-products inhibition, reaction conditions (pH, temperature and speed), etc.

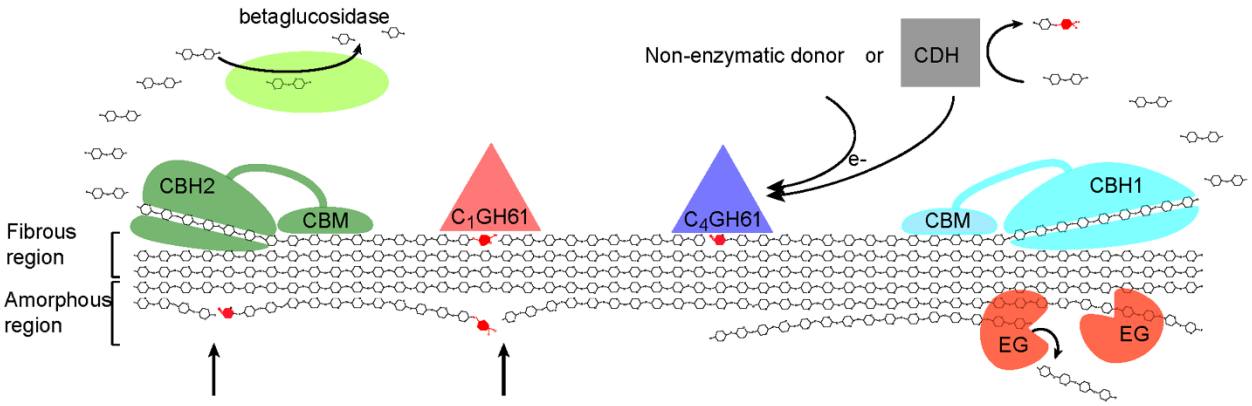

Figure 1-9 Current view on fungal enzymatic degradation of cellulose. Abbreviations: EG, endoglucanase; CBH, cellobiohydrolase; CDH, cellobiose-dehydrogenase; CBM, carbohydrate-binding module (Horn et al., 2012).

Cellulase enzyme *Trichoderma reesei* are composed of mainly endoglucanases (EG), exocellulases or cellobiohydrolases(CBH), and β-glucosidase(BG). These individual components act synergistically and break down the cellulose molecule into monosaccharides ("simple sugars"). The mechanism of enzymatic hydrolysis of cellulose by cellulase is depicted in Figure 1-9. Endoglucanases (EGs) act preferentially at amorphous cellulose regions, randomly cleave internal bond in the cellulose chain, thus producing new chains of polysaccharides with reducing and non-reducing end. CBH then attack the new polysaccharide chain cleaving off the oligosaccharides or cellobiose from the end of the chain. Two type of CBH involve in the process. CBH I begin the process from the reducing end while CBH II generate oligosaccharides from the non-reducing end. BG convert small oligosaccharides and cellobiose into monosaccharides. In addition, typical cellulases contain carbohydrate-binding modules (CBMs) that are beneficial for enzyme efficiency by adhering to and sometimes possibly disrupting the substrate (Horn et al., 2012; Yang et al., 2011). Several wild-type species of microorganisms produce this kind of enzyme cocktails. For an example, *T.reesei* cellulase generates five endo-glucanases (EG-1 to EG-5), two exo-glucanases

(CBH-1 and CBH-2), β-glucosidases and several hemicellulases. Out of these proteins, CBH-1, CBH-2 and EG-1 are three main proteins in *T.reesei* cellulase with the respective compositions of 60%, 20% and 12% (Gupta, 2008).

1.10 Fermentation

There are various modes of hydrolysis and fermentation as shown in Figure 1-10. Saccharification or hydrolysis of biomass is carried out using enzymes in the enzymatic hydrolysis reactor. Thus, cellulose degrades into glucose and hemicellulose is converted into either six-carbon sugar such as glucose, mannose and galactose or five-carbon sugar such as xylose and arabinose by the action of cellulase enzyme. Microorganism then take these monomeric sugars as their feed and produce different types of value added chemicals depending on microorganism specificity during fermentation. Traditionally, fermentation is performed as an independent unit process following the enzymatic hydrolysis; the process is called separate hydrolysis and fermentation (SHF) (Figure 1-10 a). In this mode, each step is performed at conditions optimized to give high products in each stage. However, the main disadvantage of this process is end-product inhibition. The high concentration of the main product of the hydrolysis (glucose) inhibit the activity of cellulase, thus reducing overall bioconversion yields. To reduce the end-products inhibition, two separate unit processes (enzymatic hydrolysis and fermentation of C-6 sugars) is carried out in a single reactor at compromised conditions (usually at 37 °C) which is known as simultaneous saccharification and fermentation (SSF) process. Since the sugar production by the enzyme and consumption by the microbe is occurred simultaneously, the end-products inhibition on enzymatic hydrolysis is reduced substantially. Thus, a significant improvement on overall bioconversion yield is observed during SSF (Gauss & Tagaki, 1976).

(a) Separate Hydrolysis and Fermentation:

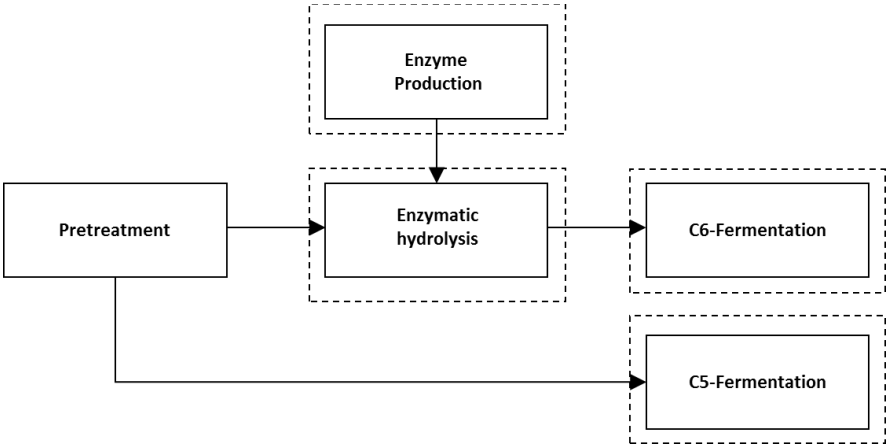

(b) Simultaneous Saccharification and Fermentation:

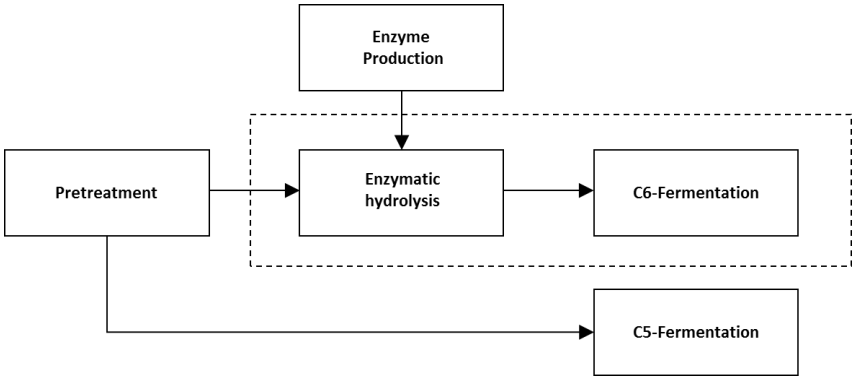

(c) **Simultaneous Saccharification and Co-Fermentation:**

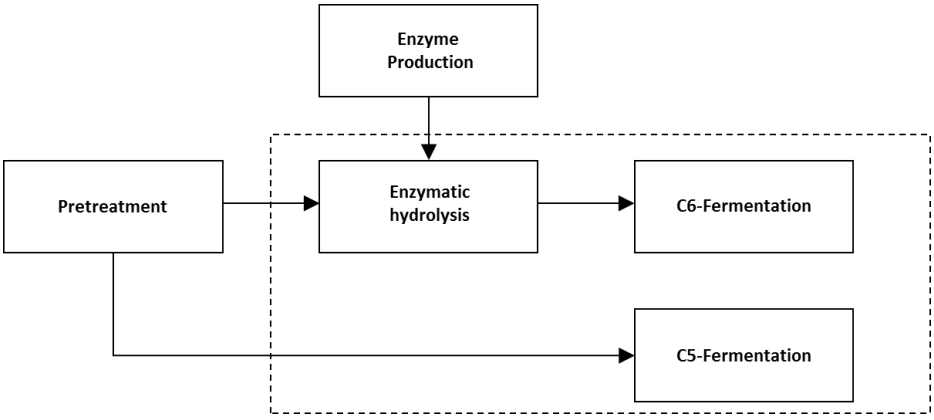

d) Consolidated Bioprocessing

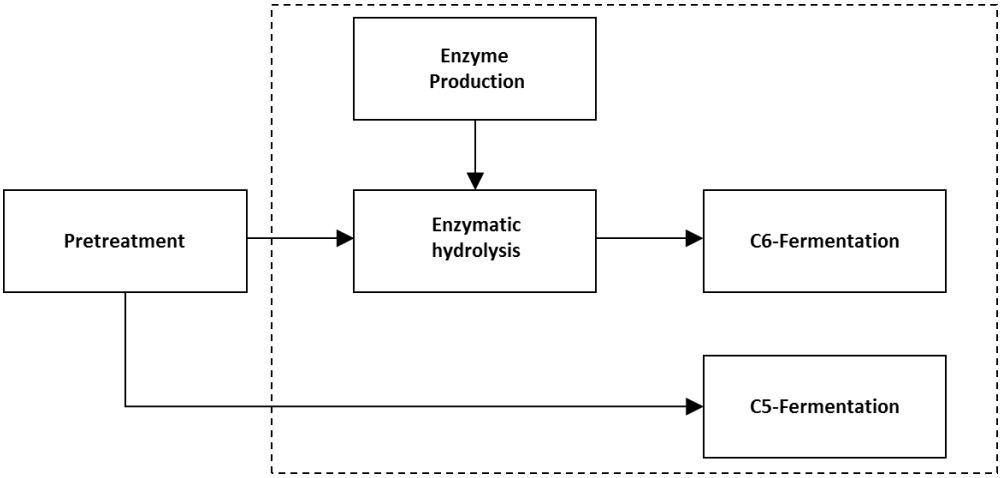

Figure 1-10 Various Modes of hydrolysis and fermentation (a) Separate Hydrolysis and Fermentation; (b) Simultaneous Saccharification and Fermentation; (c) Simultaneous Saccharification and Co-fermentation; and (d) Consolidated Bioprocessing

Depending on the microbe's capability of utilizing pentoses as carbon source, SSF can be further upgraded into simultaneous saccharification and co-fermentation (SSCF). SSCF is one-step ahead of SSF where xylose fermentation is also carried out in the same reactor with biomass hydrolysis and glucose fermentation. Consolidated Bioprocessing (CBP) is a concept where all the steps, enzyme production, enzymatic hydrolysis and fermentation, are carried out in one reactor with the use of single microorganism or group of microorganisms operating at the same conditions.

1.11 Research overview

The main objective of this study is to develop an efficient thermochemical strategy for the production of LA and a biochemical strategy for lactic acid by liquid-phase processing of biomass-derived carbohydrates.

Chapter 2 provides the details of the kinetic aspects of homogeneous acid catalyzed LA production from glucose in aqueous media. Chapter 3 describes the synthesis of LA from glucose using dual solid-acid catalysts. Chapter 4 demonstrates how cellulosic feedstock mixture can be converted into lactic acid efficiently. Chapter 5 establishes chlorine dioxide as a secondary pretreatment reagent in enhancement of enzymatic hydrolysis. Finally, Chapter 6 summaries the main conclusions drawn from this study and the direction of future research based on the current study.

Chapter 2

Sulfuric acid catalyzed conversion of glucose to levulinic acid in aqueous media: kinetics and reaction engineering to maximize yields.

2.1 Abstract

Levulinic acid (LA) is considered as a highly versatile chemical having the potential to be building-block for the synthesis of various chemicals from biomass. In this study, we have developed a kinetic model of homogeneous acid (H_2SO_4) catalyzed hydrolysis of glucose to LA in aqueous media. The model shows good agreement with experimental data using a batch reactor over the following range of conditions: 150-200 °C, sulfuric acid concentrations of 1-5 (wt. %) and initial glucose concentrations of 5-15 (wt. %). Reaction temperature and acid concentration were found to be the main factors affecting LA yield. The effect of these parameters were further investigated in detail, from which kinetics models and associated kinetics constant were determined. The model suggests that high temperature and shorter reaction times favor the yield of hydroxymethylfurfural (HMF), an intermediate in the process. It also predicts low temperature and longer reaction times favor LA yield from HMF. We also developed an optimum temperature profile for the LA production from glucose.

2.2 Introduction

The production of biomass derived fuels and chemicals have been the central focus of last couple of years to meet energy requirement and to make basic chemicals (Yan et al., 2009; Yu et al., 2008a). As mentioned before, a list of top twelve chemicals was obtained by evaluating the potential markets of the building blocks and their derivatives and the complexity of the synthetic pathways (Girisuta et al., 2007b; Werpy and Petersen, 2004). Levulinic acid (LA) is one of the top-twelve building blocks which can be produced from lignocellulosic biomass using an acid catalyst (Girisuta et al., 2007b). LA (gamma-ketovaleric acid), is a short-chain fatty acid, provide potentially important platforms for production of liquid fuels and chemicals(Shen & Wyman, 2012) . The unique feature of LA is its ketone and a carboxylic acid groups. These two functional groups make it a potentially very versatile building block for the synthesis of various organic chemicals (Girisuta et al., 2007b)

The most common method to produce LA is the acid catalyzed hydrolysis of hexose sugars or carbohydrates. Traditionally, homogeneous catalysts such as HCl and H_2SO_4 have been used to synthesis LA from glucose (Girisuta et al., 2006b), cellulose, (Girisuta et al., 2007b), normal corn starch (Cha & Hanna, 2002), water hyacinth plant (Girisuta et al., 2008), sugarcane bagasse (Girisuta et al., 2013) and Pine (Rivas et al., 2013). Developed by Biofine incorporation, one of the commercial process claims to achieve LA yields of 70-80% of the theoretical maximum from cellulosic feed stock in its two reactor system by the conversion of approximately 50% hexose sugars to LA, with 20% being converted to formic acid and 30% to tars (Fitzpatrick, 1997; Hayes et al., 2006) using wood as a raw material and H_2SO_4 as an acid catalyst.

Numerous kinetic studies on the decomposition of sugars/carbohydrate to produce LA and formic acid have been reported (Girisuta et al., 2006b). Nevertheless, a few kinetics studies incorporated

undesired byproduct formation steps to enhance accuracy of their models(Girisuta et al., 2006b; Weingarten et al., 2012; Shen & Wyman, 2012). A direct comparison of the kinetics parameters reported by researchers is rather meaningless as these parameters vary substantially depending on reaction conditions, substrates, and acid catalyst. However, it is noteworthy that there should be a consensus agreement to maximize the selectivity and yield of HMF and LA among the studies. However, a wide discrepancy in the optimum parameters selection to maximize yield and selectivity are observed among these studies. For example, some authors suggest that low temperature and long residence time are essential to maximize the HMF yield (Chang et al., 2006; Girisuta et al., 2006a).Others claim that high temperature and short residence time are essential to maximize the HMF yield (Weingarten et al., 2012). In the same study, Weingarten et al. (2012) found glucose to HMF demonstrate a near first order dependence to the acid concentration whereas glucose to humins exhibit a near third order dependence. This indicates that higher acid concentrations will have a negative effect on the selectivity of glucose to HMF formation. On the contrary, some authors claim that higher acid concentrations will have a positive effect on the selectivity of glucose to HMF formation (Chang et al., 2006). A different conclusion was deduced by Girisuta et al. (2006a) as they found the selectivity of this reaction is independent on the acid concentration. Similarly, some others viewed low temperature and long residence time is favorable for the production of LA yield from HMF whereas the selectivity of the reaction is independent on the acid concentration (Weingarten et al., 2012 ; Shen & Wyman, 2012). Conversely, Girisuta et al., (2006b) suggest, reaction should be carried out at high temperatures to achieve higher rate since the selectivity of the reaction is independent on the temperature and at high acid concentrations as higher acid concentrations will have a positive effect on the selectivity of the reaction. These discrepancy to urge a detailed understanding of acid catalyzed reactions involved

in the production of LA which will provide a new insight into interplays among the various reaction steps that can help for the successful design of an optimal hydrolysis process (Girisuta et al., 2006b; Weingarten et al., 2012; Shen & Wyman, 2012). The objective of this study is to develop a kinetic model for the acid catalyzed glucose decomposition to LA by fitting kinetic data collected in a batch reactor system and optimize the process using obtained kinetic parameters.

Here we report, the kinetics of acid catalyzed glucose decomposition to LA by fitting kinetic data collected in a batch reactor system. A series of experiments were carried out at 150, 175 and 200 °C using sulfuric acid concentrations of 1, 3 and 5 (wt. %) with initial glucose concentrations of 5,10 and 15 (wt. %). The concentrations of glucose, HMF and LA were determined at different reaction times to develop the kinetic model. We also develop optimum temperature profile for the aqueous phase production of LA from glucose by homogeneous acid catalyst.

2.3 Materials and Methods

2.3.1 Chemicals and reagents

Hydroxemethylfurfural (HMF) was obtained from Fisher Scientific Inc. (Cincinnati, Ohio). Glucose, sulfuric acid, formic acid and LA were purchased from VWR (Radnor, PA). All chemicals used in this study were of analytical grade and used without purification.

2.3.2 Experimental procedure

The reactions were carried out in tubular acid resistant alloy-400 Monel reactors, which are composed of 63% nickel and 28-34% copper with outer diameter (OD) 0.375 inch, inside diameter (ID) 0.305 inch and length 4 inch. Approximately 3 ml of reaction mixture was poured into every reactor and then the sealed reactors were placed in a constant-temperature oven that was initially set to 250 °C to reduce the heating time. The temperature was monitored with a J- type

thermocouple probe. To track the temperature profile, a reactor (filled with water) was connected with a thermocouple, which is attached to a computer to record the real-time data. This reactor with all others reactors (containing reaction mixture) were simultaneously placed in the oven. The inside temperature of the reactors containing reactor mixture is assumed to be same as the reactor containing water equipped with thermocouple. When the internal reactor temperature approached to near of target temperature, oven temperature was then reset to desired values and it took 4-7 minutes to reach aimed value depending on required temperature. At the point, when the temperature reached within 5 °C of the target value of desired temperature, time counting was started i.e. this time being defined as time zero (t=0). At different reaction time, the reactor were removed from the oven and submerged in ice water to cool it to room temperature as soon as possible to stop the reaction. After the reactor reached room temperature, the reaction mixture was taken out of the reactor and centrifuged. Then the particle-free solution was analyzed using high-pressure liquid chromatography (HPLC).

2.3.3 Analytical method

The concentrations of liquid samples were determined using an HPLC system consisting of a AcuFlow Series III pump (LabX, Midland, ON, Canada), Alcott 708 autosampler (LabX, Midland, ON, Canada), a Bio-Rad HPX-87H column (Hercules, CA) , a refractive index detector (Shodex, NY) and PeakSimple Chromatography Data Systems(Torrance, CA). The aqueous solution of 0.005 M sulfuric acid was selected as mobile phase and the flow rate was set to 0.55 ml/min. The column was operated at 85 °C. The analysis for a sample was completed within 40 minutes.

2.4 Kinetic Modeling

The kinetic modeling of glucose decomposition to LA was done according to following assumptions.

1. The model consists of four key steps: (1) glucose dehydration to form HMF; (2) glucose degradation reactions to form humins; (3) HMF rehydration to form LA and FA, and (4) HMF degradation to produce humins.

2. All the reaction rate equations were quantified using a pseudo first order approach.

Based on the above-mentioned assumptions, the analysis of our kinetic data was carried out using the reaction network of glucose dehydration in acidic medium as shown in Scheme 2-1. The overall rate equations for glucose conversion to LA are shown in following equations.

$$\frac{d[G]}{dt} = -K_1\,[G] - K_2\,[G] \quad \ldots\ldots 1$$

$$\frac{d[HMF]}{dt} = K_1\,[H] - K_3\,[HMF] - K_4\,[HMF] \quad \ldots\ldots 2$$

$$\frac{d[LA]}{dt} = K_3\,[HMF] \quad \ldots\ldots 3$$

$$K_i = K'_i C_H = A_i\, C_{H+}^{n} e^{-(\frac{Ei}{RT})} \qquad (i = 1-4) \quad \ldots\ldots 4$$

in which G, HMF, LA and C_{H+}, n represent glucose, HMF, LA, proton concentrations (mol/dm^3) and reaction order with respect to acid concentration respectively. The rate constants K_1, K_2, K_3, and K_4 take into account proton concentration for reactions 1–4(min^{-1}) whereas the rate constants K'_i (dm^3/(mol. min)) do not incorporate the proton concentration. The A_i (dm^3/(mol. min)) and E_i (J/mol) are pre-exponential factors and activation energies for reactions 1–4, respectively, R is the universal gas constant (J/(mol. K)), and T is the reaction temperature (K).

Scheme 2-1 Acid catalyzed glucose conversion to LA via HMF

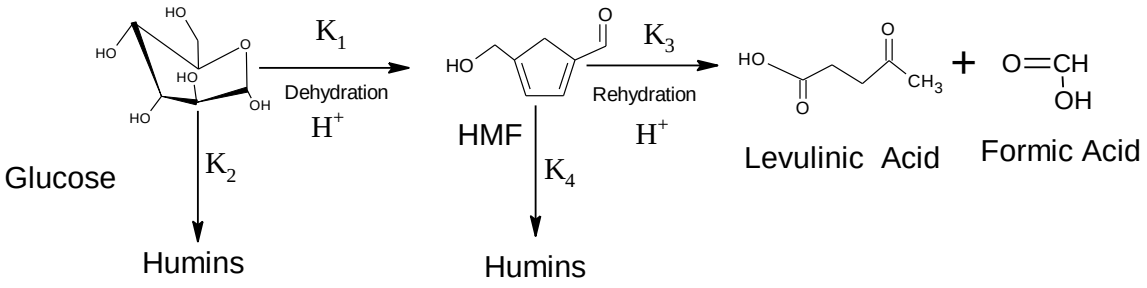

2.4.1 Calculations procedure

The glucose decomposition is hydrogen ion catalyzed reactions and the reaction rates depend on the catalyst amount (Lamminpaa et al., 2012). Conventionally, the amount of homogeneous acid catalyst is incorporated into the kinetic models as hydrogen ion concentration (Lamminpaa et al., 2012; Saeman, 1945), weight percentage (Liu et al., 2012), or activity (Marcotullio et al., 2009). In weight percentage approach, the hydrogen ion concentration remains constant irrespective of the temperature changed. On the other hand, activity-based models are useful to evaluate solution properties although the selection of the appropriate excess Gibbs energy model determines the accuracy of this approach. In this study, the hydrogen ion concentration of sulfuric acid was used in kinetic modeling according to Girisuta's approach (Girisuta et al., 2006a) . The H^+ concentrations in reaction temperature were calculated using the following equation.

$$C_{H+} = C_{H2SO4} + \frac{1}{2}\left(-K_{a,HSO4} + \sqrt{\left(K_{a,HSO4}^2 + 4C_{H2SO4}K_{a,HSO4}\right)}\right) \quad \ldots\ldots 5$$

where C_{H2SO4}, $K_{a,HSO4}$ represents concentration of H_2SO_4 and the dissociation constant of HSO_4, respectively, which ranges between $10^{-4.5}$-$10^{-3.6}$ in the temperature window 140–200 °C (Dickson et al., 1990).

The system of differential equations (1)–(4) can be solved by using experimental measurements of the concentrations of glucose, HMF and LA at various reaction times, temperatures, and acid concentrations. We used the least-squares sum of the residuals between experimental measurements and predicted values of the concentrations to estimate the kinetic parameters. For this analysis, the Levenberg-Marquardt algorithm built in Mathcad 15 (Korobov and Ochkov, 2011) was used to minimize the objective function φ given by:

$$\varphi = \sum_i \sum_j (X_{i,predict} - X_{i,exp})^2 \quad \ldots\ldots 6$$

The regression analysis was repeated several times with different initial values of the parameter set to confirm the validity of the regression parameters.

The average molecular weights of glucose and LA are 180.16 and 116.11 respectively. LA concentrations (g/l) measured from HPLC were converted to LA yields as a percent of the theoretical maximum as follows.

$$LA\ Yield\ (\%) = \frac{LA\ concentration\left(\frac{g}{l}\right) * \text{glucose MW}}{\text{Initial glucose concentration}\left(\frac{\text{g}}{\text{l}}\right) * \text{ LA MW}} \quad \ldots\ldots 7$$

$$Conversion\ (\%) = 100 * \frac{\left(Initial\ \ concentration\left(\frac{g}{l}\right) - Final\ concentration\left(\frac{g}{l}\right)\right) * \text{glucose MW}}{\text{Initial glucose concentration}\left(\frac{\text{g}}{\text{l}}\right) * \text{ glucose MW}} \quad \ldots 8$$

Instantaneous yield of LA

$$\frac{d[LA]}{d[G]} = -\frac{K_3\,[HMF]}{K_1\,[G] + K_2\,[G]} \quad \ldots\ldots 9$$

Instantaneous yield of humin

$$\frac{d[Humin]}{d[G]} = -\frac{K_2\,[H] + K_4\,[HMF]}{K_1\,[G] + K_2\,[G]} \quad \ldots\ldots 10$$

2.4.2 Optimum temperature profile

With the kinetic model and associated parameters at hand, attempts were made to determine the optimum temperature profile in batch reactor. The optimum temperature profile was determined in consideration of either maximum instantaneous yield of desired product or minimum instantaneous yield of undesired product during the course of the reaction. Having all the parameters with concentration of reactants and products, one can calculate instantaneous yield of LA (desired) or humin (undesired) as a function of temperature at a given time using equation 9 and 10 respectively. It is also possible to determine the optimum temperature at this particular time by maximizing instantaneous yield of LA or minimizing instantaneous yield of humins formation. Suppose, x, y and z are the concentrations of glucose, HMF and LA at a given time t. The optimum temperature, $T_{opt,}$ was calculated by maximizing instantaneous yield of LA at that point (t) using equation 9. The "maximization" function in Mathcad was incorporated with equation 9 to determine the optimum temperature at every instant. This procedure was applied until glucose conversion is reached 99%. However, at the very beginning of the reaction (at t=0), the theoretical optimum temperature is infinity. For practical operation, an upper limit of the temperature must be chosen. For example, if the upper temperature was chosen as 180° C, then the reaction is carried out at 180°C isothermally until it meets the predetermined optimum temperature profile curve.

2.5 Results and Discussion:

2.5.1 Effect of process variable on the HMF decomposition to LA in acid medium

Acid catalyzed HMF decomposition reaction were carried out in tubular batch reactor at three different temperature 140, 155, and 170 ˚C using 1-5% sulfuric acid with an initial concentration of 4 wt.% HMF. The effect of temperature on HMF conversion and LA production is illustrated in Figure 2-1 &2-2 for the acid concentration of 1 % H_2SO_4.

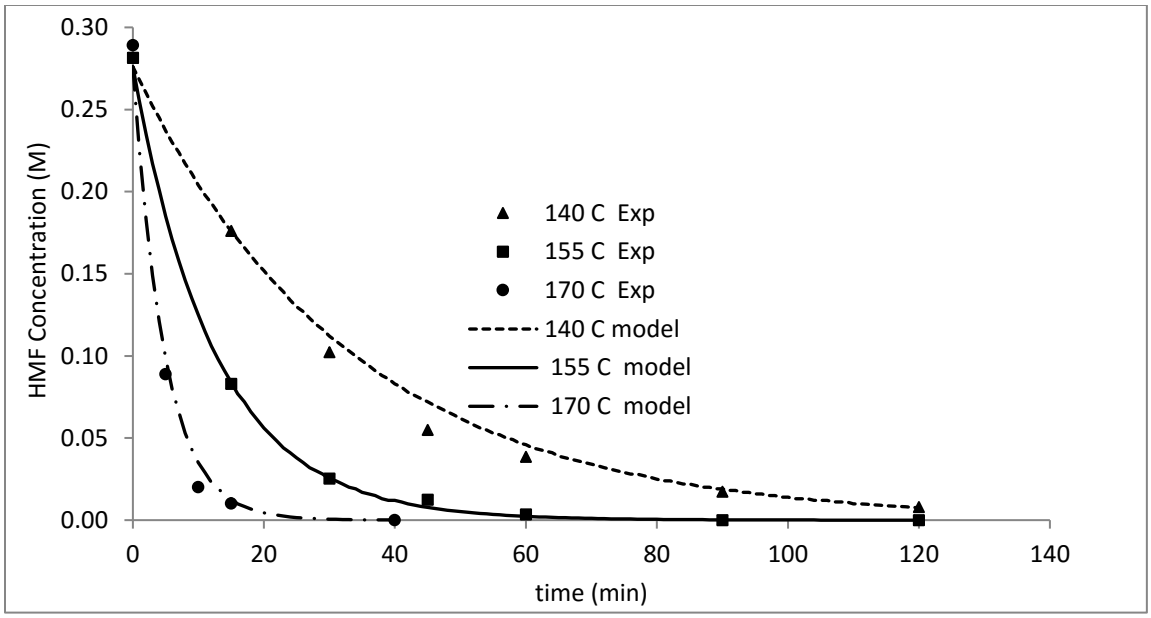

Figure 2-1 Effect of temperature on HMF conversion to LA. Experimental data (symbols) and kinetic model data (lines). Conditions: 1 (wt. %) H_2SO_4, 4 (wt. %) HMF

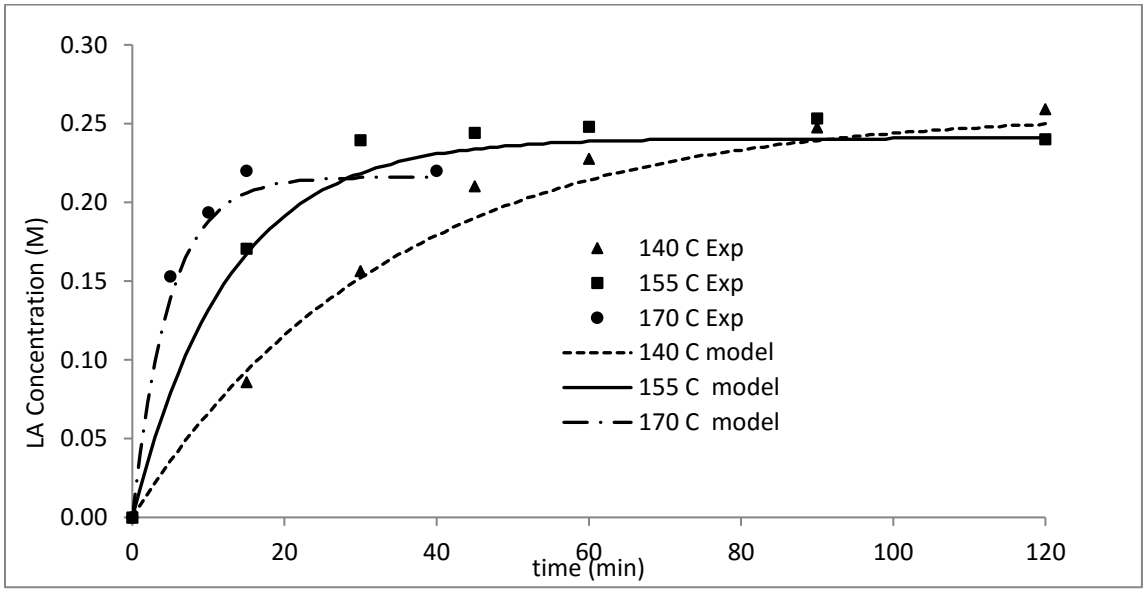

Figure 2-2 Effect of temperature on LA production from HMF. Experimental data (symbols) and kinetic model data (lines). Conditions: 1 (wt. %) H_2SO4 and 4 (wt.%) HMF.

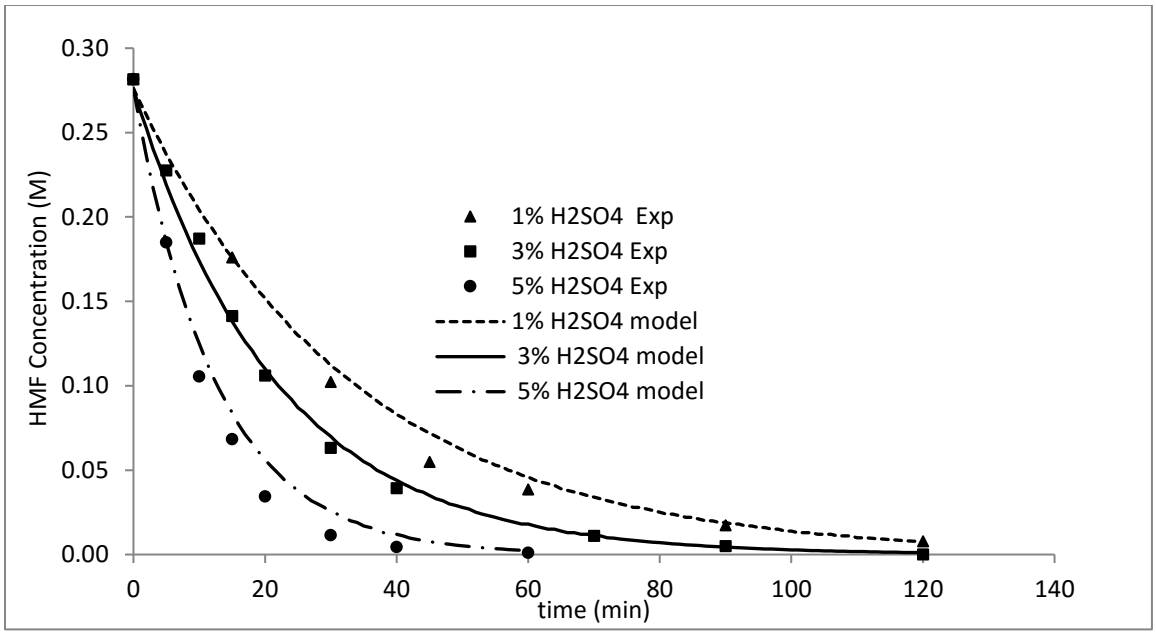

Figure 2-3 Effect of acid concentration on HMF conversion to LA. Experimental data (symbols) and kinetic model data (lines). Conditions: 140 ˚C, 4 (wt. %) HMF

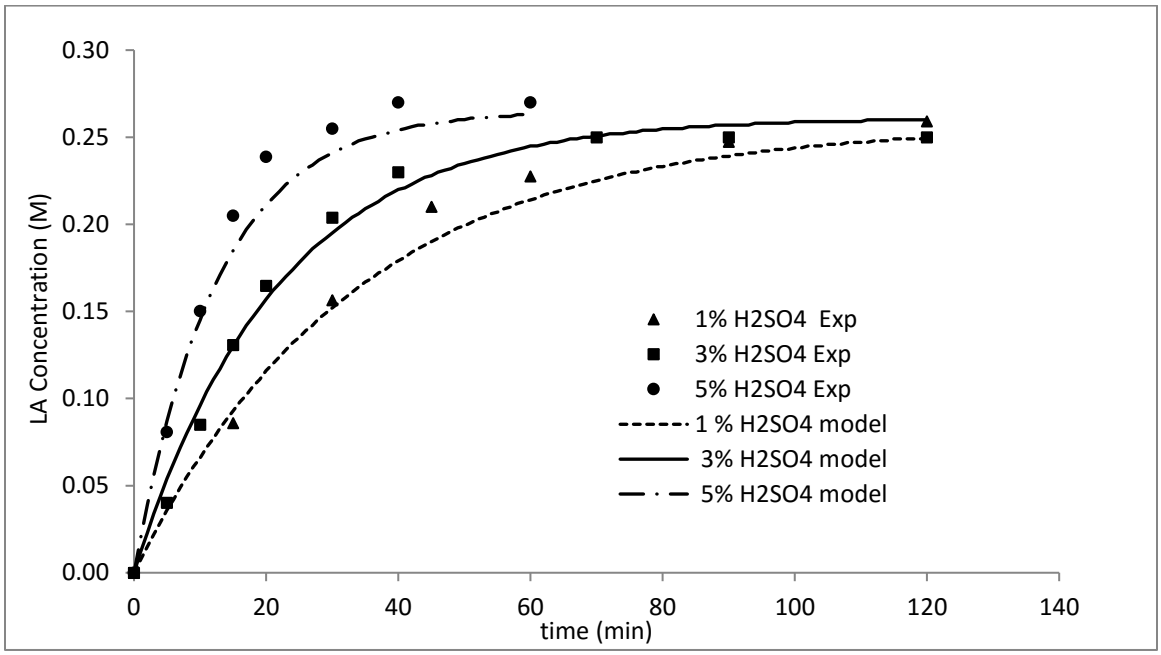

Figure 2-4 Effect of acid concentration on LA production from HMF. Experimental data (symbols) and kinetic model data (lines). Conditions: 140 ˚C, 4 (wt. %) HMF

With the increase of reaction temperature, LA yield is decreased whereas the rate of HMF decomposition increased sharply as expected. In addition, the effect of sulfuric acid concentrations on HMF conversion and LA production is illustrated in Figure 2-3 &2-4 for the experiments which were carried out at 140 ˚C with acid concentrations ranging between 1-5 %. As observed, acid concentration has positive impact on reaction rate i.e. higher acid concentration give high HMF conversion as well as higher LA production.

2.5.2 Kinetic model for HMF decomposition to LA:

Based on the mechanism proposed by Horvat et al. (1985), the acid-catalyzed conversion of HMF produces levulinic and formic acids in equal amounts. Highly polymerized insoluble dark-colored solids, known as humins, are also formed in a parallel reaction presented in 2nd part of Scheme 2-1. However, some kinetics studies proposed an additional pathway to form humins from LA. For simplicity, we assumed all humins were produced from HMF because there is a very little chance of humins formation from LA in our experimental conditions (Girisuta et al., 2006a; Weingarten et al., 2010).

2.5.2.1 Modeling results

All experimental data, nine batch experiments (three temperatures, 140, 155 and 170 ˚C, and three acid concentrations 1, 3 and 5 %), for HMF decomposition to LA were fitted to the proposed kinetic model (2nd part of scheme 2-1) to estimate the rate constants. Then rate constants data from all nine batch experiments were used in a non-linear regression algorithm to determine the values of activation energies, acid exponents and the pre-exponential factors that were presented in Table 2-1. The relatively lower activation energies of the main reaction (E_{3HMF}= 86 kJ mol$^{-1)}$ compare to the side reaction (E_{4HMF}= 139 kJ mol^{-1}) indicates that low temperatures will favor the formation of LA from HMF. In this model, HMF conversion to LA exhibit less than a 1st

order dependence to the acid concentration. (α= 0.74). The slightly higher value of acid concentration order (n) in LA production indicate higher acid concentration has positive effect of LA production from HMF.

Table 2-1 Estimated kinetic parameter for acid catalyzed HMF decomposition to LA

Rate Constant	Log A (dm^3.mol.min)	E (KJ/mol)	order(n)
k_3	9.95	85.55	0.74
k_4	15.66	139.30	0.73

2.5.3 Kinetic model for glucose conversion to LA

A series of kinetics experiments were carried out in a batch reactor over the following range of conditions: at three different temperatures 150, 175 and 200 °C; sulfuric acid concentrations of 1-5 (wt. %) and initial glucose concentrations of 5-15 (wt. %).

2.5.3.1 Modeling results

Reactions 3 and 4 (HMF rehydration and decomposition, respectively) were assumed independent of reactions 1and 2 (glucose dehydration and glucose decomposition, respectively). Therefore, the same rate parameters obtained for HMF rehydration (Table 2-1) were combined with those derived for glucose dehydration to fit the experimental data to our proposed model for LA production. The experimental data for glucose dehydration, HMF, and LA production are shown in Figure 2-5 along with the fitted kinetic model. The rate parameters obtained for glucose dehydration appear in Table 2-4. Since we did not consider initial glucose concentration as a function of LA yield for simplicity, therefore, when we modelled the systems we used the average of corresponding rate constant of all three different set of experiment (5 %, 10 % and 15 % glucose) obtained independently.

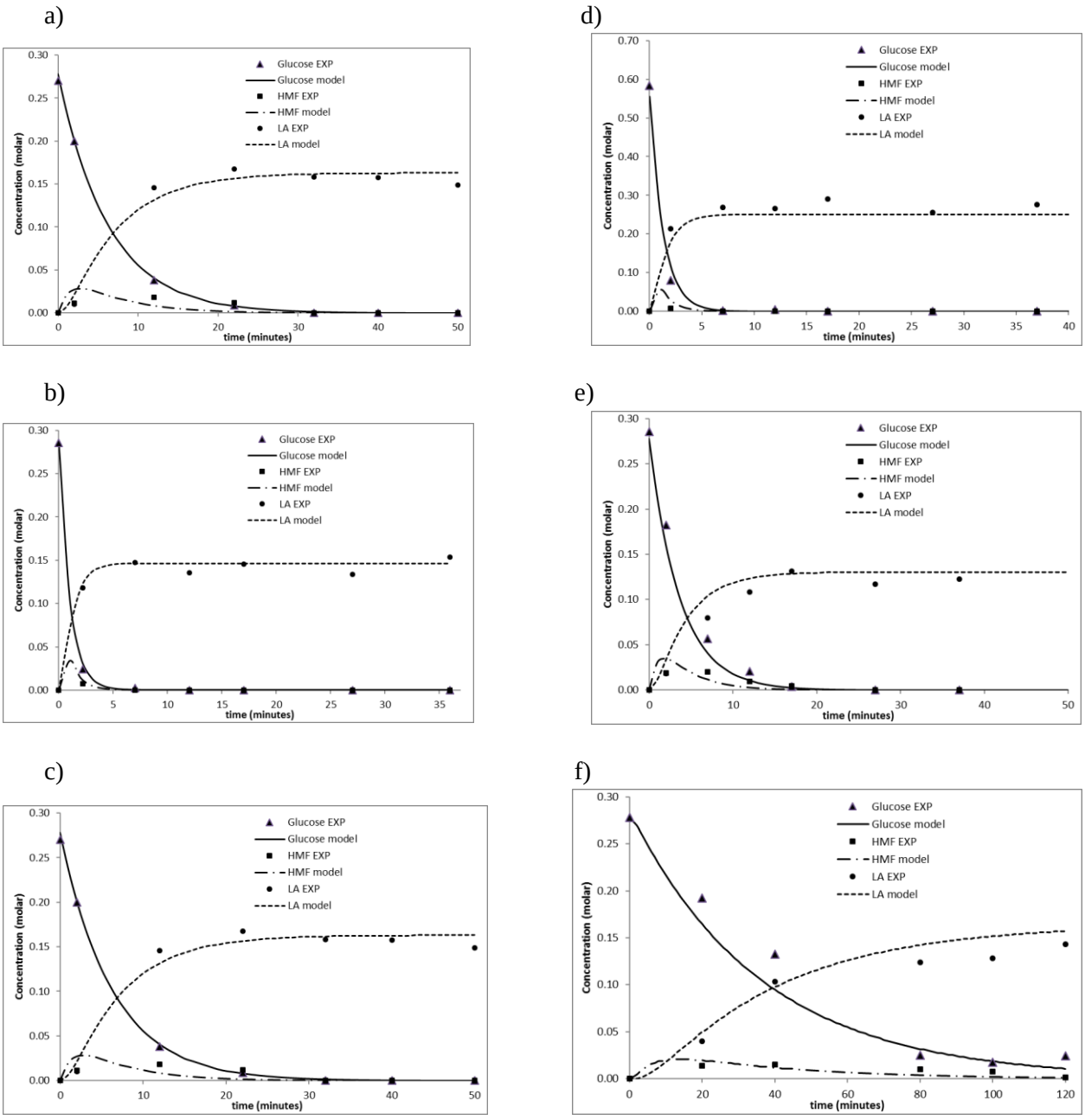

Figure 2-5 Data fitting for LA production at different initial concentration of glucose. Experimental data (symbols) and kinetic model data (lines) for different experimental concentration. Conditions a) 175˚C, 5% glucose, 5 (wt. %) H_2SO_4. b) 200˚C, 5% glucose, 5 (wt. %) H_2SO_4. c) 175˚C, 5 (wt. %) H_2SO_4 with 5 % initial glucose. d) 175˚C, 10 % glucose, 5 (wt. %) H_2SO_4. e) 200˚C, 5% glucose, 1 (wt. %) H_2SO_4.) e) 200˚C, 5% glucose, 1 (wt. %) H_2SO_4. f) 150˚C, 5% glucose, 5 (wt. %) H_2SO_4.

2.5.3.1.1 Model predictions for HMF and LA yield in batch reactor

2..5.3.1.1.1 Effect of initial hexose concentration

To study the effect of initial hexose concentration on HMF and LA yield, a three different set of experiments (total 3× 9=27) were carried out with sulfuric acid concentrations of 1, 3 and 5 (wt. %) and initial glucose concentrations of 5, 10 and 15 (wt. %) at temperatures 150, 175 and 200 °C. The effect of initial glucose concentration on glucose conversion and on the production of HMF and LA are summarized in Figure 2-6, 2-7 &2-8 respectively. The conversion of glucose seems to be independent of the initial concentration as shown in Figure 2-6. Therefore, when we modelled the system, we considered that rate constants are dependent on the first order of glucose concentration. That mean HMF and LA yields are not a function of initial glucose concentration as shown in Figure 2-7 and 2-8. However, in our experiments we have seen, in some cases, maximum LA yield is decreased with the increase of glucose.

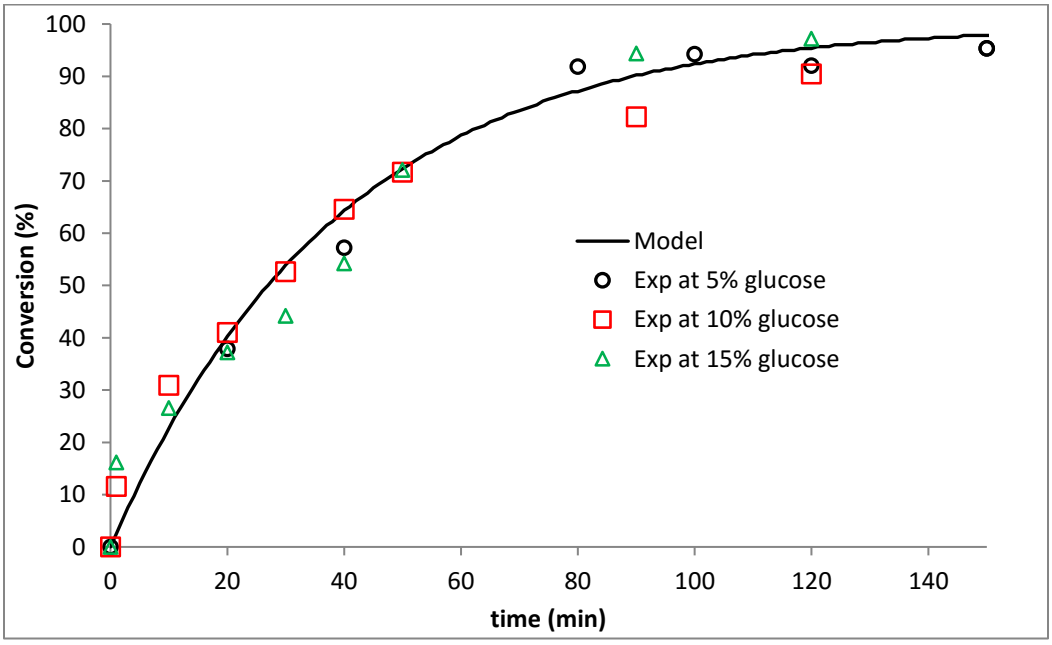

Figure 2-6 Effect of initial concentration on glucose conversion. Experimental data (symbols) and kinetic model data (lines) .Conditions: 150 ˚C and 5 (wt.%) H_2SO_4.

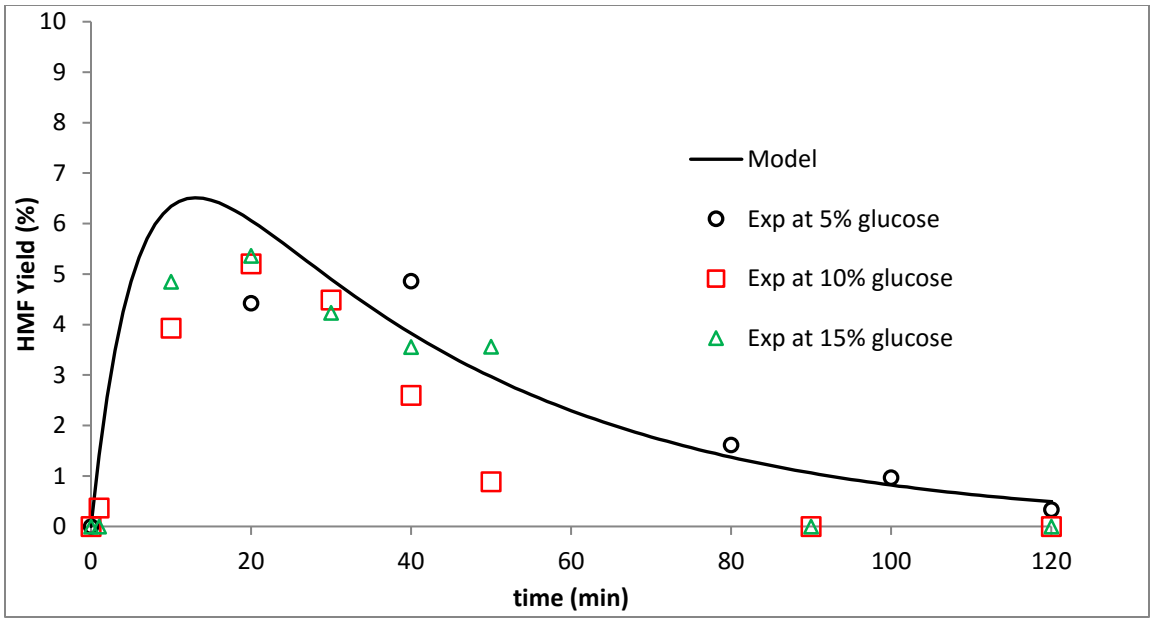

Figure 2-7 Effect of initial glucose concentration on HMF yield. Experimental data (symbols) and kinetic model data (lines). Conditions: 150 ˚C and 5 (wt. %) H_2SO_4.

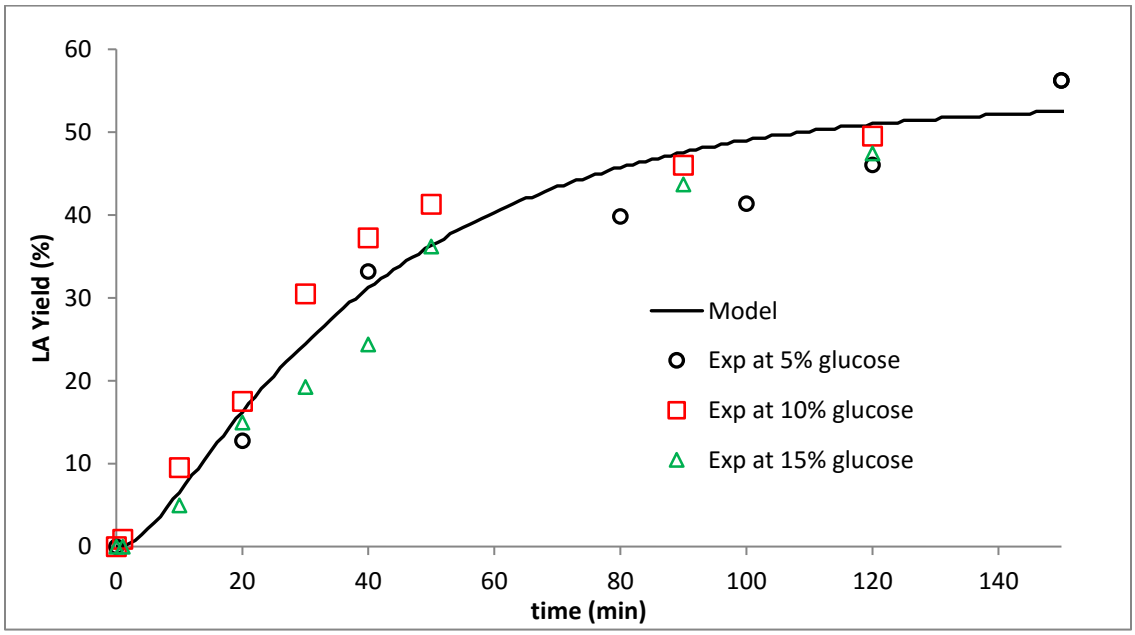

Figure 2-8 Effect of initial glucose concentration on LA yield. Experimental data (symbols) and kinetic model data (lines). Conditions: 150 ˚C and 5 (wt. %) H_2SO_4.

We also compared rate constants to see the effect of rate constant on glucose concentration as shown in Table 2-3 corresponds of Figures 2-6, 2-7 & 2-8. As rate constants k_i did not change monotonically with increasing initial glucose concentration, maximum LA yield may be independent of the initial hexose concentration as shown in Table 2-2.

Table 2-2 Estimated first order rate constant at three initial glucose concentration. Condition: 150 ˚C and 5 % H_2SO_4.

Glucose initial Concentration (%)	Glucose	
	K_1 (dm^3/mol.min)	K_2 (dm^3/mol.min)
5	0.018	0.009
10	0.014	0.01
15	0.014	0.011
Average	0.015	0.01

2..5.3.1.1.2 Effect of Temperature on HMF and LA yield

The effect of temperature on glucose conversion and HMF &LA yields are summarized in Figures 2-9, 2-10, & 2-11 at the following conditions: an acid concentration of 5 % and glucose concentration of 15 % for temperatures of 150, 175, and 200°C. As expected, the rate of reaction is increased with the temperature i.e. glucose concentration decline rapidly, as shown in Figure 2-9. The maximum achievable HMF yield is a function of the temperature, with the highest temperature leading to the highest HMF yield as shown in Figure 2-10. For example, the maximum HMF yield is increased from 7% to 12% as temperature is increased from 150 to 200 °C. On the other hand, maximum LA yield was decreased with increased temperature shown in Figure 2-11 in accordance with other studies for glucose (Shen and Wyman, 2012; Weingarten et al., 2012; Girisuta et al., 2006a). As expected, with the increase of temperature, there is a decrease of time to reach maximum LA concentration. For example, the time to achieve highest LA Yield is more than 100 min at 150 °C whereas it is 5 min for 200 °C (figure 2-11).

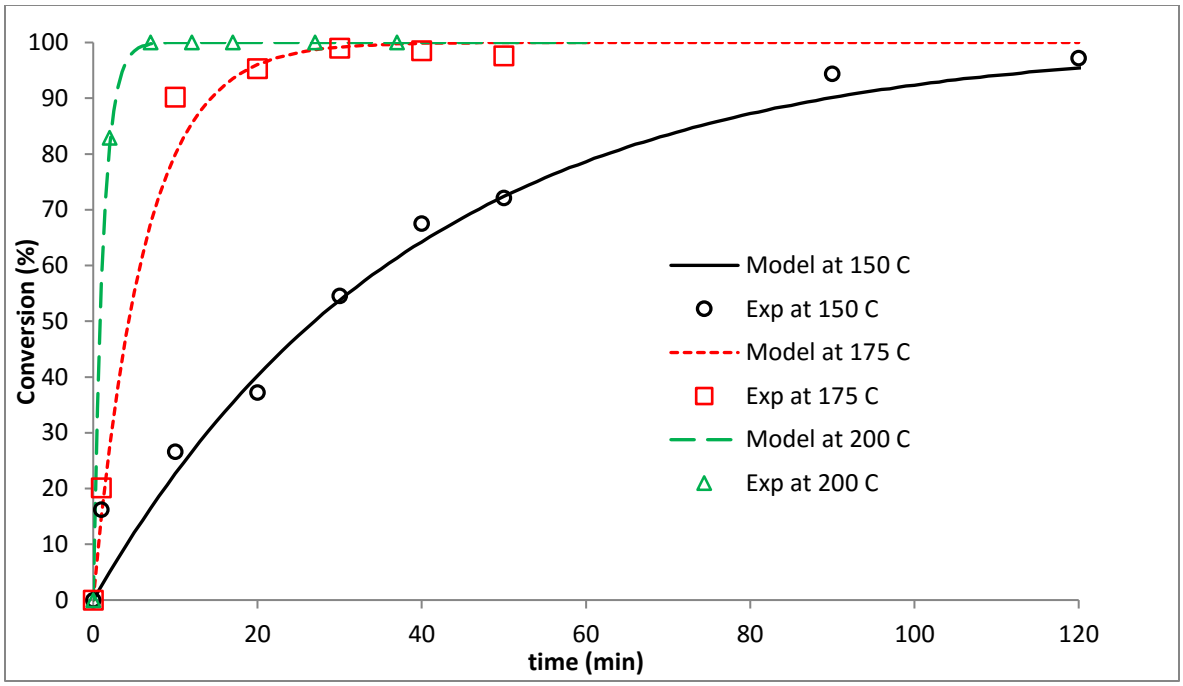

Figure 2-9 Effect of temperature on glucose conversion. Experimental data (symbols) and kinetic model data (lines). Conditions: 5 (wt. %) H_2SO_4 and 15 (wt. %) glucose.

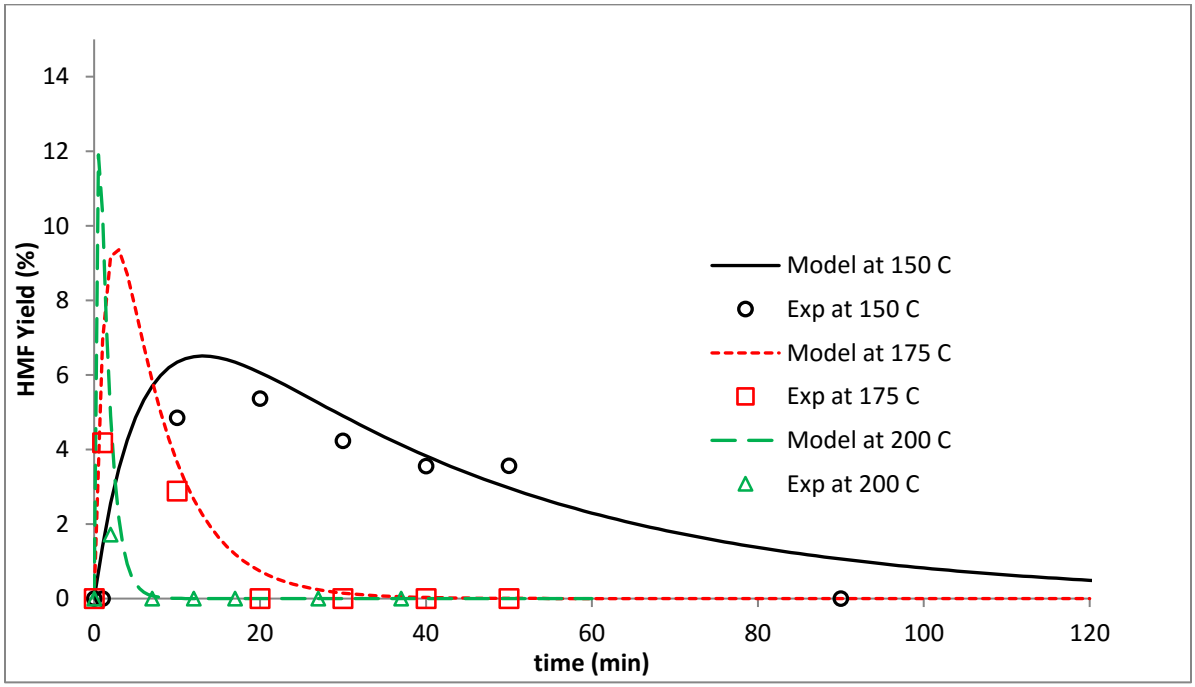

Figure 2-10 Effect of temperature on HMF production. Experimental data (symbols) and kinetic model data (lines). Conditions: 5 (wt. %) H_2SO_4 and 15 (wt. %) glucose.

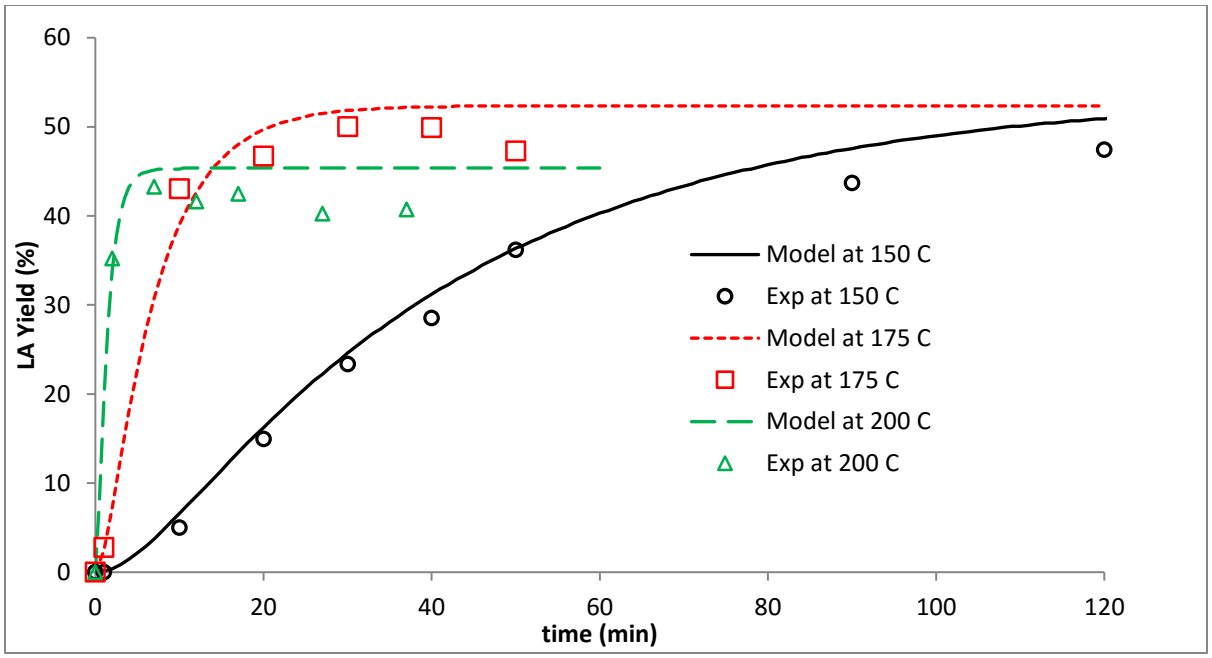

Figure 2-11 Effect of temperature on LA production. Experimental data (symbols) and kinetic model data (lines). Conditions: 5 (wt. %) H_2SO_4 and 15 (wt. %) glucose.

The effects of temperature on rate constant of glucose conversion to LA are summarized in Figure 2-8 and table 2-2 based on Figures 2-9, 2-10 &2-11. The rate constants k_i increase with increasing temperature in the following orders $k_1>k_2$ indicate HMF formation from glucose increase with the increase of temperature. On contrary, the rate constants k_i increase with increasing temperature in the following orders $k_4>k_3$ indicate humins formation from HMF increase with the increase of temperature. The ratio of k_{200}/k_{150} for side reaction (HMF to humins) is higher than other reactions implying humins formation from HMF is most sensitive to temperature as shown in Table 2-2. It should be noted here, rate constant follows Arrhenius law in every case, which is shown in Figure 2-12.

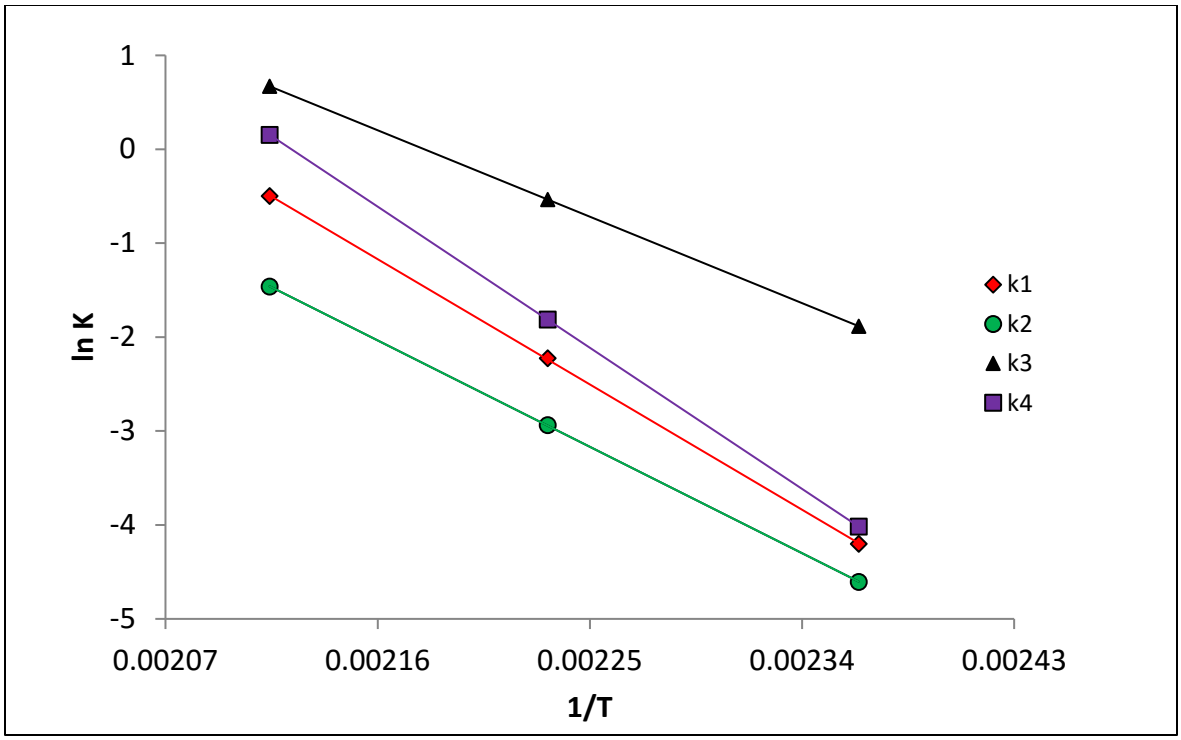

Figure 2-12 Effect of Temperature on rate constant. Experimental data (symbols) and kinetic model data (lines). Conditions: 150-200 ˚C and 5 (wt.%) H_2SO_4 and 15 % glucose

Table 2-3 Estimated first order rate constant at three temperatures. Conditions: 15 % glucose and 5 % H_2SO_4.

	Glucose to HMF		HMF to LA	
Temperature (°C)	k_1(dm^3/mol.min)	k_2(dm^3/mol.min)	k_3(dm^3/mol.min)	k_4(dm^3/mol.min)
150	0.015	0.01	0.152	0.018
175	0.108	0.053	0.588	0.162
200	0.608	0.232	1.974	1.168
Ratio K_{200}/K_{150}	40.53	23.20	12.99	64.89

2..5.3.1.1.3 Effect of sulfuric acid concentration on HMF and LA yield

The effect of H_2SO4 acid concentration on glucose conversion as well as on HMF and LA yield are depicted in Figure 2-13, 2-14 & 2-15 at 200°C for an acid concentration of 1, 3 and 5 % and glucose concentration of 15 %. The maximum HMF yield is increased slightly with the increase of acid concentration in this experimental range. Similarly, maximum LA yield is increased with

the increase of acid concentration. The maximum LA yields were 42, 45 and 46 % for glucose at acid concentration of 1, 3 and 5 % H_2SO_4 at 200°C. The time required to reach the maximum LA yield is reduced with increasing acid concentration. For example, the time to achieve highest LA yield is more than 400 min for 1% acid concentration while 5 % acid take less than 100 min .

Table 2-4 Estimated rate constant at three acid concentrations. Condition: 15 % glucose and 200˚C

Acid concentration (%)	Glucose	
	K_1 (dm^3/mol.min)	K_2 (dm^3/mol.min)
1	0.19	0.09
3	0.42	0.17
5	0.61	0.23

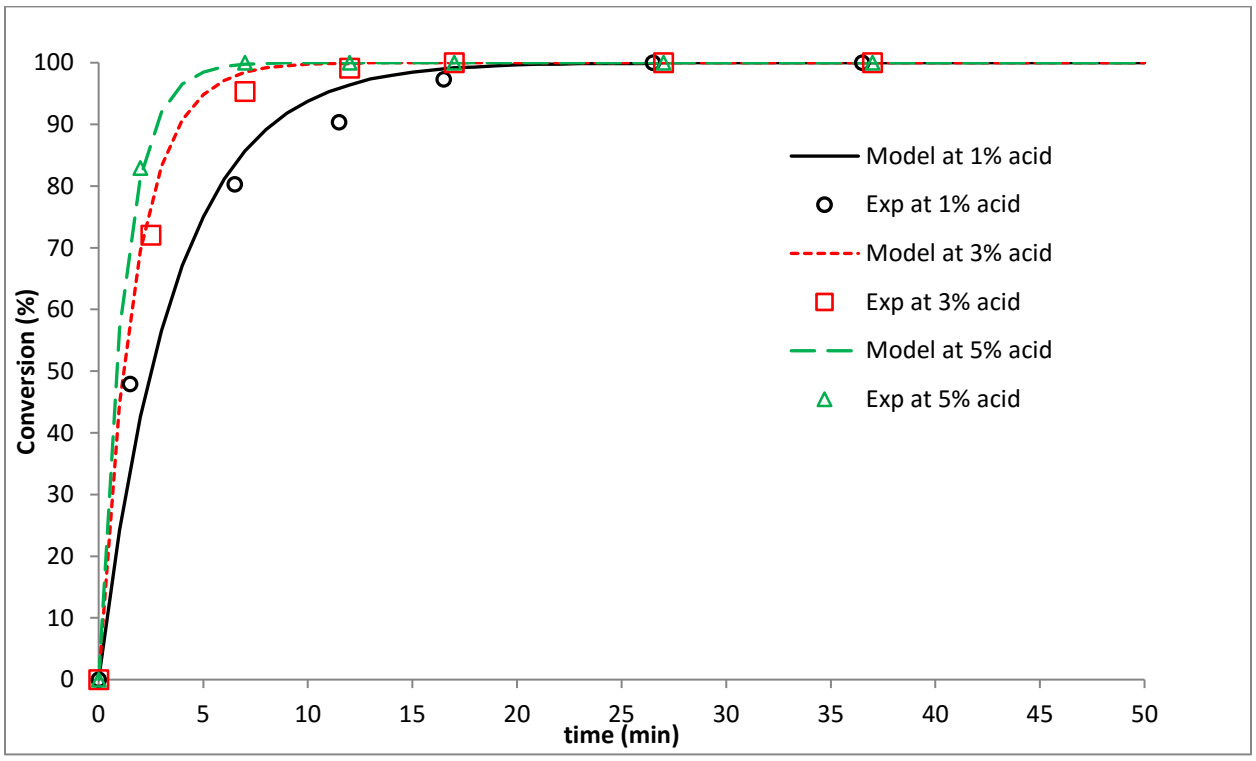

Figure 2-13 Effect of acid concentration on glucose conversion. Experimental data (symbols) and kinetic model data (lines). Conditions: 200 ˚C, 15 (wt. %) glucose.

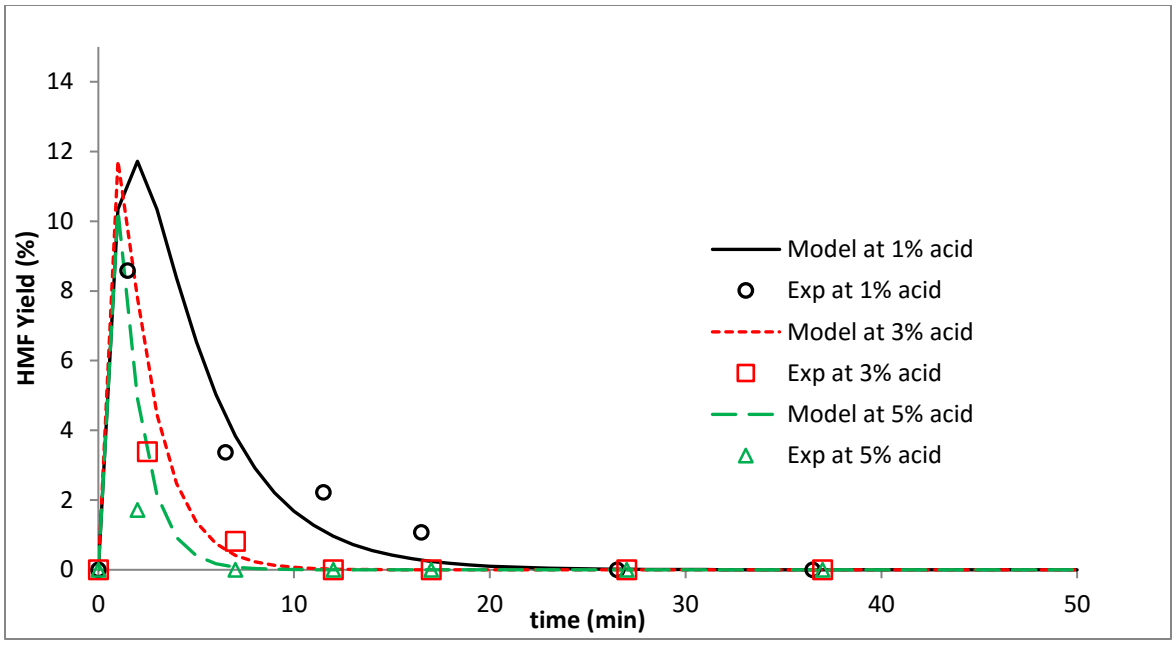

Figure 2-14 Effect of acid concentration on HMF yield. Experimental data (symbols) and kinetic model data (lines). Conditions: 200 ˚C, 15 (wt. %) glucose.

.

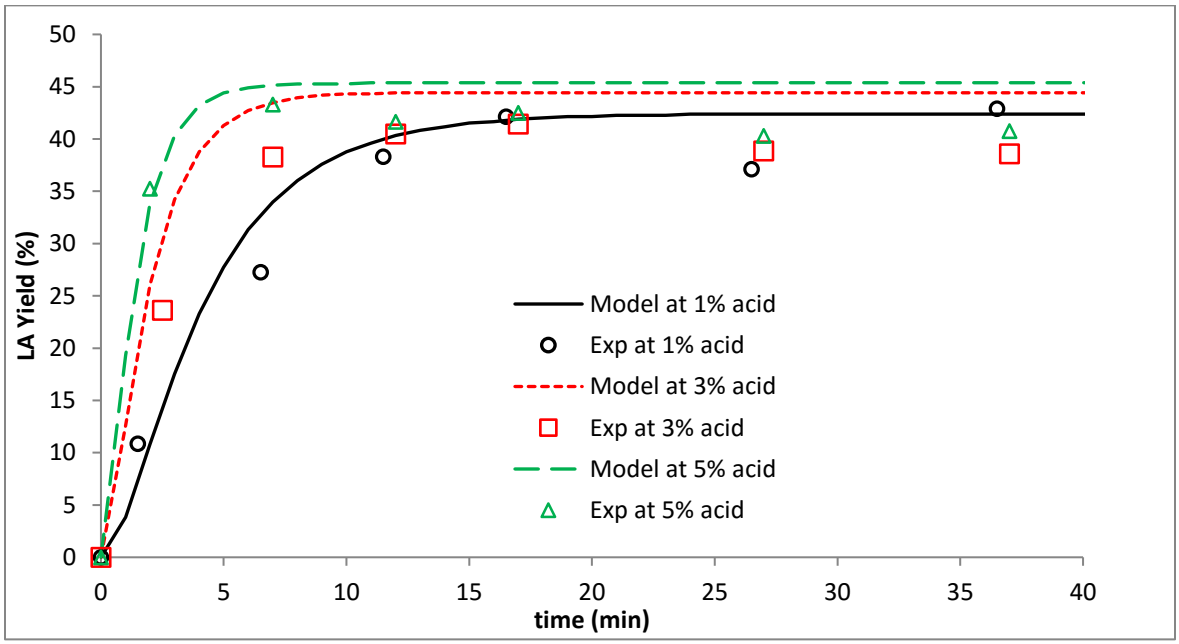

Figure 2-15 Effect of acid concentration on LA yield. Experimental data (symbols) and kinetic model data (lines) .Conditions: 200 ˚C, 15 (wt. %) glucose.

2.5.3.1.2 Comparison with previous kinetic model

The yield and conversion predicted by model are in good agreement with those obtained in experiments. Table 2-4 shows the kinetic parameter for glucose decomposition to LA. In this study, the activation energy of glucose to HMF was found to be 122 (kJ mol^{-1}) which lie in the range 86-160 (kJ mol^{-1}) of previous studies (Song and Lee, 1984; Weingarten et al., 2012; Girisuta et al., 2006a). In addition, the activation energy of the glucose conversion to humins was found to be 104 kJ mol^{-1} which is in the range of 51-210 (kJ mol^{-1}) of previous studies (Weingarten et al., 2012; Girisuta et al., 2006a). The relatively higher activation energies of the main reaction (E_{1g}= 122 kJ $mol^{-1)}$ compare to the side reaction (E_{2g}= 104 kJ mol^{-1}) indicates that high temperatures will favor the formation of HMF from glucose and will increase its maximum concentration in the reaction solution.

Table 2-5 Estimated kinetic parameter for acid catalyzed glucose decomposition to HMF at different initial glucose concentration.

Glucose concentration	Parameter	Glucose to HMF	
		Main reaction	Side reaction
5%	log A	13.10	10.45
	E (KJ/mol)	118.61	99.51
	n	0.73	0.65
10%	log A	13.50	10.78
	E (KJ/mol)	122.65	101.98
	n	0.70	0.63
15%	log A	14.09	11.73
	E (KJ/mol)	127.24	109.44
	n	0.79	0.58

Table 2-6 Estimated kinetic parameter for acid catalyzed glucose decomposition to LA used for model.

Glucose concentration	Parameter	Glucose to HMF		HMF to LA	
		Main reaction	Side reaction	Main reaction	Side reaction
5-15%	log A	13.54	11.06	9.95	15.66
	E (KJ/mol)	122.55	104.23	85.55	139.30
	n	0.74	0.62	0.74	0.73

By assessing the reaction orders in acid concentration, glucose conversion to HMF was found to exhibit a near first order dependence to the acid concentration (α_g= 0.74), lower than other studies (Girisuta et al., 2006a; Weingarten et al., 2012). On the other hand, glucose to humins formation also exhibits lower than first order dependence (β_g=0.62) in agreement with Girisuta et al. (2006a) reported values but lower than Weingarten et al. (2012) reported values. The reaction orders with respect to acid concentration in the main reactions (α_g=0.74) higher than that of the side reaction (β_g=0.62), indicate that high acid concentrations will have a positive effect on the selectivity of the HMF formation from glucose.

The activation energy for the reaction HMF conversion to LA (85 kJ mol^{-1}) are in agreement with those reported in other studies (Girisuta et al., 2006a; Weingarten et al., 2012; Patil et al., 2012) and it is the lowest activation energy of the reactions involved in the glucose conversion to LA. On the other hand, the decomposition reaction of HMF to the undesired humins product has the activation energy (139 kJ mol^{-1}) consistent with other reported values (Girisuta et al., 2006a; Patil et al., 2012). Comparing with the activation energies of the other reactions, one can say that low temperatures will favor the formation of LA while high temperature will favor humins formation consistent with our finding in Figure 2-12.

In their study of acid-catalyzed HMF decomposition, Girisuta et al. (2006a) reported reaction odder of 1.38 and 1.07 for the formation of LA and humins respectively. Weingarten et al. (2012) also reported values of 1.176 for both case. These values are higher than our calculated values of 0.74 and 0.73 respectively. Nevertheless, they agree that the reaction of LA formation has a higher order (0.74) than that of the humins formation reaction (0.73). However, the relatively small gap between these two orders indicate not a significant change will occur if we change the acid concentration. This indicates that high acid concentrations will promote LA formation from HMF to a little bit higher extent than the humins formation as observed in experiments.

2.5.4 Reactor design for production of HMF and LA

The kinetic model developed here can be used further to model continuous reactor system. Considering the mixing of the reactant, CSTR and PFR are the two type of reactor that were modelled for LA production from sugar in aqueous conditions. The reactor design equations of the PFR are similar to the design equations for the batch reactor . Under steady state operating conditions, their design equations are described as equations.

$$\text{PFR} \qquad \tau = C_{i,0} \int_0^x \frac{dx}{r_i}$$

$$\text{CSTR} \qquad \tau = -\frac{C_{i,o} X}{r_i}$$

Where τ is the residence time, $C_{i,o}$ is the initial concentration of species i, r_i corresponding reaction rate, x_i the conversion of species. The process variables such as initial concentration of glucose, acid concentration, temperature and residence time can be manipulated to maximize HMF and LA. The theoretical calculation of HMF and LA yields as a function of glucose conversion for an ideal PFR and CSTR is presented in Figure 2-16 & 2-17. At 30 % glucose conversion in PFR, the maximum yields of HMF is increased from 7% to 13% with the increase of temperature from 150

°C to 200 °C. In CSTR, with the increase of temperature same degree, the maximum yields of HMF is increased from 5% to 8% at same conversion level. These indicate higher temperatures are essential to maximize the HMF yields and higher yield of HMF can be obtained in a PFR compared to CSTR at equal conversion. This is because the relatively higher activation energies of the main reaction (E_{1g}= 122 kJ mol^{-1}) compare to the side reaction (E_{2g}= 104 kJ mol^{-1}) favor the formation of HMF from glucose at high temperature and will increase its maximum concentration in the reaction solution. The shorter residence time minimizes the further decomposition of HMF and maximize the HMF production in PFR over CSTR.

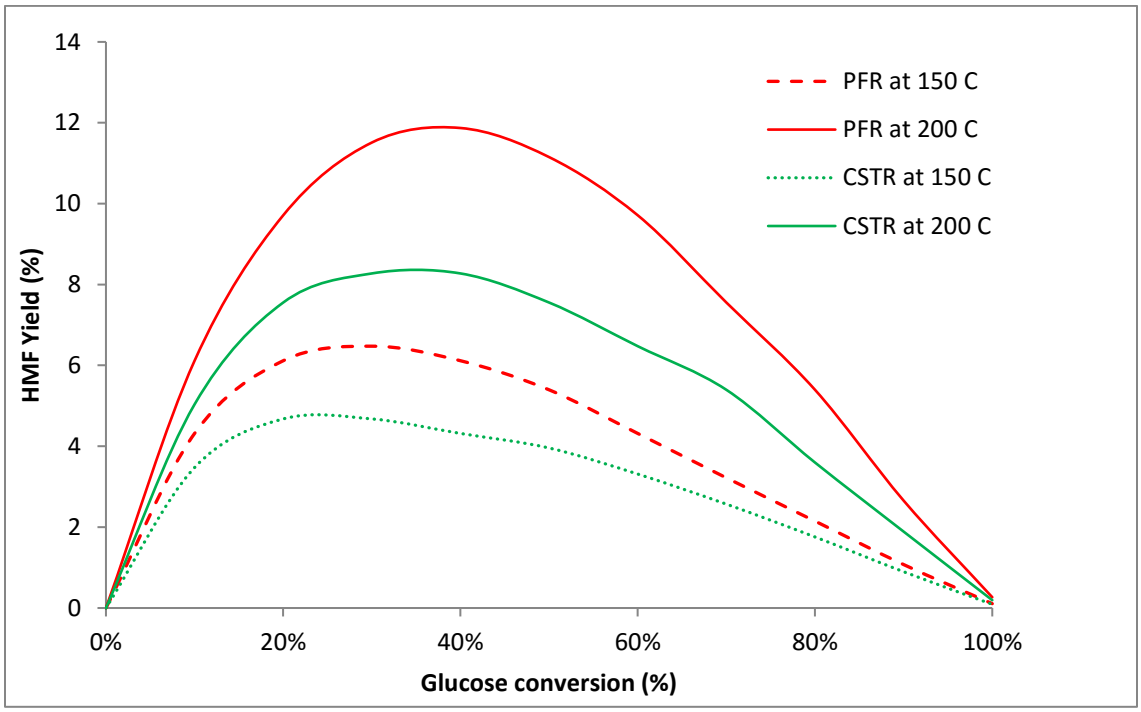

Figure 2-16 Continuous reactor modelling for HMF yield in a single continuous reactor. Conditions: 150-200 ˚C and 5 (wt. %) H_2SO_4

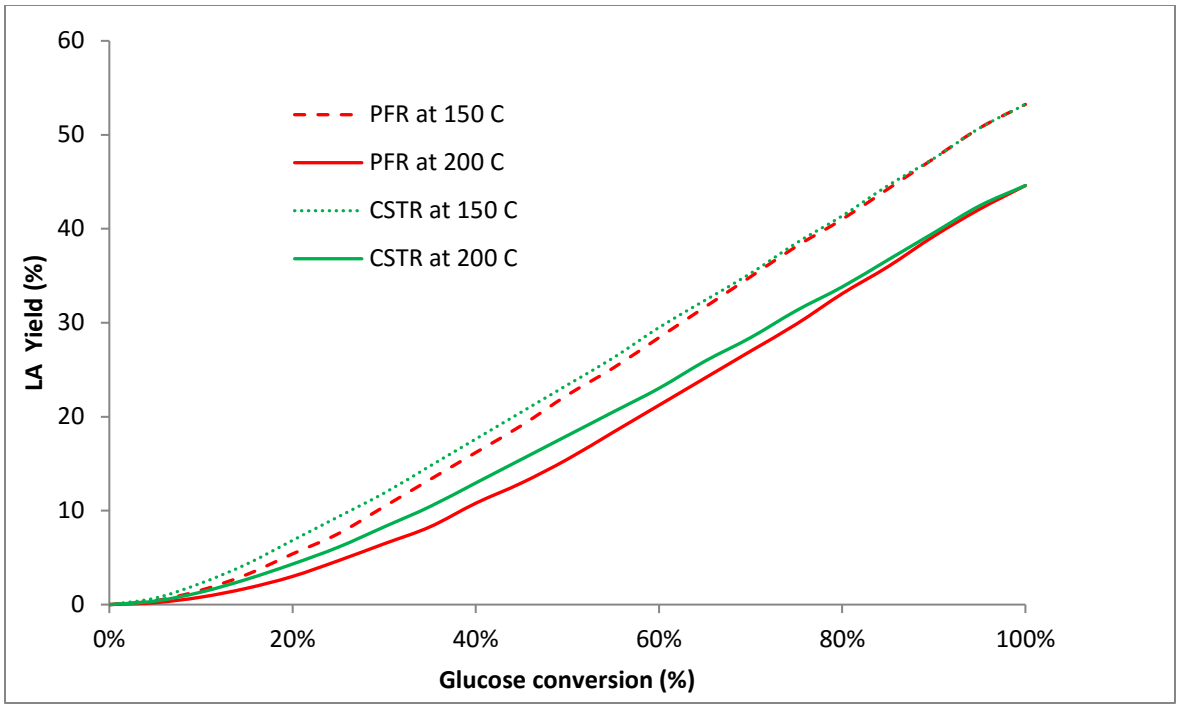

Figure 2-17 Continuous reactor modelling for LA yield in a single continuous reactor. Conditions: 150-200 ˚C and 5 (wt. %) H_2SO_4.

However, an opposite scenario was found for the production of LA. In PFR, when temperature is increased from 150 to 200 °C, the yield of LA is decreased from 11 % to 7 % at 30 % glucose conversion. At same conversion level, the yields were decreased from 12% to 8 % with the increased of temperature from 150 to 200 °C in CSTR. However, at higher conversion, no difference in LA yield is observed for PFR and CSTR. These imply that low temperatures favor the formation of LA. The relatively lower activation energy associated with LA production than that of humins formation from HMF is attributed to this.

To see the yield variations along with temperature and residence time, contour plot for CSTR and PFR were sketched in Figure 2-18 & 2-19. Figure 2-18 clearly shows that higher temperatures (200 °C and more) and short residence time (less than one minute) are essential to maximize the HMF yield and these conditions are favored in PFR type reactor. On the other hand, Figure 2-19

shows, in a PFR, 50 % LA can be achieved at 175 °C after 50 min where as in a 50 % LA can be achieved at 175 °C after 200 min CSTR. These indicate longer residence times are required in a CSTR compared to a PFR to obtain equivalent LA yield.

a)CSTR b) PFR

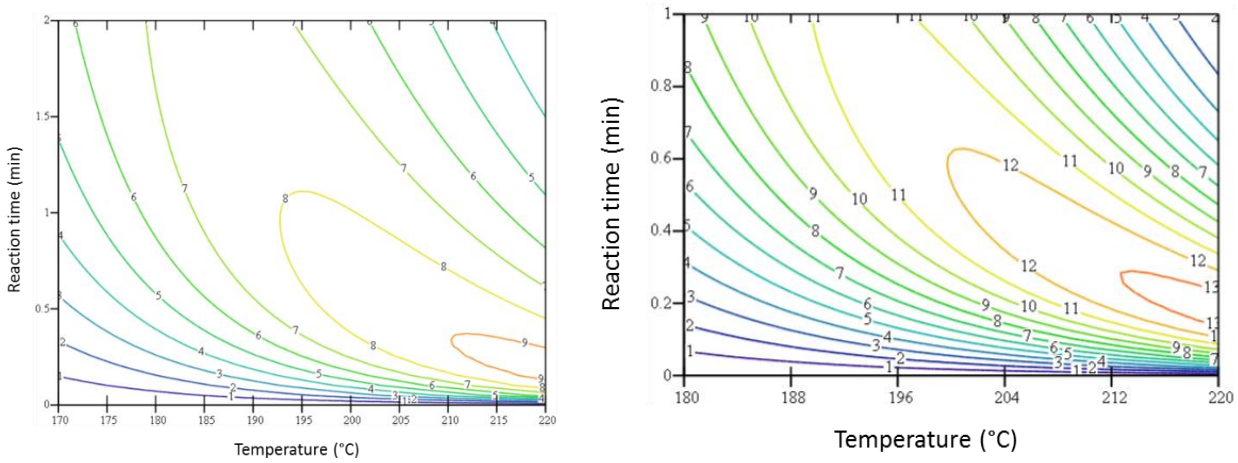

Figure 2-18 Contour plot for continuous reactor modelling for HMF yield in a single continuous reactor. Conditions: 5 (wt. %) H_2SO_4, a) in CSTR, b) in PFR

a) PFR b)CSTR

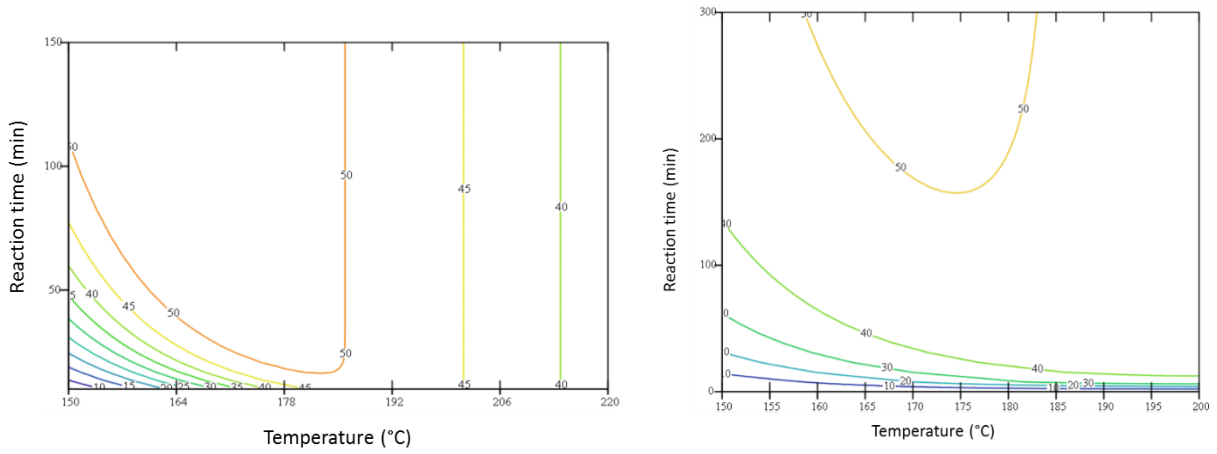

Figure 2-19 Contour plot for continuous reactor modelling for LA yield in a single continuous reactor. Conditions: 5 (wt. %) H_2SO_4 a) in CSTR, b) in PFR

2.5.5 Optimum temperature profile

The LA yield has an optimum with respect to temperature and residence time. The "isothermal optimum temperature" is a fixed temperature (dT/dt=0) at which maximum concentration of LA can be achieved. Table 2-5 demonstrates the optimum temperatures of LA production with others reaction conditions where a good yield of LA can be obtained. It shows that at optimum temperature (156 °C), the maximum yield of LA is calculated 54%. Figure 2-20 shows how the optimum temperature profile is varied with time. To follow the optimum temperature profile, a hypothetical reaction is started at 180 °C and ran until it meets the optimum temperature curve at t= 8 min. The effect of optimum temperature profile and isothermal optimum temperature on glucose conversion and on the production of HMF & LA yields are summarized in Figure 2-21, 2-22, & 2-23 at an acid concentration of 5 %. It is clear from the figure with optimum temperature profile, 52 % yield of LA can be achieved within 20 min of the reaction at 95% glucose conversion. On the other hand, "isothermal optimum temperature" policy give maximum yield of 20% LA with 50 % conversion at 20 min . That means by using optimum temperature profile we can reduce the reaction time substantially.

Table 2-7 Isothermal optimum temperature vs other isothermal conditions.

Temperature (°C)	Maximum LA yield (%)	Time (min)
140	52.88	800
150	53.9	400
160	54.03	200
170	53.23	100
180	51.48	50
190	48.85	20
200	45.33	7
Opt Temperature (156.54)	54.9	300

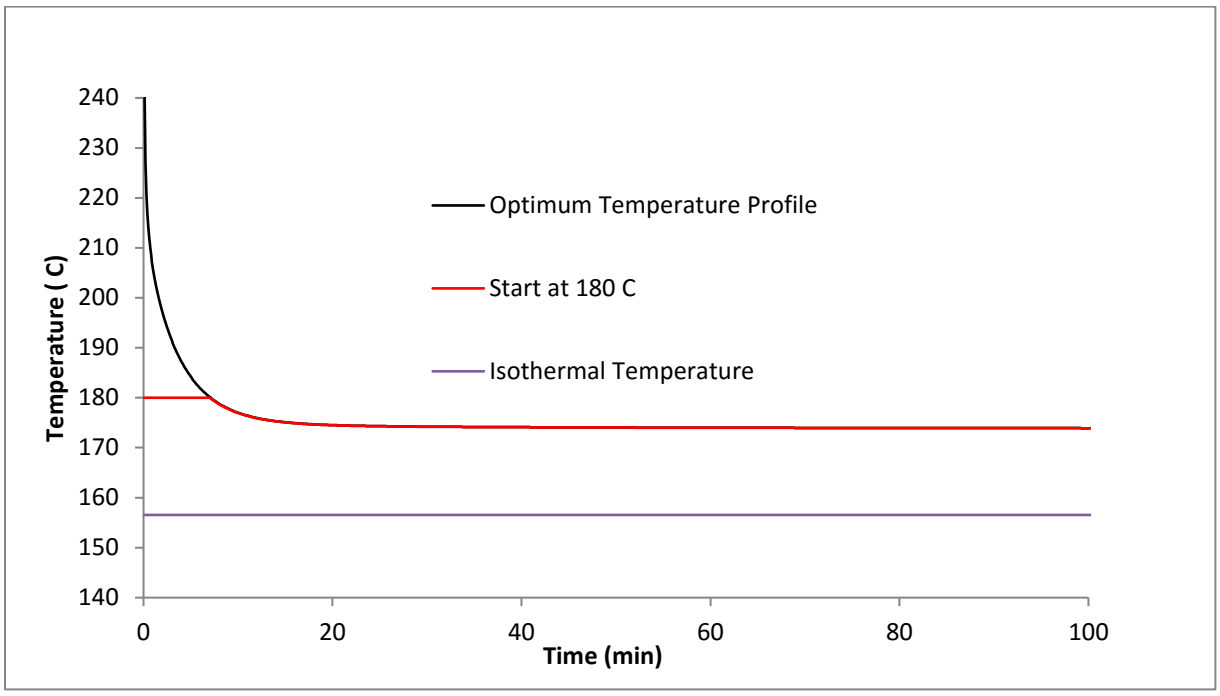

Figure 2-20 Optimum temperature profile for LA yield in a single batch reactor. Conditions: 5 (wt.%) H_2SO_4, 5-15 % glucose

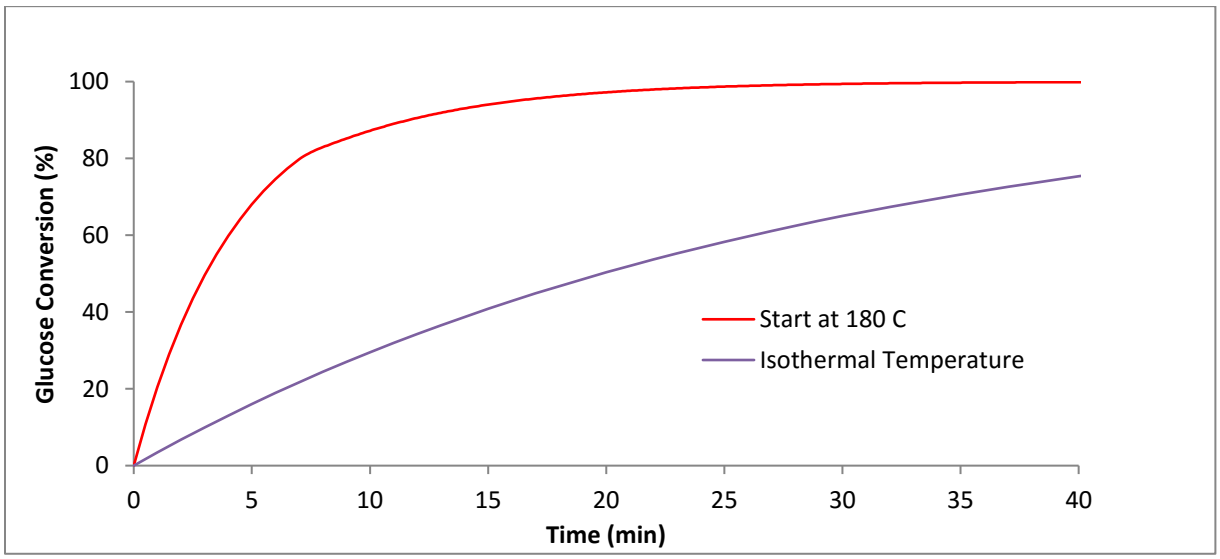

Figure 2-21 Glucose conversion profile based on optimum temperature profile and isothermal optimum temperature in a single batch reactor. Conditions: 5 (wt.%) H_2SO_4

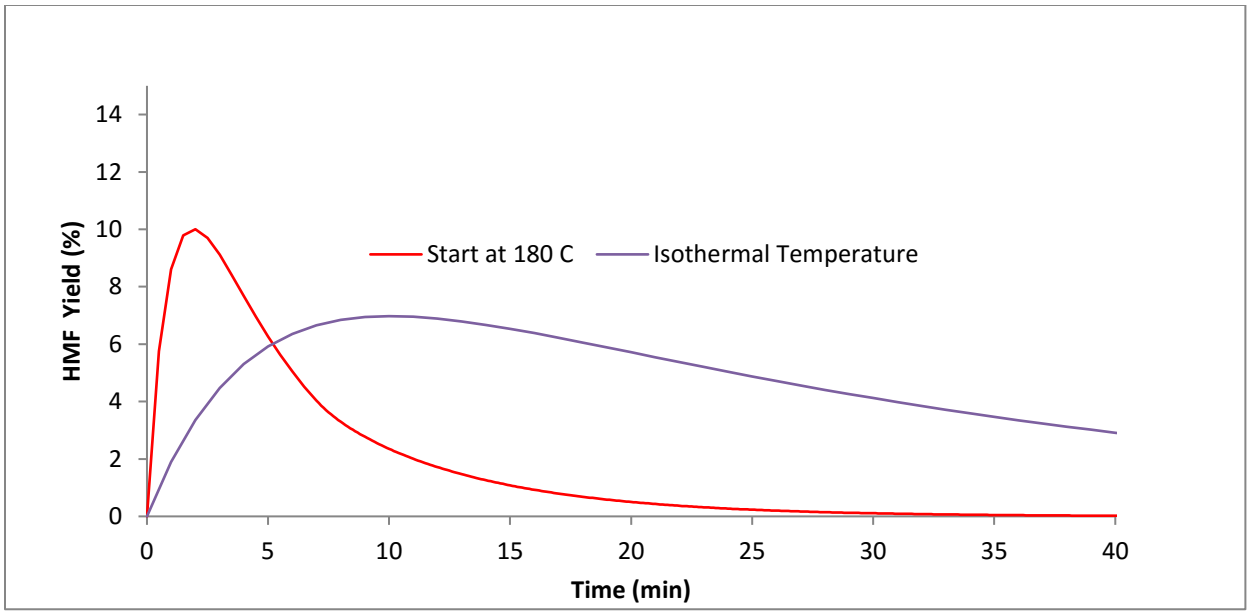

Figure 2-22 HMF yield profile based on optimum temperature profile and isothermal optimum temperature in a single batch reactor. Conditions: 5 (wt.%) H_2SO_4

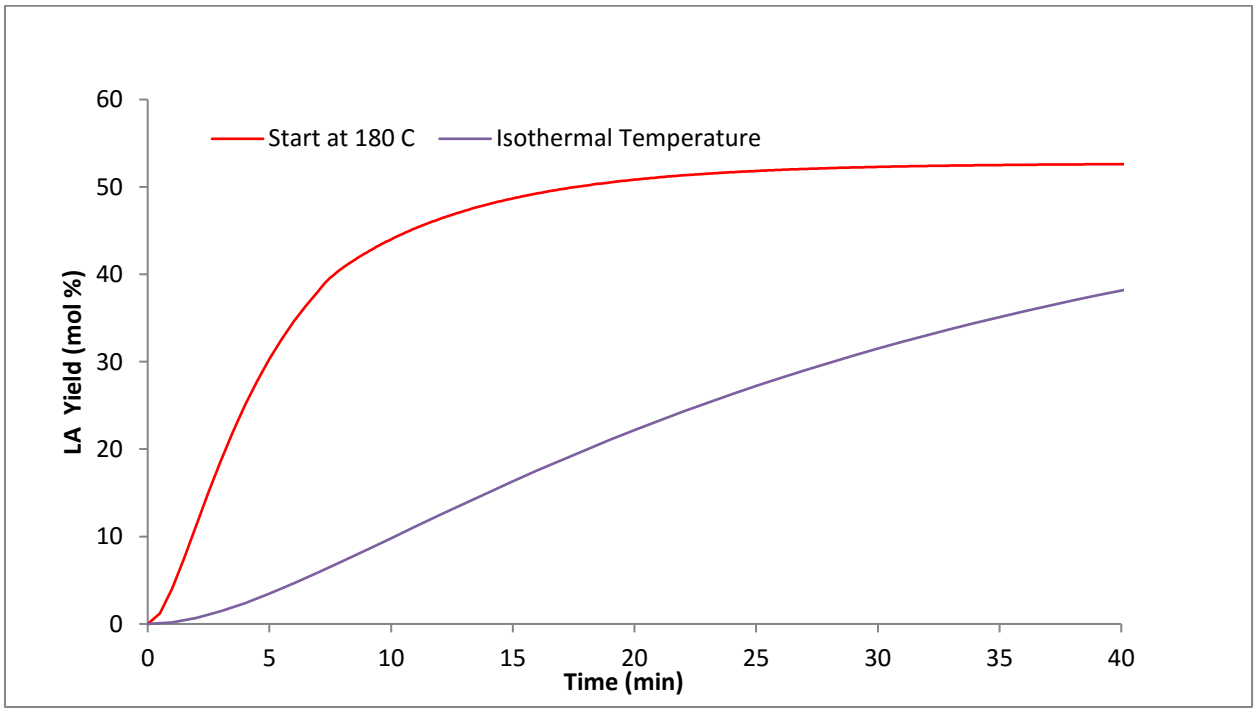

Figure 2-23 LA yield profile based on optimum temperature profile and isothermal optimum temperature in a single batch reactor. Conditions: 5 (wt.%) H_2SO_4.

2.6 Conclusion

This study describes an experimental study on the acid-catalyzed decomposition of glucose into LA and formic acid in a batch reactor. In this study, we have developed a kinetic model for LA production from glucose that consists of four steps: (1) glucose dehydration to form HMF; (2) glucose degradation reactions to form humins; (3) HMF rehydration to form LA and formic acid, and (4) HMF degradation to produce humins. Some parameters such as reaction temperature, acid concentration and initial hexose concentration that impact LA yield have been investigated in detail. The results shows LA yields depend on sulfuric acid concentration. Although temperature speed up the reaction rate and allowed the maximum LA yield to be reached sooner, the maximum LA yield is decrease with increasing temperature. The acid concentration has little positive effect on maximum LA yield. The kinetic model derived for batch reactor was further used to model continuous reactor system. The model suggests that high temperature and shorter reaction times are required to maximize hydroxymethylfurfural (HMF), an intermediate in the process. It also predicts low temperature and longer reaction times are essential to maximize LA yield. By following optimum temperature profile, a near maximum LA yield can be obtained within short period of time.

Chapter 3

Production of levulinic acid from glucose by dual solid-acid catalysts

3.1 Abstract

Levulinic acid is a versatile specialty chemical usable as a building-block for synthesis of various chemicals. In this study, we have prepared a series of solid Lewis acid catalysts and tested them for glucose to fructose isomerization. We also tested a Brønsted solid acid catalyst (Amberlyst-15) to investigate conversion of fructose to levulinic. Among the Lewis solid acid catalysts tested, tin imbedded on large-pore zeolite (Sn-Beta) has shown the highest specific activity in isomerization of glucose to fructose in aqueous media. The concurrent use of the dual-catalysts of Sn-beta and Amberlyst-15 was further investigated. The dual-acid catalyst has improved the yield of LA over that of Amberlyst-15 alone, from 37% to 45% of the theoretical maximum. The improvement was due to enhanced isomerization of glucose to fructose by Sn-Beta. Stability tests have shown that the Sn-beta zeolite catalyst loses 20 % of its activity after five consecutive batch-cycles. The activity of this catalyst, however, was fully regenerated by calcination. Ambelyst-15 also suffers from deactivation, which is lower than that of Sn-Beta. The deactivation is primarily due to humin deposit on the surface of the catalyst.

3.2 Introduction

LA (gamma-ketovaleric acid), is a short-chain fatty acid, provide potentially important platforms for production of liquid fuels and chemicals(Shen & Wyman, 2012). The unique feature of LA is its ketone and a carboxylic acid groups. These two functional groups make it a potentially very versatile building block for the synthesis of various organic chemicals (Girisuta et al., 2006b). For example, Levulinic ester, which is produced from the esterification of LA, is suitable to be used as additives for gasoline and diesel of transportation fuels (Peng et al., 2011). LA can also be hydrogenated to g-valerolactone (GVL), a non-toxic solvent, has the functionality to be upgraded to a variety of chemicals, fuels additives, and fuels (Alonso et al., 2013). Serrano –Ruiz et al. (2011) have developed a cost effective route for the conversion of lignocellulosic biomass to liquid hydrocarbon fuels via catalytic decarboxylation of GVL to butene followed by alkene oligomerization.

The most common method to produce LA is the acid catalyzed hydrolysis of hexose sugars or carbohydrates. Traditionally, homogeneous catalysts such as HCl and H_2SO_4 have been used to synthesis LA from glucose (Girisuta et al., 2006b), cellulose, (Girisuta et al., 2007b), normal corn starch (Cha & Hanna, 2002), water hyacinth plant (Girisuta et al., 2008), sugarcane bagasse (Girisuta et al., 2013) and Pine (Rivas et al., 2013). A wealth of research have been conducted on conversion of lignocellulosic biomass to LA using homogeneous catalysts, but relatively few address heterogeneous catalyst in the process of LA production from soluble sugars. The difficulty in recovery of the homogeneous catalyst and disposal problem along with equipment corrosion issues make heterogeneous catalyst a viable option. Use of solid catalysts, however, is restricted to liquid feedstocks. There are liquid carbohydrates available from various sources that can compete cost-wise with lignocellulosic feedstocks. The examples are industrial byproducts such

as sugarcane molasses (Pradeep & Reddy, 2010),cheese whey (Ferchichi et al., 2005), and pulp mill prehydrolysates (Shi et al., 2015), which is extracted from hemicellulose of pulp feed. This fraction of pulp feed is discharged as black liquor in pulping process and it only carries a fuel value. Successful recovery of hemicellulose sugars from pine without loss of the quality and yield of pulp and its conversion to fuels and chemicals have been reported (Fu et al., 2011; Helmerius et al., 2010; San Martin et al., 1995; Shi et al., 2015). The main intent of using solid acid catalyst is to utilize such cheaply available liquid carbohydrates.

Catalytic conversion of glucose to LA involves a multi-step complex reaction sequence. The reaction pathway includes glucose↔fructose→hydroxymethyfurfural (HMF)→LA and various side-reactions. Each of these reactions behaves differently depending on the type of acid catalyst. Specifically, Lewis acid has much higher selectivity for the first reaction (glucose↔fructose) whereas Brønsted acid favors the latter reactions (Choudhary et al., 2013).

Scheme 3-1 Overall reaction scheme of acid catalyzed production of levulinic acid from glucose in aqueous phase.

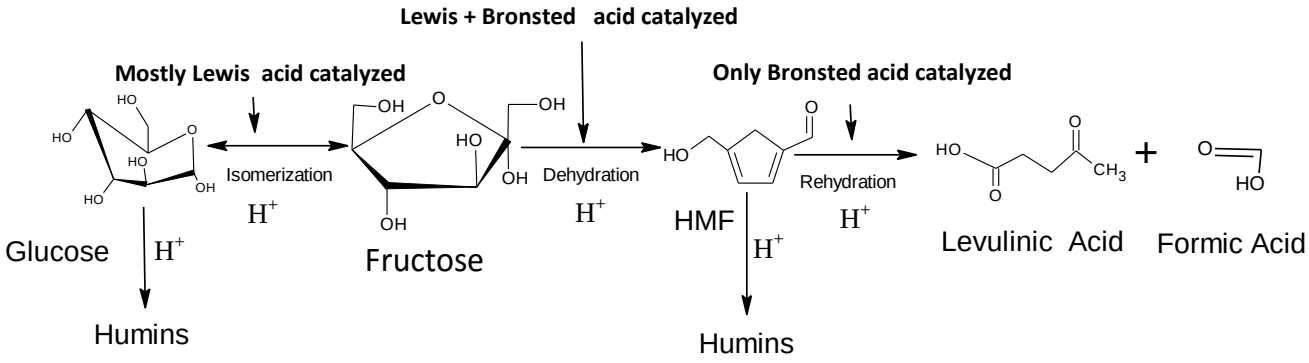

Recently, Moliner et al. (2010) reported on a tin-containing zeolite (tin in the framework of a pure-silica analog of zeolite beta, denoted by Sn-beta) that it has high activity over a wide range

of temperature (110– 140 °C) for isomerization of glucose into fructose in aqueous media with glucose feed as high as 45 wt.%. In another study, Son et al. (2012) reported that the synthesis of LA from fructose with high yield (56% molar yield) using Amberlyst-15, an ion-exchange resin with strongly acidic sulfonic groups that contains more Brønsted acid sites than Lewis acid sites. Results of these studies collectively suggest that yield of levulinic from glucose can be improved applying the dual-acid catalyst system, each carrying out the respective reaction steps.

In this work, we have explored the use of solid-acid Lewis acid catalysts including post-transitional metal (tin-containing zeolite), transitional metal (vanadium-containing zeolite, iron-containing zeolite), lanthanoide metal (lanthanum-containing zeolite) to identify their roles in catalyzing the glucose isomerization reaction as well as to investigate the combined effect of Lewis acid and Brønsted acid (Amberlyst-15) on glucose conversion to levulinic. Our strategy was to separately investigate the two independent reactions involved in the synthesis of LA from glucose: (1) isomerization of glucose into fructose catalyzed by Lewis acid (Sn-beta, V-beta, La-beta, Fe-beta) and (2) dehydration of fructose into LA by Brønsted acid (Amberlyst-15).

3.3 Materials and Method

3.3.1 Chemicals and reagents

Hydroxymethylfurfural (HMF) was obtained from Fisher Scientific Inc. (Cincinnati, Ohio). Zeolite beta, Tin (II) acetate, ammonium metavandate (NH_4VO_3), Iron chloride hexahydrate ($FeCl_3.6H_2O$), $LaCl_3.7\ H_2O$, glucose, fructose, nitric acid, LA and formic acid were purchased from VWR (Radnor, PA). All chemicals used in this study were of analytical grade and used without further purification.

3.3.2 Catalyst preparation

Lewis acid doped zeolites are typically obtained by direct incorporation of the Lewis acid into the framework during hydrothermal synthesis. However, this procedure has some disadvantages such as undesirable formation of metal oxide particles, significant retardation of the zeolite nucleation, and hence excessively time-consuming synthesis procedure (up to 40 days for Sn-beta), and undesirable crystal formation during the catalyst synthesis. To avoid these, Sn-beta was synthesized according to the solid-state ion-exchange (SSIE) procedure described by Hammond et al. (2012). Zeolite beta was treated with 13 M HNO_3 mixing them in proportion of 1 g zeolite per 20 ml solution. This treatment was carried out at 90 °C for 20 h to remove the aluminum content. Then de-aluminated zeolite beta was recovered by filtration, extensively washed with water, and dried at 45 °C overnight. The SSIE reaction was then applied by grinding the appropriate amount of de-aluminated zeolite together with required amount of tin (II) acetate for 15 minutes to prepare 10% (w/w) Sn-beta/dealuminated zeolite and then calcined in an air-flow furnace at 550 °C for 6 h. To prepare V-beta, Fe-beta and La-beta, SSIE reactions were carried out the same way as that of Sn-beta except that NH_4VO_3, $FeCl_3.6\ H_2O$, and $LaCl_3.7\ H_2O$, in place of tin (II) acetate, were used as starting material. The detailed procedures are described elsewhere (Capek et al., 2005; Dzwigaj et al., 1998; Jia et al., 1998). For Fe-beta and La-beta, the calcined samples were washed thoroughly with water to remove any Cl- anions, and dried at 45 °C overnight.

3.3.3 Catalyst characterization

The method of Brunauer, Emmett, and Teller (BET) was used to determine the total surface area of catalysts and the micro pore volume. The surface areas and pore volumes of catalysts were determined by nitrogen adsorption at 77 K using Quantachrome automated gas sorption

system/Nova 2200e surface area and pore volume analyzer (Boynton Beach, Florida). The catalyst samples were degassed in vacuum for 12 h at 200 °C before measurement. The XRD patterns were obtained using a Bruker D8 Discover diffractometer. The spectra were acquired at a scan rate of 1.6 degrees/min between 2 theta = 5 to 35. An accelerating voltage of 40 kV was used at 40 mA. The SEM pictures of the catalysts were taken by a ZEISS DSM940 scanning electron microscope.

3.3.4 Catalytic reaction procedure

All of the catalytic reactions were carried out using batch reactors made out of SS-316 tubes with dimension of 0.75 inch ID x 1.89 inch L. For the dual catalysts experiments, the two catalysts were premixed and placed into reactor containing glucose solution. The reactors were filled with 2 ml of reaction mixture, sealed with screw-cap ends, and placed in a constant-temperature oven to initiate the reaction. The reactor was preheated for 15–30 min to reach the set temperature and maintained at the level for desired period of time. The reaction time in this report is defined as the duration after it reached the set temperature. The reactors were shaken at 200 rpm connecting them to a laboratory arm shaker externally located. The reactors and the shakers were connected by a rod through a hole on top of the furnace. It was done to keep the catalyst particles uniformly suspended in the reactor maintaining vigorous solid-liquid contact. The reactors were removed from the oven with predetermined interval and placed into ice-bath to quench the reaction. The reaction mixture was centrifuged, and the particle-free solution was analyzed for its composition by HPLC.

3.3.5 Catalyst stability test

The relative activity of the Sn-Beta catalyst was measured over five-consecutive isomerization cycles at 140 °C for 20 min. After each cycle, catalyst was separated from the liquid by filtration

and dried without washing at 45 °C in oven for 12 h. Its relative activity was measured by conversion of glucose over 20-minutes period. The activity test for Amberlyst-15 was carried out slightly different way. Unlike Sn-beta, the catalyst particles were separated from the liquid after each cycle by filtration and air-dried without washing at room temperature for 2 days. The activity test run was then carried out adding fresh fructose solution to react at 140 °C for 1 h. The conversion of the reactant after 1 hour was taken as the relative activity. This was done over five cycles of batch runs. In each of the batch runs, the reaction was carried out for 8 hours at 140 °C.

3.3.6 Product analysis

Composition of the liquid samples were determined by HPLC system equipped with Bio-Rad HPX-87H column (Hercules, CA), refractive index detector (Shodex, NY), Alcott 708 Autosampler, PeakSimple Chromatography Data Systems (Torrance, CA).

Conversion is defined as moles of feed reacted divide by the initial moles of feed in the reactor as shown by the following equation.

$$Conversion\ (\%) = 100 * \frac{(Initial\ \ concentration\left(\frac{g}{l}\right) - Final\ concentration\left(\frac{g}{l}\right)) * \text{hexose MW}}{\text{Initial hexose concentration}\left(\frac{\text{g}}{\text{l}}\right) * \text{hexose MW}}$$

Yield is defined as moles of product divided by the initial moles of feed in the reactor. LA concentration (g/l) was converted to LA percent-yield on the basis of the theoretical maximum as follows.

$$Levulinic\ acid\ Yield\ (\%) = 100 * \frac{levulinic\ acid\ concentration\left(\frac{g}{l}\right) * \text{hexose MW}}{\text{Initial hexose concentration}\left(\frac{\text{g}}{\text{l}}\right) * \text{levulinic acid MW}}$$

3.4 Results and discussions

Preliminary test of catalytic conversion of glucose to LA was conducted for various solid acid catalysts including ZSM-5, Nafion SAC-13, and Amberlyst-15. As shown by the results summarized in Table 3-1, the yields of LA are low and the catalytic activity as indicated by conversion of glucose varied widely. For example, the maximum LA yield of 15 % with a conversion of 81 % was achieved for an initial glucose concentration of 10 wt. % at 180 °C in 8 h for ZSM-5 (Table 3-1, entry 3). Similarly, Nafion SAC-13 converted glucose into LA with 13 % yield under identical reaction conditions (Table 3-1, entry 6). To enhance the yield of LA, sodium halide was added to ZSM-5 as Lucht and co-workers found NaCl plays an important role on the yield of LA from cellulose with use of Nafion SAC-13 (Liu et al., 2013; Potvin et al., 2011). Addition of sodium halide to ZSM-5, however, did not show any effect on the yield of LA (Table 3-1, entry 4-5). A nominal enhancement was observed for Nafion SAC-13 (Table 3-1, entry 8) due to the interaction of NaCl with the hydrogen bonding network of the glucose structure (Liu et al., 2013; Potvin et al., 2011) . It appears that the interaction of NaCl with Nafion SAC-13 is different from that with ZSM-5 in aqueous media. Upon observation of low overall yields of LA from glucose, a new set of experiments were carried out using fructose as the reactant instead of glucose under the same conditions, in which significant improvement in LA yield was observed with these catalysts (Table 3-1, entry 9-13). Particularly notable was that LA yield of 58 % with a conversion of 100 % was achieved at 140 °C in 8 h when Amberlyst-15 was used as a solid catalyst (Table 3-1, entry 16). This value agrees closely with that reported by Son et al. (2012). It was also the highest fructose-to-LA yield observed in this work. Further experiments with Amberlyst-15 to produce LA from glucose resulted LA yield of only 27 % under the identical conditions (Table 3-1, entry 17).

Table 3-1 Production of LA from hexoses. Feed was 10% hexose solution

Entry	Feed	Catalyst	Catalyst/ Feed ratio (wt./wt.)	Temperature (°C)	Time (h)	Conversion (%)	LA Yield (% of theoretical maximum)
1	Glucose	ZSM-5	0.5	180	4	53.3	5.2
2	Glucose	ZSM-5	0.5	180	6	68.9	10.3
3	Glucose	ZSM-5	0.5	180	8	80.8	15.0
4	Glucose	ZSM-5+ NaI	0.5	180	4	53.5	5.1
5	Glucose	ZSM-5+ NaCl	0.5	180	4	57.6	7.1
6	Glucose	Nafion SAC-13	0.5	180	4	51.7	13.6
7	Glucose	Nafion SAC-13+ NaI	0.5	180	4	54.0	12.5
8	Glucose	Nafion SAC-13+ NaCl	0.5	180	4	65.3	18.1
9	Fructose	ZSM-5	0.5	180	4	98.5	19.8
10	Fructose	ZSM-5	0.5	180	6	99.3	19.3
11	Fructose	Nafion SAC-13	0.5	180	4	98.1	36.1
12	Fructose	Nafion SAC-13+ NaI	0.5	180	4	99.6	32.5
13	Fructose	Nafion SAC-13+ NaCl	0.5	180	4	99.4	30.3
14	Fructose	Amberlyst-15	0.5	140	8	85.0	45.2
15	Fructose	Amberlyst-15	1	140	8	97.8	52.9
16	Fructose	Amberlyst-15	2.2	140	8	100	58.9
17	Glucose	Amberlyst-15	1	140	8	67.3	26.7

A significant increase in levulinic yield with substitution of glucose from reactant to suggests that the first-stage reaction of glucose-to-fructose isomerization represents a major resistance in the sequential conversion process of glucose-to-LA. Recent investigation on acid catalyzed sugar conversion indicates that glucose isomerization to fructose is catalyzed mostly by Lewis acid whereas fructose to LA via HMF route (shown in Scheme 3-1) is promoted by Brønsted acid (Choudhary et al., 2013; Moliner et al., 2010).

3.4.1 Glucose isomerization to fructose by Lewis acid catalyst

3.4.1.1 Characterization of Lewis acids

The structures of solid acids were studied by XRD and the XRD patterns of these catalysts were compared with the standard patterns of zeolite beta and de-aluminated zeolite beta as shown in Figure 3-1. The high crystallinity of the Sn-beta, V-beta, Fe-beta and La-beta were observed in the XRD pattern consistent with the typical diffraction lines characteristic for the BEA-type framework topology. It indicates that the framework structure is well preserved after de-alumination and incorporation of elements does not cause any loss of crystallinity.

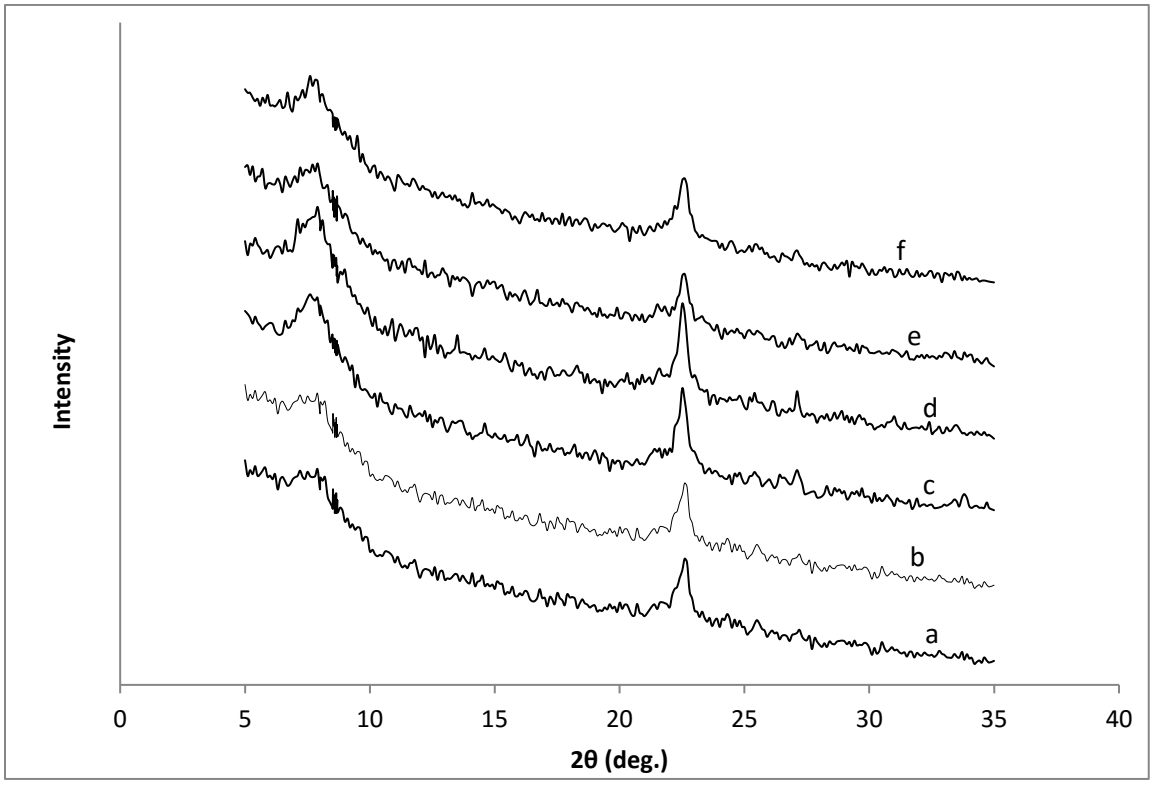

Figure 3-1 XRD Pattern of a) zeolite beta, b) dealuminated zeolite beta, c) Sn-beta, d) V-beta, e) La-beta and, f) Fe-beta.

Additional characterizations using BET were conducted to determine the surface area and porosity of the catalysts (Table 3-2). The surface area of the Sn-beta was larger than those of other solid acids which contributed to high specific catalytic activity/site as evidenced by data of Figure 3-2 and Table 3-2.

Table 3-2 Physicochemical properties of the catalysts.

Catalyst	Treatment	Surface area [m^2g-1]	Pore volume [$cm^{-3}g^{-1}$]
Zeolite beta	N/A	405	0.4
De aluminated zeolite beta	H+	620	0.31
Sn-Beta	H+/SSIE	505	0.33
V-beta	H+/SSIE	418	0.38
La-beta	H+/SSIE	386	0.46
Fe-beta	H+/SSIE	401	0.47
Amberlyst-15 (dry)	Fresh	53	0.4
Amberlyst-15 (dry)	Used	46	0.17
Sn-Beta	Used	303	0.24
Sn-Beta+ Amberlyst-15 mixed	Used	52	0.22

3.4.1.2 Catalyst screening for glucose isomerization reaction

A number of solid acid catalysts (Sn-beta, V-beta, Fe-beta, and La-beta) were screened to determine their relative activity in the glucose isomerization reaction. All screening experiments were conducted at 140°C and 60 minutes reaction time using 10 % glucose solution. As demonstrated in Figure 3-2, Sn-beta showed the highest glucose isomerization activity; V-beta, moderate activity, whereas La-beta and Fe-beta catalyst were virtually inactive. Sn-beta was therefore chosen for investigation.

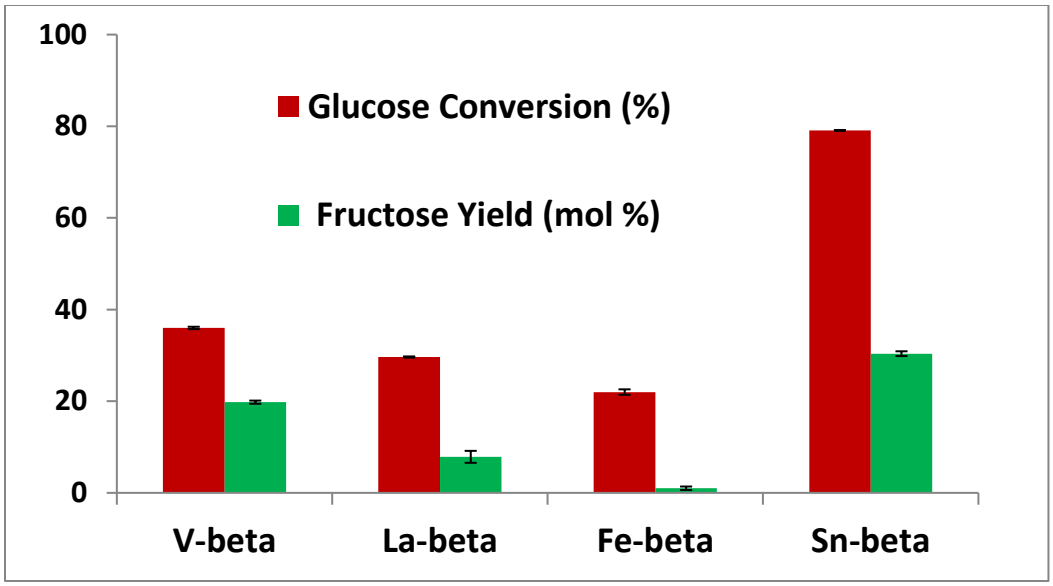

Figure 3-2 Glucose isomerization to fructose using solid acids. Reaction conditions: 10% glucose, 0.5 g catalyst/g glucose, 140 °C, 60 minutes

3.4.1.3 Sn-beta for glucose isomerization reaction

To determine suitable reaction conditions for glucose isomerization to fructose, batch reaction experiments were conducted covering the conditions of 110-140 °C, 10-60 minutes, and with catalyst loading of 0.125-0.5 g-catalyst/g-glucose. The upper limit of temperature was set at 140 °C because beyond this temperature Amberlyst-15 is inoperable. The experimental data concerning glucose isomerization to fructose over 110-140 °C with catalyst loading 0.5 g-catalyst/g-glucose are presented in Table 3-3a. Glucose-fructose conversion is a reversible reaction. The equilibrium constants and the corresponding equilibrium conversion (which is equal to equilibrium fructose yield) were also calculated over this temperature range using the data reported by Moliner et al. (2010). We note that the equilibrium data in the table applies only to the isolated reaction of glucose to fructose.

Table 3-3 Glucose isomerization to fructose using Sn-beta. Feed was 10% glucose solution.

a) Effect of temperature on the yield of fructose at catalyst loading 0.5 g catalyst/g glucose.

Temperature	Time (30 min)		Time (60 min)		Equilibrium Constant (K_{eq})	Equilibrium conversion =Eq. Yield (%)
	Conversion (%)	Fructose Yield (%)	Conversion (%)	Fructose Yield (%)		
110	16.6	12.2	48.3	31.4	1.45	60.1
130	41.7	28.5	76.7	35.6	1.72	65.1
140	71	34.1	79.1	30.4	1.81	67.2

b) Effect of catalyst loading on the yield of fructose at temperature 140 °C.

Catalyst loading (g cat/g glucose)	Time (10 min)		Time (30 min)	
	Conversion (%)	Fructose Yield (%)	Conversion (%)	Fructose Yield (%)
0.5	41.5	23.9	71	34.1
0.25	12	8.3	30.3	24.8
0.125	10.5	0	26.2	18.4

c) Effect of reaction time on fructose yield at catalyst loading 0.5 g catalyst/g glucose.

Reaction time (min)	Temperature (110 °C)		Temperature (140 °C)	
	Conversion (%)	Fructose Yield (%)	Conversion (%)	Fructose Yield (%)
10	5.5	0	41.5	23.9
30	16.6	12.2	71	34.1
60	48.3	31.4	79.1	30.4

Although Sn-beta has high selectivity toward glucose isomerization to fructose, in these test runs, isomerization reaction is accompanied by various other reactions (decomposition of glucose and fructose and subsequent reaction of fructose). The equilibrium data are presented

only as reference information. The data collectively indicate that above 70% conversion is attained within 60 minutes at 140 °C. The maximum observed fructose yield was 35.6%, which occurred at 140 °C and 60 minutes. The data of Table 3-3a show that the observed conversion surpass the equilibrium conversion. It is so because the equilibrium conversion was calculated on the basis of the isolated reversible reaction of glucose-to-fructose. We refer to an explanation provided by Moliner et al. that high temperature and long reaction time forces fructose degradation and more glucose is being converted into fructose to re-establish the thermodynamic equilibrium (Moliner et al., 2010). In order to reduce the reaction time, more experiments were performed varying the catalyst-glucose ratio, keeping other reaction conditions constant. As expected, the maximum glucose conversion of 71 %, which corresponds to fructose yield of 34 %, is reached within 30 minutes of reaction at 140°C with 0.5 g-catalyst/g-glucose (Table 3-3b). However, upon prolonged reaction time, the yield of fructose started to decrease as seen at 140 °C in Table 3-3c for the aforementioned reason.

3.4.2 Production of LA from glucose with solid acid catalysts

As previously mentioned, Sn-beta has the highest glucose isomerization activity; V-beta has moderate activity; Fe-beta is virtually inactive (Figure 3-2). Nonetheless, LA is, although in low amount, produced by all of these catalysts. From this one can deduce that these "Lewis acid catalysts" that contain not only Lewis acid sites but also Brønsted acid site, since HMF is produced on both Brønsted and Lewis sites, whereas LA is produced exclusively on Brønsted sites (Choudhary et al., 2013; Moliner et al., 2010). Also notable is that lactic acid was detected as a byproduct of Sn-beta. Lactic acid has previously been reported to be a byproduct in Lewis acid treatment of glucose (Chambon et al., 2011; Weingarten et al., 2013). As shown in Table 3-4, these catalysts alone are not effective in production of HMF and/or LA. Hence, it became of

our interest to use the Lewis solid acids jointly with Amberlyst-15 that has been proven to be highly effective in production of LA from fructose.

Table 3-4 Glucose transformation to LA using solid acids. Reaction conditions: 10% glucose, catalyst loading 0.5 g catalyst/g glucose. [a] fructose as a starting material instead of glucose.

Catalyst	Temperature (° C)	Time (h)	Conversion (%)	LA Yield (mol %)	HMF Yield (mol %)	Lactic Acid Yield (mol%)
Sn-beta	140	8	88.7	2.9	9.8	9.7
Sn-beta	140	16	92.7	4.7	7.2	4.2
Sn-beta [a]	140	8	96.3	7.7	2.6	10.2
Sn-beta [a]	140	16	94.4	7.9	4.3	6.9
Fe-beta	140	8	76.0	11.4	0.0	0.0
Fe-beta	140	16	91.0	18.1	0.0	0.0
V-beta	140	8	77.0	11.8	0.0	0.0
V-beta	140	16	92.8	18.8	0.0	0.0

To see the effect of the Lewis acid and Amberlyst-15 ratio on the reactions, a series of experiments were carried out applying varying ratio of the catalysts. From the results of these experiments the optimum ratio that maximizes the synergetic effect was determined to be 10 (Amberlysi-15/Sn-beta). In order to assess the effectiveness of the combined solid-solid catalyst system in production of LA from glucose, another series of batch experiments were performed and the results were compared with those of Amberlyst-15 alone. The experiments were carried out at 140 °C, for 12 hours using 10 % glucose solution with catalyst loading of 2.2 g-cat./g-glucose. As shown in Figure 3-3, the most effective dual-catalysts was found to be Sn-beta and Amberlyst-15 that has shown LA yield of 41 % of the theoretical maximum.

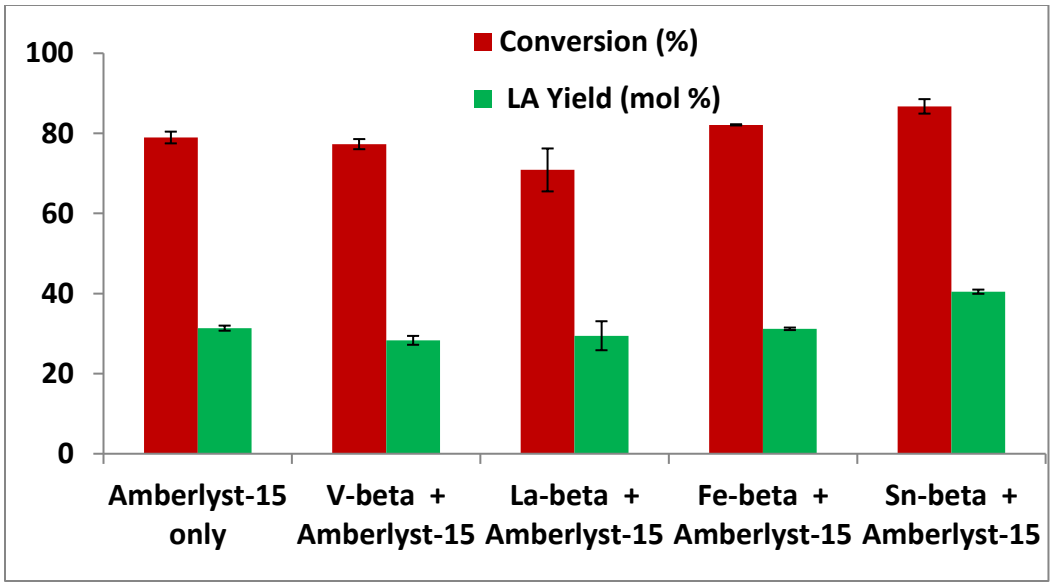

Figure 3-3 Conversion of glucose to LA using dual solid-acid catalysts. Reaction conditions: 10% glucose, 2.2 g total catalyst/g glucose, Amberlyst-15 to Lewis acid catalyst ratio 10, 14 0 °C and 12 h.

Sn-beta and Amberlyst-15 was therefore selected as the dual solid-acid catalyst system for further investigation. Figure 3-4 shows the glucose conversion and yield data of the key products obtained from duel solid-acid experiments. Notable in the data of Figure 3-4 and Figure 3-5 was that the LA yield of 44 % was achieved with a conversion of 92 %. It occurred at 140 °C, after 15 hours of reaction. On the other hand, with Amberlyst-15 alone, maximum LA yield reached only 37%, which occurred after 24 hours. The results prove that combining the best sides of the two catalysts is effective in raising the yield of the LA and reducing the reaction time and/or the amount of the catalyst. Sn-beta's capability in rapid isomerization of glucose into fructose and its transformation to LA by Amberlyst-15 reduces the formation of unwanted side products, such as soluble polymer and humins; hence a higher LA yield was achieved.

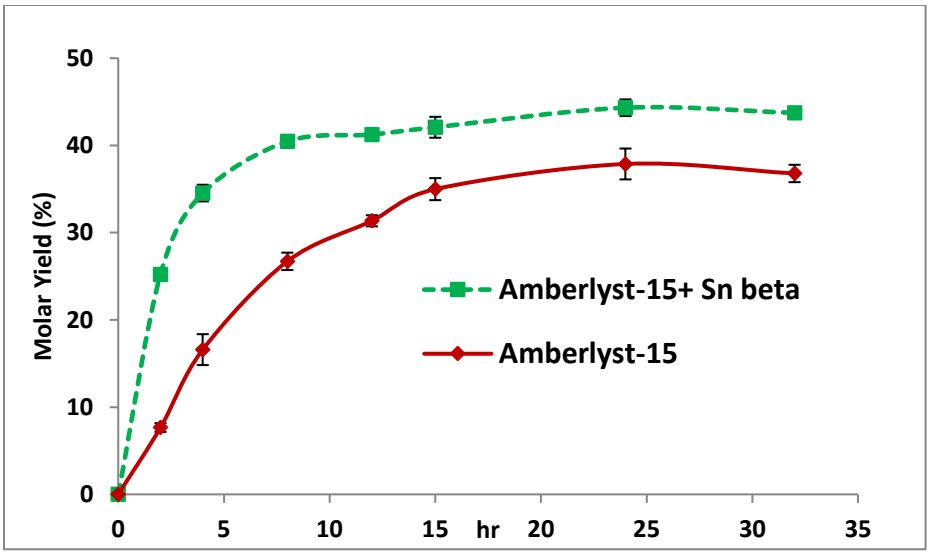

Figure 3-4 LA yield using dual solid-acid catalysts. Reaction conditions: 10% glucose, 2.2 g catalyst/g glucose, Amberlyst-15 to Sn-beta ratio 10, 140 °C.

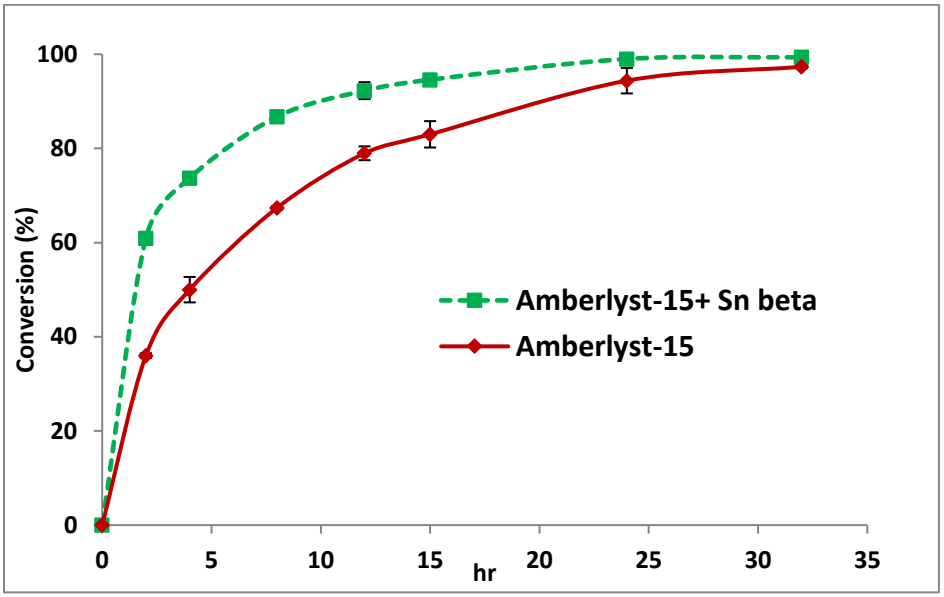

Figure 3-5 Conversion of glucose using dual solid-acid catalysts. Reaction conditions: 10% glucose, catalyst loading 2.2 g catalyst/g glucose, Amberlyst-15 to Sn-beta ratio 10,140 °C.

Production of LA from hexoses involves isomerization, dehydration, fragmentation, reversion, and condensation reactions. Two schools of thought have been reported with regard to the HMF formation from C_6 sugars in literature. One pathway postulates that the isomerization of glucose into fructose is the primary reaction pathway together with a small amount of mannose (Choudhary et al., 2013; Moliner et al., 2010). Then fructose is converted to HMF by dehydration and subsequently hydrolyzes to form levulinic and formic acids. The other theory suggests that dehydration of glucose does not involve the isomerization of glucose to fructose as the first step of the reaction. According to this theory, glucose is converted into HMF through cyclization of the 3-deoxyglucosone (3-DG) intermediate formed from the open-ring form of glucose (Chidambaram & Bell, 2010; Locas & Yaylayan, 2008). The relatively low conversion of glucose to HMF is observed due to the low propensity of glucose to exist in an open ring form as well as many other side reactions of 3-DG (Locas & Yaylayan, 2008).

The data of Table 3-4, especially on Sn-beta, show that both yield of LA and conversion of hexose are always higher when fructose is used as the reactant than glucose. Since Sn-beta is the only catalyst that is responsible for glucose to fructose isomerization and subsequent reaction, we conclude that isomerization of glucose into fructose is the first step in production of HMF. If glucose to fructose isomerization were not the first step then higher glucose conversion along with more LA yield from glucose would have been seen. Glucose isomerization to fructose in acidic solution proceeds by way of an intramolecular hydride shift mechanism between the carbonyl-containing C-1 and the hydroxyl-bearing C-2 of glucose. The solid Lewis acid catalyst Sn- beta promotes the carbonyl oxygen atom to facilitate a hydride shift mechanism (Moliner et al., 2010; Roman-Leshkov et al., 2010) . Once formed, fructose can be converted to HMF through the intermediate fructofuranosyl cation from its cyclic forms (Locas & Yaylayan, 2008).

Computational molecular model studies also corroborated the generation of fructofuranosyl intermediates in the formation of LA and HMF from glucose and fructose, respectively (Assary et al., 2012; Assary et al., 2011; Maldonado et al., 2012). Although, our findings support the formation of HMF from glucose proceeds via fructose, we do not rule out the other pathway, which is cyclization of 3-deoxyglucosone (3-DG) intermediate formed from the open-ring form of glucose, as it may occur in the formation of HMF with different acid catalyst and conditions.

Scheme 3-2 Proposed mechanism of acid catalyzed production of LA from glucose in aqueous phase.

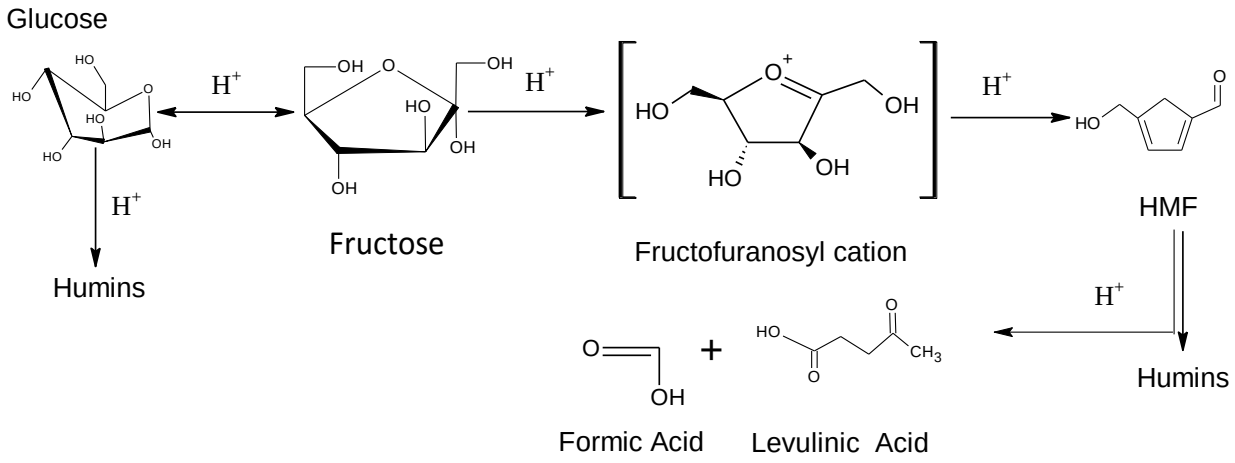

3.4.3 Catalyst stability test

Stability test was done first on the Sn-Beta catalyst. For this purpose, batch reaction was carried out for 20 minutes under the conditions of 10% glucose, catalyst loading 0.5 g catalyst/g glucose, temperature 140 °C and the conversion at this point was taken as the relative activity. It was repeated five times, each time using fresh glucose. As shown in Figure 3-6, the glucose conversion decreased from 62 % to 52 % after five consecutive batch runs.

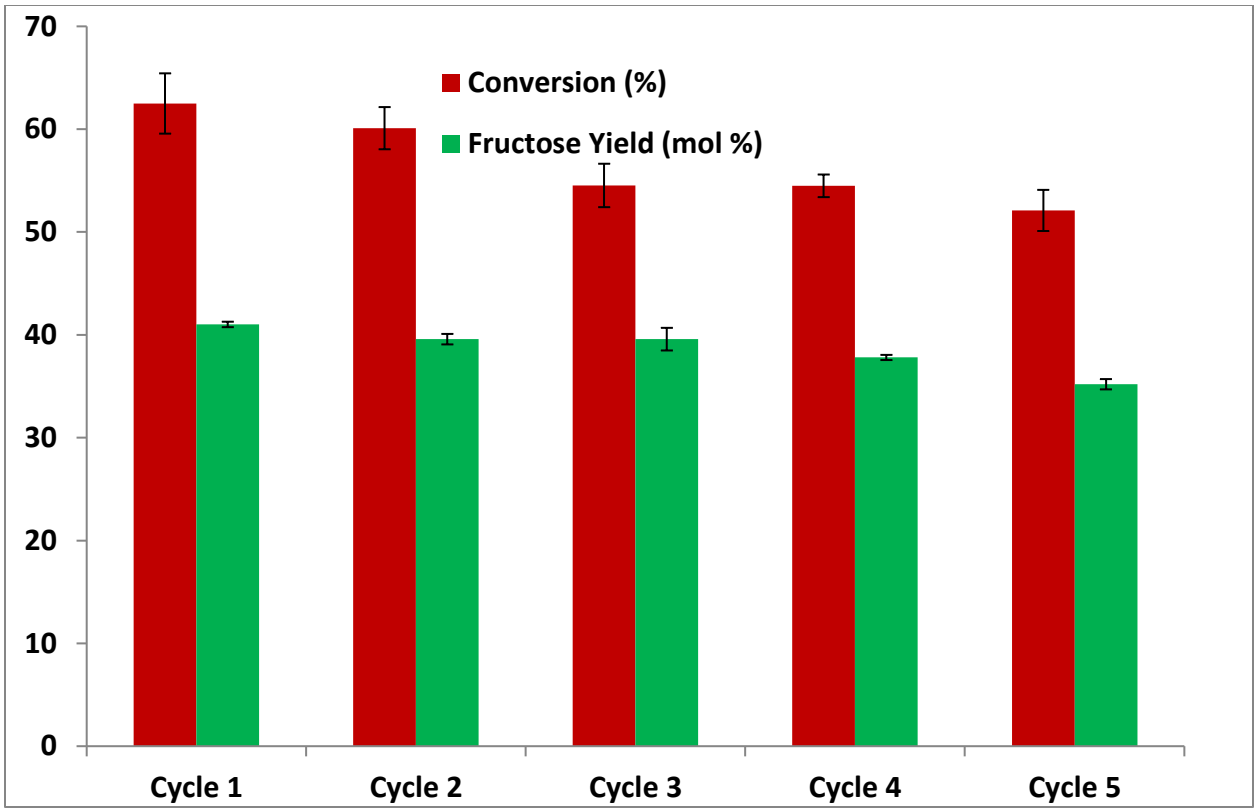

Figure 3-6 Stability test of Sn-beta in glucose isomerization to fructose. Reaction conditions: 10% glucose, catalyst loading 0.5 g catalyst/g glucose 140 °C , 20 min.

The relative activity profile in Figure 3-9 (a) indicates that deactivation of Sn-Beta follows the first order deactivation pattern with deactivation constant (k_d) of 0.14 h^{-1}, which is equivalent to 5 hours of half-life. BET surface area and pore volume of the used catalyst significantly decreased after repeated use (Table 3-2). From this and the SEM pictures of Figure 3-9-a-b, humin deposition on the surface of catalyst appears to be the main cause of deactivation. Our deactivation data do not agree with that of Moliner et al. (2010) who reported that Sn-beta maintained its original activity and product distribution after 3rd-cycle. The difference in synthesis method of the catalyst and the reaction conditions may be the reason for the difference.

To regenerate the catalyst activity, Sn-Beta was calcined at 550 °C for 6 h between the cycles 2 and 3.

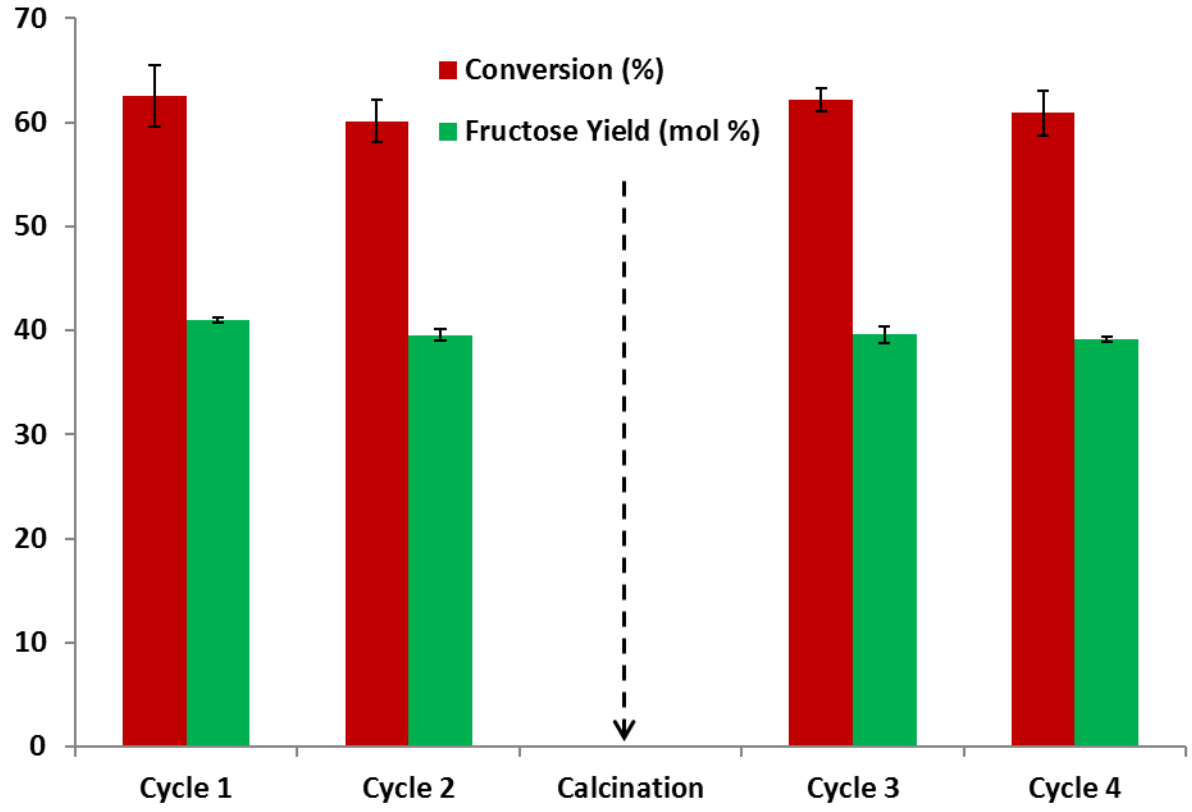

Figure 3-7 Regeneration of Sn-beta in glucose isomerization to fructose. Reaction conditions: 10% glucose, 0.5 g catalyst/g glucose, 140 °C , 20 min. Calcination performed between cycles 2 & 3

Data of Figure 3-7 show that the catalyst was fully restored to regain its original activity and the product distribution. The stability test for Amberlyst-15 was also done by a procedure slightly difference than that of Sn-Beta. LA production from fructose was carried out five times at 140 °C. The fructose conversion decreased from 32% to 12% with Amberlyst-15 after five consecutive run as shown in Figure 3-8.

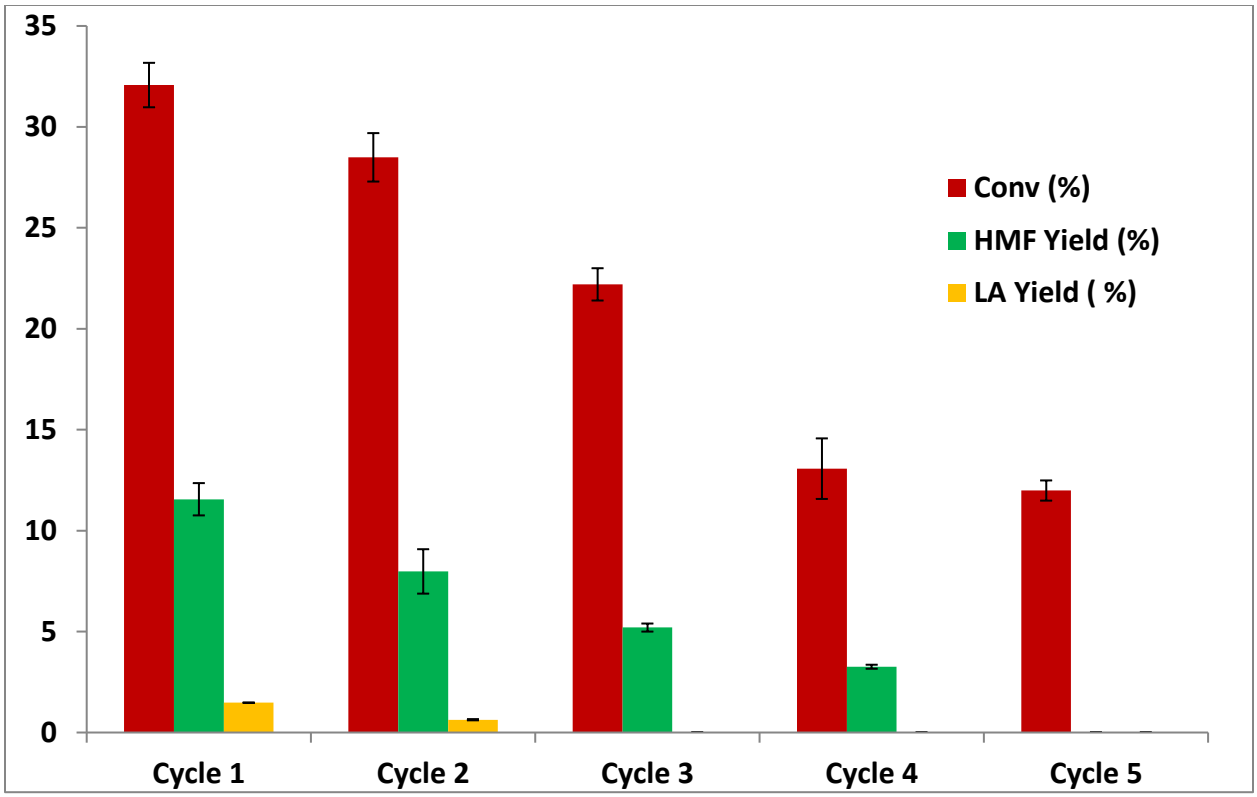

Figure 3-8 Recycling study of Amberlyst-15 in LA production from fructose. Reaction conditions: 10% fructose, 0.25 g catalyst/g fructose, 140 °C, 1h.

Neither LA nor HMF was detected after five cycle indicating one hour reaction time was not sufficient to produce LA under the reaction conditions applied in these tests. Here also, a plausible cause for this drop is deposition of organics such as humins formed during the reaction which is seen in figure 3-10d .The reduction of BET surface area also play an important role to lower the catalyst activities (Table 3-2). The activity of Amberlyst-15 is reduced more than 20 % per batch cycle as shown in Figure 3-9(b). An effective method of reactivation of Amberlyst-15 is yet to be developed.

(a) Activity of Sn-beta in glucose to fructose isomerization. Reaction conditions: 10% glucose, 0.5 g catalyst/g glucose, 140 °C, k_d (deactivation rate constant) = 0.14 h^{-1}, equivalent to half-life of 4.9 h.

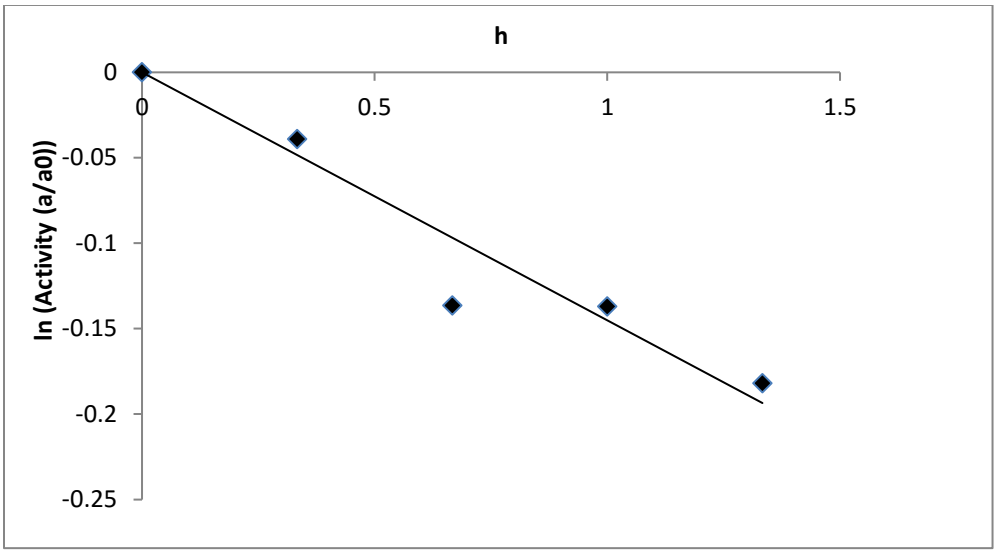

(b) Activity of Amberlyst-15 in LA production from fructose. Reaction conditions: 10% fructose, catalyst loading 0.25 g catalyst/g fructose 140 °C, k_d (deactivation rate constant) = 0.03 h^{-1}, equivalent to half-life of 23h.

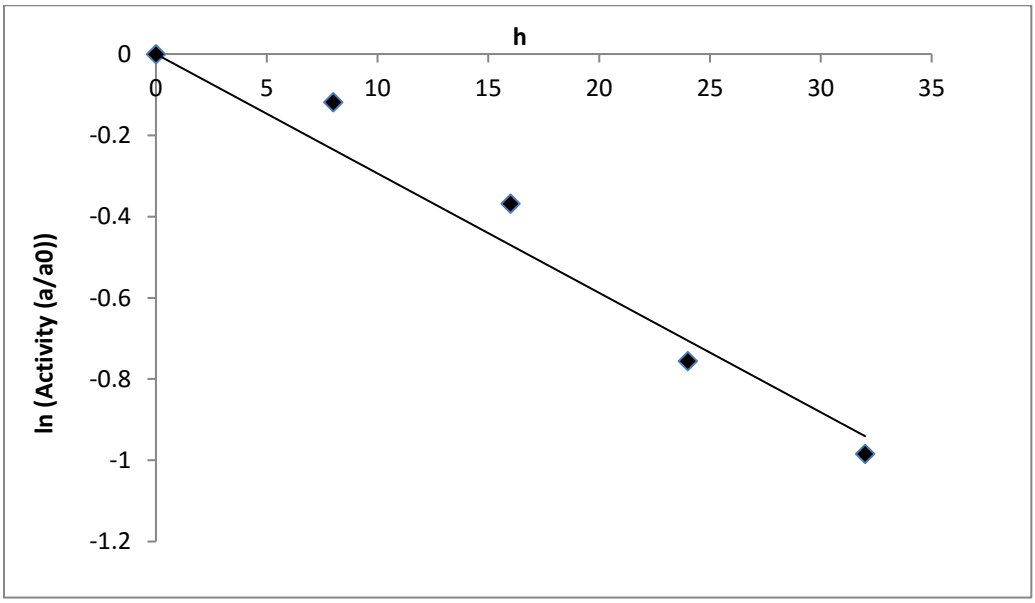

Figure 3-9 Stability test of Sn-beta and Amberlyst-15.

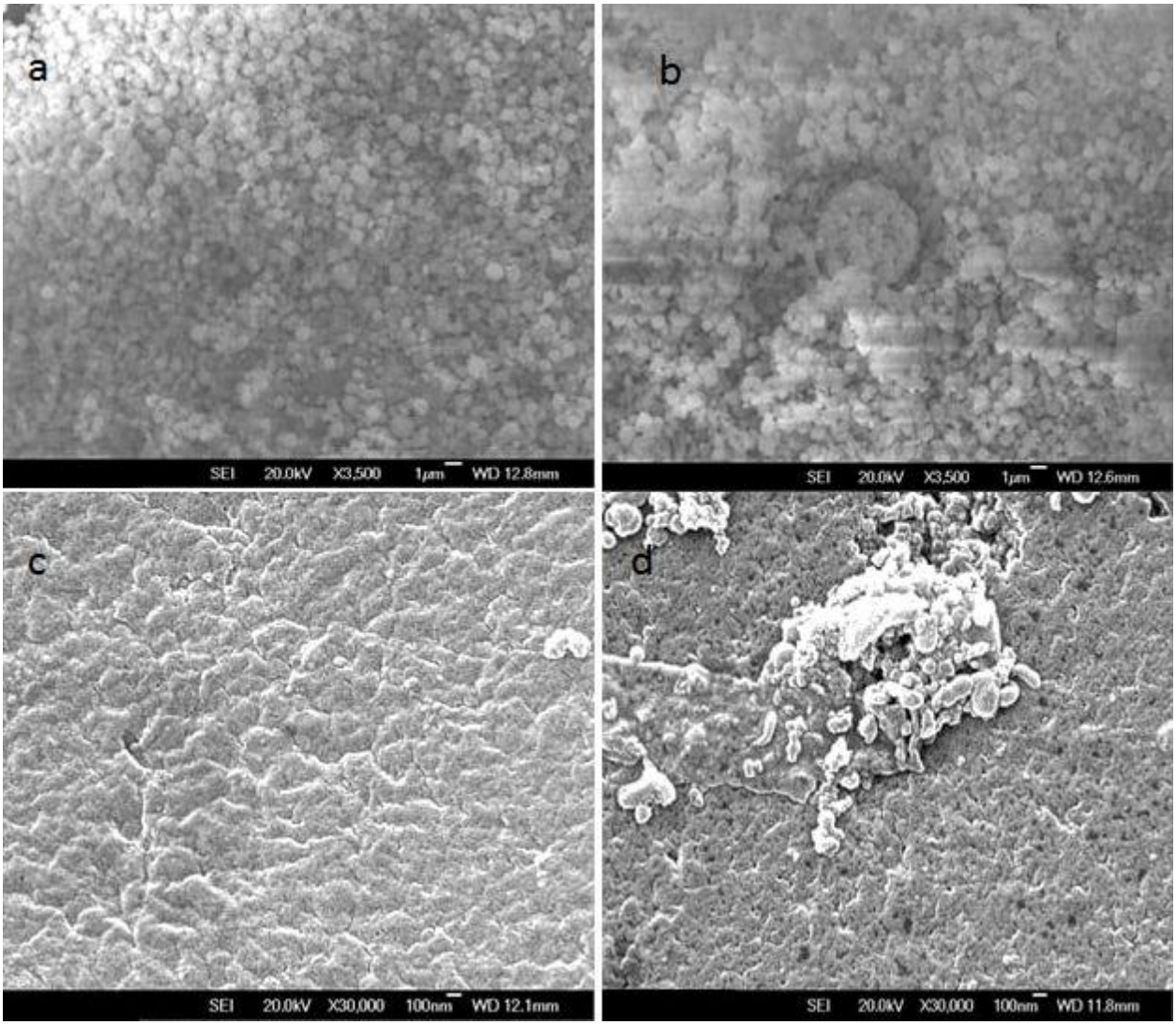

Figure 3-10 Scanning electron microscope images of a) Fresh Sn-beta b) Used Sn-beta c) Fresh Amberlyst-15 d) Used Amberlyst-15

3.5 Conclusions

Acid-catalyzed synthesis of LA from glucose involves a number of sequential and branching reactions including isomerization, dehydration, and rehydration. A cation exchange resin, Amberlyst-15, is a proven solid-acid catalyst capable of converting glucose into LA. It is primarily a Brønsted acid, but also carries limited Lewis acid sites. Its low Lewis acid activity limits the yield of LA to the level of 37% of the theoretical maximum. As a means to improve the product yield, Sn-Beta embodied on large-pore Zeolite was synthesized and found to be highly effective in the glucose isomerization to fructose, a rate-limiting step in the overall conversion process. Concurrent use of this catalyst along with Amberlyst-15 significantly improved the yield of LA over that of Amberlyst alone, from 37% to 44%. Stability study has shown that both of these catalysts deactivates during the reaction, showing the respective deactivation rate constants of 0.14 h^{-1} and 0.03 h^{-1} for Sn-beta and Amberlyst-15. The main cause of deactivation was humin deposit on the surface of catalyst surface for both catalysts. Activity of Sn-Beta can be fully recovered by calcination.

Chapter 4

Simultaneous saccharification and co-fermentation of paper mill sludge mixed with hemp hurd for the production of lactic acid

4.1 Abstract

Mixture of paper mill sludge and hemp hurd, was investigated as a raw material for lactic acid production by way of simultaneous saccharification and co-fermentation (SSCF). Hemp hurd is an industrial waste material generated during pulping of hemp for bast fiber production. The SSCF was carried out employing Cellic C-Tec2 enzyme and *Lactobacillus pentosus* (ATCC-8041) without pH control utilizing the ash content existing in the sludge (primarily calcium carbonate) as a neutralizing reagent. Calcium lactate is therefore obtained as the end product of the SSCF. The neutralizing capacity of the ash in the sludge is high enough to accommodate additional lignocellulosic feedstock. From SSCF experiments applying various ratio of the two solid feedstocks, the sludge to hemp hurd ratio of 3:1 was found to be the minimum in that it maintains the pH at near optimum and provided highest lactic acid yield. From multiple runs of SSCF, lactic acid concentration of 52-67 g/L and lactic acid yield of 0.69-0.82 g/g sugars were achieved from the mixed feed under the conditions of 10-12 % solid loading and 15 FPU/g-glucan enzyme loading.

4.2 Introduction

Lactic Acid is an important industrial commodity with large and fast growing market due to its widespread applications, mainly in food, chemical, cosmetic, and pharmaceutical industries (Xu et al., 2006). Currently, most lactic acid is produced by microbial fermentation of carbohydrates due to low temperature, low energy consumption, and high product specificity as it produces a desired stereoisomer, optically pure L-(+)- or D-(−)-lactic acid when the appropriate microorganism is selected as the lactic acid producer (John et al., 2007). The main obstacle for the fermentative production of lactic acid is the high cost of feedstocks (Abdel-Rahman et al., 2013). Therefore, lignocellulosic feedstocks are promising for lactic acid production. However, the biochemical conversion of lignocellulosic feedstock requires several processing steps to convert structural carbohydrates to monomeric sugars, e.g., glucose, xylose, arabinose, and mannose. These monomeric sugars can be fermented to lactic acid through different types of microorganisms (Abdel-Rahman et al., 2013).

The main objective of this study is to utilize wastes materials, especially available from pulp and paper plants to reduce the raw material cost. Among the various wastes from pulp and plants, paper mill sludge, emerge as the most attractive feedstock as it has a number of advantages (Shi et al., 2015). Being a waste material, the cost of disposal is about $20-$50 per wet ton sludge (Kang et al., 2010). Sludge can be biologically converted to value-added products without pretreatment due to its high carbohydrate content and well-dispersed structure (Guan et al., 2016). Pretreatment is one of the major cost factors in bioconversion of lignocellulosic materials. Its elimination can significantly reduce the processing cost (Kim et al., 2003). Hemp hurd, available as a waste material from bast fibers production which is currently discarded as solid waste, can also be considered as a promising feedstock for lactic acid production due to its greater sustainability and

low cost compared to refined sugars (Gandolfi et al., 2015). Comparing to the paper mill sludge, raw hemp hurd consists of a similar amount of cellulose (40-45%) but a much higher amount of hemicellulose (around 18-24%). Due to lower degree of cellulose polymerization and crystallinity the treated hemp hurd might be somewhat amenable for bioconversion without further pretreatment same as paper mill sludge (Gandolfi et al., 2013).

A large number of studies related to lactic acid fermentation through Simultaneous saccharification and fermentation (SSF) using Lactobacillus (LAB) from lignocellulosic feedstocks have been investigated (Abdel-Rahman et al., 2011; Bustos et al., 2005; Monteagudo et al., 1997; Zhu et al., 2007). The growth of LAB i.e. lactic acid production is significantly affected by pH, nutrient concentration, substrate concentration, products concentration, and temperature (Abdel-Rahman et al., 2011). For an example, low pH has an inhibitory effect on cellular metabolism and lactic acid production (Adachi et al., 1998). Hence, neutralizing agents such as calcium carbonate, sodium hydroxide, or ammonium hydroxide must be added to keep the pH at a constant value in order to reduce the inhibitory effects of low pH (Hofvendahl & Hahn-Hagerdal, 2000). Since paper mill sludge is a pretreated material from Kraft pulping, which contains mainly glucan, xylan and ash ($CaCO_3$), we hypothesize that both glucan and xylan can be directly converted into lactic acid in a SSF process without pH control. Besides, treated hemp hurd which contain mostly glucan can be converted into lactic acid using sludge $CaCO_3$ as a buffer reagent simultaneously.

In this study, we explored a novel process scheme wherein the two different carbohydrate resources available from pulp mills are biologically converted to lactic acid. Here, we used three different mixing schemes such as sludge rich mixture (sludge and hemp hurd = 75:25), equal mixture (sludge and hemp hurd = 50:50), and hemp hurd-rich mixture (sludge and hemp hurd = 25:75). The main objective of this study is to investigate the technical feasibility of one-step

bioconversion of mixed feedstock into lactic acid through simultaneous saccharification and co-fermentation (SSCF).

4.3 Materials and Methods

4.3.1 Feedstock and reagents

The paper mill sludges were collected a Kraft paper mill in Alabama. Two different types of sludges were used in the study. The primary sludge which was collected from the primary wastewater clarifier unit was a discharge from the paper machine and the digester and the deink sludge also known as recycle sludge was obtained from reprocessing unit (Kang et al., 2010) Hemp hurd and pretreated hemp hurd, provided by Pure Vision Technology Inc. (Fort Lupton, CO), were examined in this work. Hemp hurd were pretreated by soaking in 2% (w/w) sodium hydroxide solution at 200 °C for 10 minutes and pretreatment was done at Fort Lupton location. All the feedstocks as received were stored in 4 °C until further analysis. The chemical compositions of paper mill sludge and hemp hurd were determined according to the NREL standard procedure (NREL/TP-510-42618). Lactic acid, glucose, xylose, acetic acid, used in this study purchased from VWR (Radnor, PA) were of analytical grade and used without purification. Recycle sludge and pretreated hemp hurd are termed as sludge and hemp hurd, respectively hereafter.

4.3.2 Enzymes and microorganism

The cellulose enzyme (Cellic C-Tec 2), a generous gift from Novozymes (North America, Franklinton, NC), having specific enzyme activity of 119 FPU/mL and total protein number of 255 mg protein/mL was applied to feedstocks. *Lactobacillus pentosus* (ATCC-8041), purchased from American Type Culture Collection (ATCC), was used as the microorganism in the SSCF.

4.3.3 Culture maintenance and inoculum preparation

The stock of *Lactobacillus pentosus* was maintained at -20 °C in 50% (v/v) of glycerol. The spores were revived by transferring 1 mL of spore into 50 mL of Lactobacilli MRS Broth (Acumedia) and cultivated for 36 h as seed inoculum anaerobically at 37 °C. The cultured bacteria (3 mL) were inoculated into 50 mL fermentation medium. The lactic acid fermentation medium formula was as follows (g/L): yeast extract, 5; protease peptone, 5; KH_2PO_4, 0.5; K_2HPO_4, 0.5; ammonium acetate, 1; $MgSO_4$ $7H_2O$, 0.5; $FeSO_4$ $7H_2O$, 0.05; $MnSO_4$ H_2O, 0.12; NaCl, 0.01.

4.3.4 Enzymatic hydrolysis

The cellulose enzyme (Cellic C-Tec 2) was applied to pretreated feedstocks. The enzymatic digestibility tests were carried out in 125 mL Erlenmeyer flasks at 50°C, and pH 4.8 using 0.05 M sodium citrate buffer in an incubator shaker (New Brunswick Scientific, Innova-4080) agitated at 150 rpm. Sodium azide was added into the reaction media to maintain sterile conditions. The digestibility tests for treated hemp hurd were performed with 1 g dry hemp hurd /50 mL of total reactant volume. The hydrolysate samples taken at different time period (12, 24, 48, and 72 h) were analyzed in HPLC to measure the level of glucose and xylose. The released glucose was used to calculate the enzymatic digestibility according to the following formula (Kothari & Lee, 2011).

$$\text{Digestibility}(\%) = \frac{\text{Glucose released(g)} + 1.053 \times \text{Cellobiose released (g)}}{1.111 \times \text{Glucan added (g)}} \times 100$$

4.3.5 Simultaneous Saccharification and Co-Fermentation (SSCF)

The lactic acid fermentation of paper mill sludge and hemp hurd were carried out in 125 mL serum bottle with a working volume of 50 mL applying various solid loadings. During SSCF, the sludge was suspended in fermentation medium and put into the flasks to reach a total working volume of

50 mL. The SSCF tests of the hemp hurd were carried out with fermentation medium and with addition of CaCO3 to neutralize pH of the medium. In the SSCF of sludge and hemp hurd mixtures, the feedstocks were suspended in fermentation medium without adding any $CaCO_3$. The sludge containing 29.3 wt. % ash acts as a neutralizing agent. The bottles were loaded with feedstocks and fermentation medium, autoclaved at 121 °C for 15 min. Cellulase enzyme (C-Tec2) was added at different enzyme loading (15-25) FPU/g-glucan after sterilization. Once anaerobic condition was developed by sparging nitrogen gas into the headspace of the bottle, the actively growing seed-culture transferred into bottle. Then the sealed bottles were placed into incubator shaker (New Brunswick Scientific, Innova-4080) at 37 °C with 150 rpm. The hydrolysate samples taken at different time period (12, 24, 48, 72, 96 and 120 h) were analyzed in HPLC to measure glucose, xylose, acetic acid and lactic acid.

$$\text{Lactic acid yield}(\%) = \frac{\text{Lactic acid concentration}(\text{g/L})}{\text{Initial hexose concentration (g/L)}} \times 100$$

4.3.6 Analytical method

The compositions of the feedstocks were analyzed by the NREL standard protocols to determine sugar components in carbohydrates, lignin, and ash. Each sample was analyzed duplicate. The moisture content was measured by infrared moisture balance (Denver Instrument, IR-30). Sugars were determined were determined by HPLC system equipped with Bio-Rad HPX-87H column (Hercules, CA), refractive index detector (Shodex, NY), Alcott 708 Autosampler, PeakSimple Chromatography Data Systems (Torrance, CA). Ultrapure DI water was used as a carrier at a flow rate of 0.55 ml/min for the Bio-Rad HPX-87P. The aqueous solution of 0.005 M sulfuric acid with a flow rate of 0.55 ml/min was selected as a mobile phase for Bio-Rad HPX-87H column. In both cases, the columns were operated at 85 °C. The analysis for a sample was completed within 30 minutes.

4.4 Results

The experimental work in this investigation was structured to perform the following specific tasks: characterization of the sludge and hemp hurd including the bioconversion compatibility and assessment of the SSCF as a bioconversion process converting the mixed feed to lactic acid.

4.4.1 Composition

The chemical compositions of sludge and hemp hurd are shown in Table 4-1. Glucan and xylan are the two major organic components in the sludge. Sludge contains high amount of ash, about one third of the total mass and the main component of the sludge is $CaCO_3$ (Kang et al., 2010). On the other hand, the hemp hurd are composed of mainly glucan (39%), xylan (22%) and lignin (29%). The treated hemp hurd contain 85 % glucan and 11 % lignin as pretreatment removes almost all xylan and a significant amount lignin; thus increasing glucan percentage in the feedstock.

Table 4-1 Composition of paper mill sludge and hemp hurd.

	[a] Hemp hurd	Treated Hemp hurd	[b] Primary sludge	Deink sludge
Glucan (%)	39.3	84.9	43.7	51.8
Xylan (%)	22.7	1.5	10.5	12.6
Mannan (%)	0.0	0.0	1.3	1.1
Lignin (%)	28.5	10.5	3.9	2.5
Ash (%)	1.6	1.3	38.3	32.7

In this study, deink sludge and pretreated hemp hurd were used as feedstocks. [a] Hemp hurd and [b] primary sludge shown only as reference.

4.4.2 Enzymatic hydrolysis of hemp hurd

To assess the compatibility of hemp hurd with sludge on the SSCF, enzymatic hydrolysis tests were performed at 2 % solid loading under 10-20 FPU/g-glucan and. Although the optimum temperature for enzymatic hydrolysis was 50°C, tests were made at 37°C in consideration of SSCF

investigated in this work. The digestibility data of hemp hurd was then compared with sludge data based on our previous report as shown in Table 4-2 (Kang et al., 2010).

Table 4-2 Enzymatic digestibility data of sludge and hemp hurd

Feedstocks	Enzyme and its loading	Protein Number (mg /g-glucan)	72 h glucan digestibility	72 h xylan digestibility
[a]Sludge	Spezyme CP (15 FPU)+ Novozyme-188 (30 NBU)	27	30.2	28.7
[a]Hardwood pulp with 0.5 g CacCO3/g-glucan	Spezyme CP (15 FPU)+ Novozyme-188 (30 NBU)	27	32.9	25.2
[a]Hardwood pulp with 0.05 M citrate buffer (pH=4.8)	Spezyme CP (15 FPU)+ Novozyme-188 (30 NBU)	27	82.0	56.8
Pretreated Hemp hurd with 0.05 M citrate buffer (pH=4.8)	Cellic C-Tec 2 (10 FPU)	16	48.4	-
Pretreated Hemp hurd with 0.05 M citrate buffer (pH=4.8)	Cellic C-Tec 2 (15 FPU)	24	58.7	-
Pretreated Hemp hurd with 0.05 M citrate buffer (pH=4.8)	Cellic C-Tec 2 (25 FPU)	40	69.6	-

[a] Data was adapted from the literature (Kang et al., 2010). Hardwood pulp was taken as the reference substrate because the composition is similar to the organic portion of the sludges.

However, hardwood pulp was taken as the reference substrate because the composition is similar to the organic portion of the sludges. The 72-h glucan digestibility of pretreated hump under the enzyme loading of 25 FPU/g-glucan of Ctec-2 (= 40 mg protein/g-glucan) was found to be 70%. On the other hand, 72-h glucan digestibility of hardwood pulp is 82% with (15 FPU/g-glucan of Spezyme-CP) and β-glucosidase (30 CBU/g-glucan of Novozyme-188) (equivalent to 27 mg protein/g-glucan). The results clearly indicate that sludge is more easily digestible than hemp hurd.

4.4.3 SSCF of sludge and hemp hurd

The SSCF of sludge was performed with a solid loading of 10% (w/v) and enzyme loading of 15 FPU/g-glucan as shown in Figure 4-1. The lactic acid concentration reached 51.8 g/L at 72 h. The maximum glucose concentration reached 3.9 g/ L which is well below the product inhibition threshold (15 g/L) (Kang et al., 2010; Shen & Xia, 2006). The xylose concentration was in the range of 1.9-2.3 g/ L during the fermentation. The acetic acid increased to 5 g/L at 48 h and was kept at 5-6 g/L until 120 h.

The SSCF of alkali-treated hemp hurd were performed with a solid loading of 10% and enzyme loading of 15 FPU/g-glucan as sown in Figure 4-2. Under these conditions, the maximum lactic acid concentration was found to be 29.5 g/L at 48 h and then stayed same until 120 h. The glucose concentration was remained low (around 1.8 g/L) throughout the fermentation. No significant amount of xylose was observed as it contains negligible amount xylose. The acetic acid was stabilized at 3.3 g/L after 72 h. The results indicated that enzymatic hydrolysis was the rate limiting step since inhibition on microbial fermentation was not observed in this case.

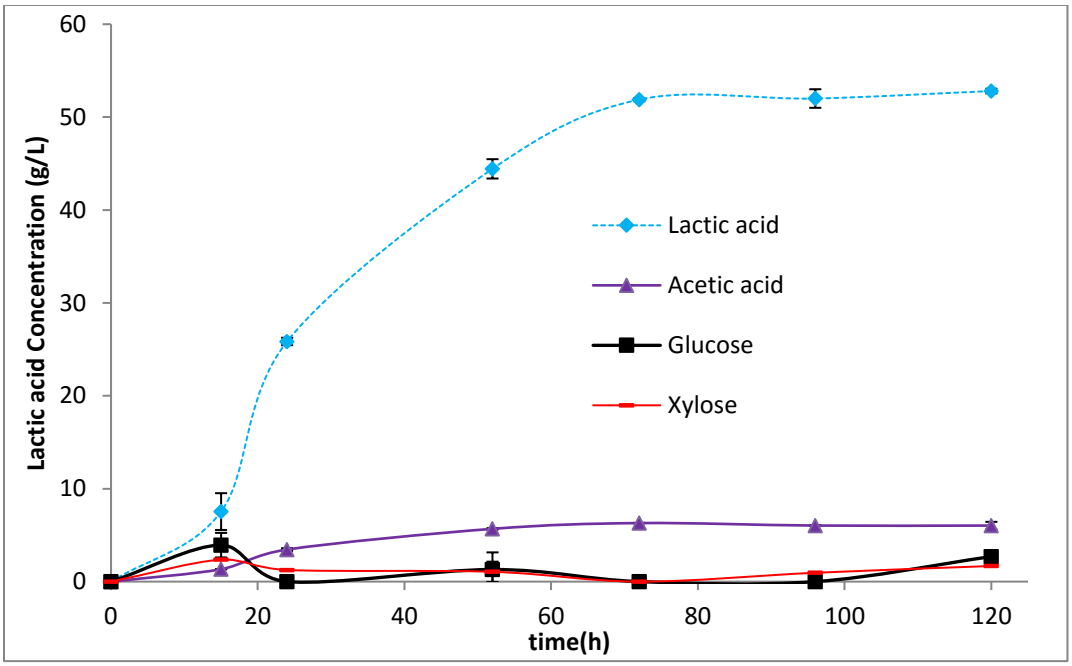

Figure 4-1 Simultaneous saccharification and co-fermentation (SSCF) of paper mill sludge under the solid loading of 10% and enzyme loading of 15 FPU/g-glucan

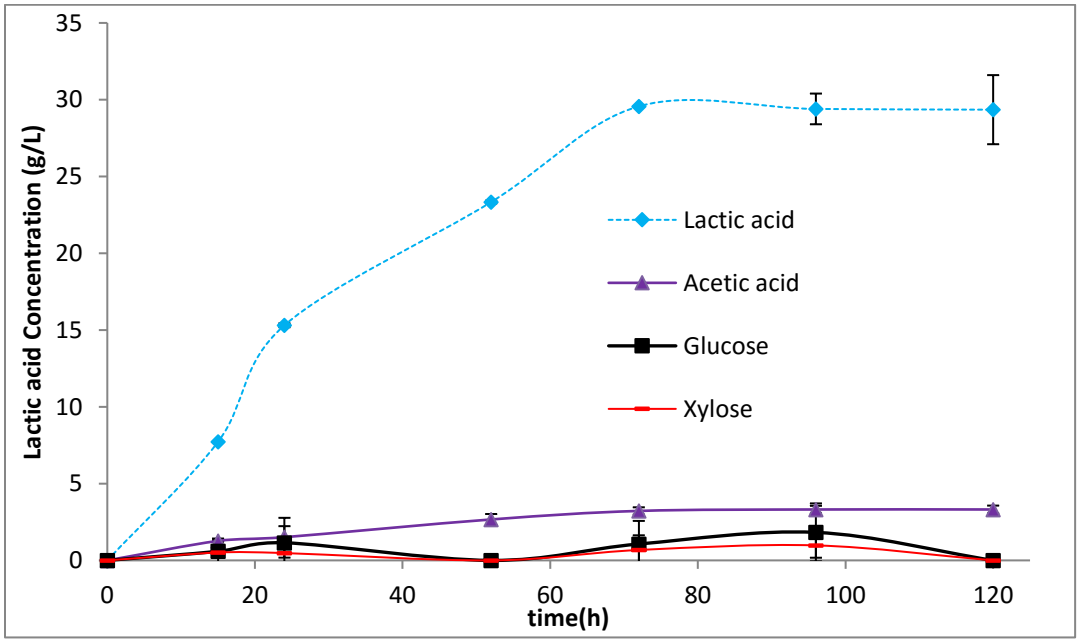

Figure 4-2 Simultaneous saccharification and co-fermentation (SSCF) of alkali-pretreated hemp hurd under the solid loading of 10% and enzyme loading of 15 FPU/g-glucan.

4.4.4 SSCF of the mixture of sludge and hemp hurd

4.4.4.1 Effect of mixing ratio on SSCF

The SSCF of the mixture were performed at three different mixing ratios of sludge and hemp hurd at 15 FPU/g-glucan under two different solid loading (5 & 10%) as shown in Figure 4-3 &4-4. Three mixing ratios were as follows- sludge rich mixture (sludge and hemp hurd = 75:25), equal mixture (sludge and hemp hurd = 50:50), and hemp hurd-rich mixture (sludge and hemp hurd = 25:75). The SSCF profiles of sludge and hemp hurd were taken as the reference substrates and plotted along with other graphs.

When the 5% solid loading was used in SSCF, the lactic acid concentration reached maximum 21.1 g/L in sludge-rich mixture and 22.4 g/L in equal-mixture at 72 h as shown in Figure 4-3a. The maximum lactic acid concentration was found to be 19.3 g/L for hemp hurd-rich mixture which occurred at 48 h. These values are equivalent to yield of 60, 60, and 48 % of lactic acid respectively (Figure 4-3b). After that, lactic acid concentrations were decreased to 18.6, 19.2, and 17.2 g/L in these mixtures respectively. The acetic acid increased to 2.9 g/L in sludge-rich mixture, 2.3 g/L in equal-mixture and 1.6 g/L in hemp hurd-rich mixture at 48 h. Then the respective concentrations were decreased to 2.3, 1.8 and 1.4 g/L at 120 h (Figure 4-3c). Figure 4-3d demonstrates that glucose started to accumulate after 72 h. It reached 2.1 g/ L in hemp hurd-rich mixture and 3.3 g/ L in equal-mixture at 120 h. However, no glucose was accumulated during SSCF of sludge-rich mixture. In sludge-rich mixture, xylose increased to 1.9 g/L at 12 h and decreased to 0.8 g/L at 48 h and then stayed in the range of (0.83 - 0.9) g/L until 120 h as shown in Figure 3e. Xylose continued to increase 2.2 g/L in equal mixture and 4 g/L in hemp hurd-rich mixture at 120 h.

a) Lactic acid concentration

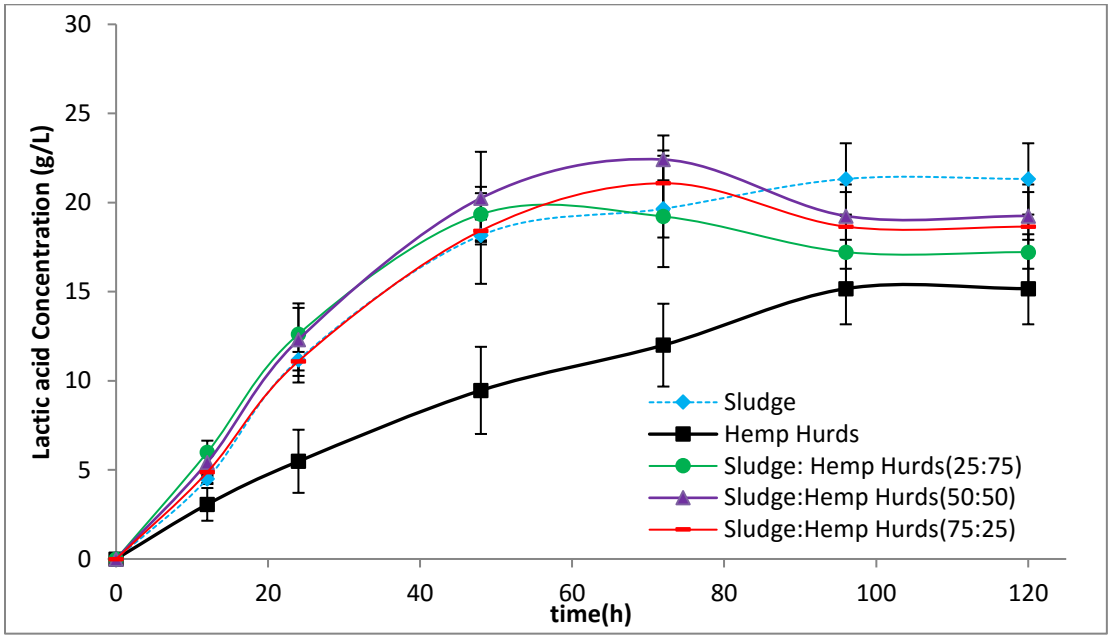

b) Lactic acid yield

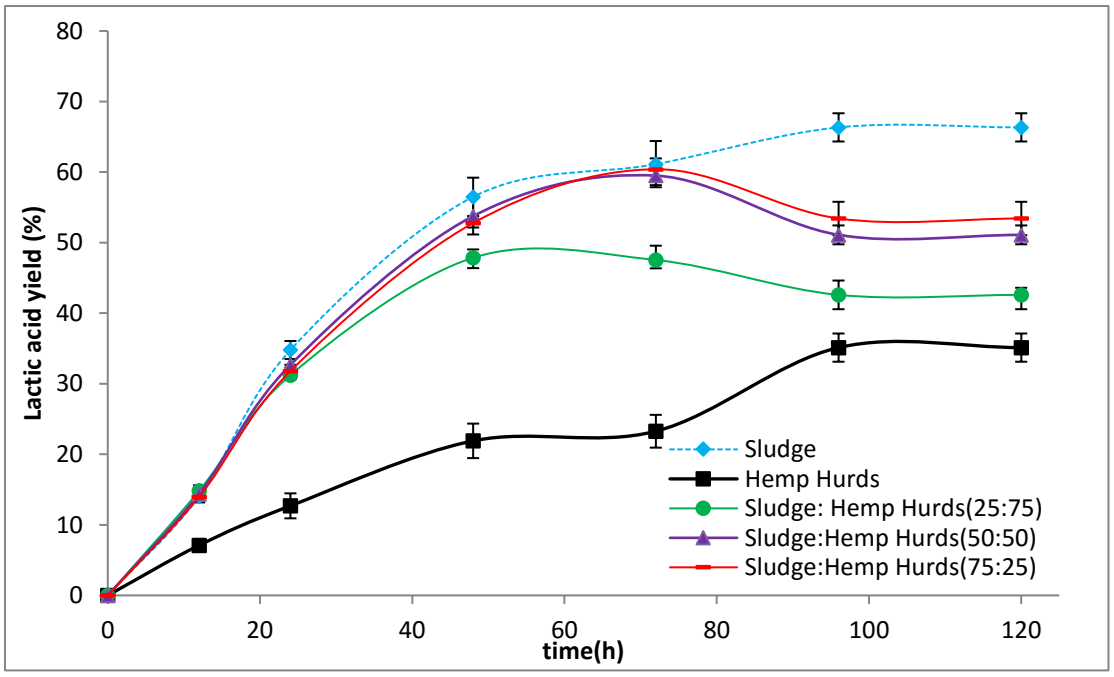

c) Acetic acid concentration

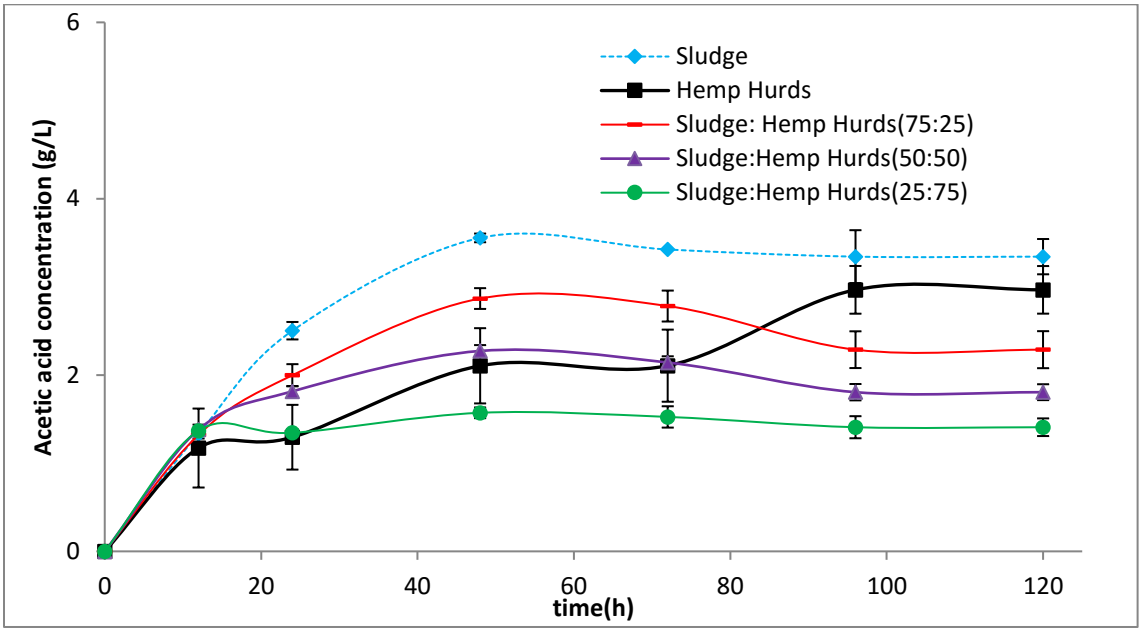

d) Glucose concentration

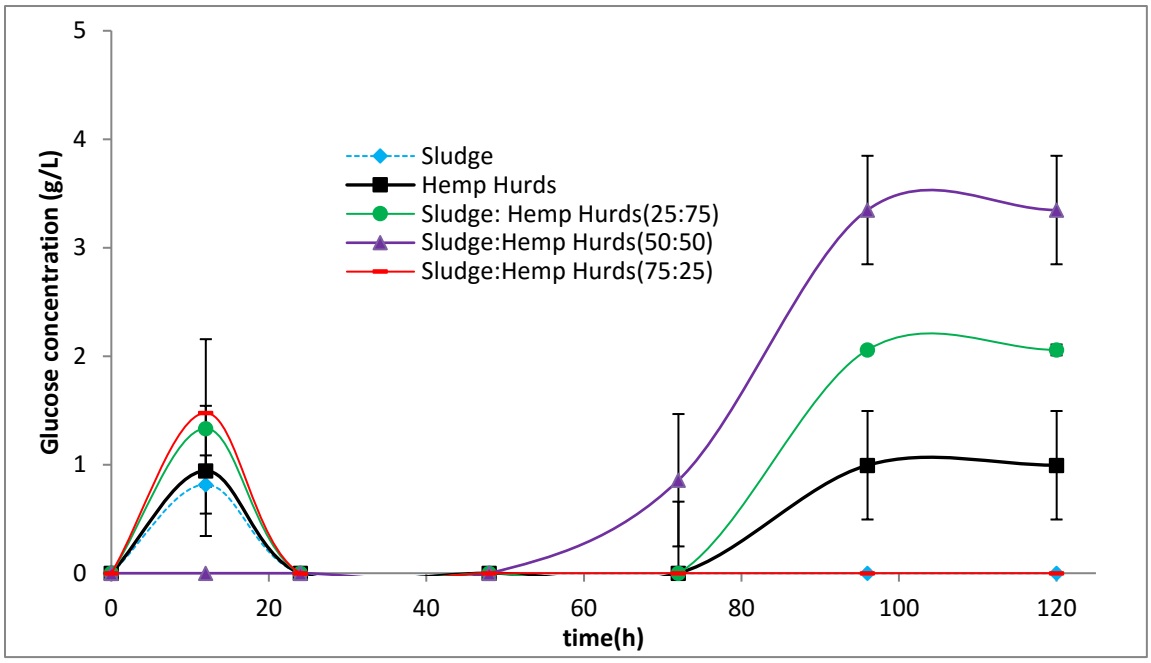

e) Xylose concentration

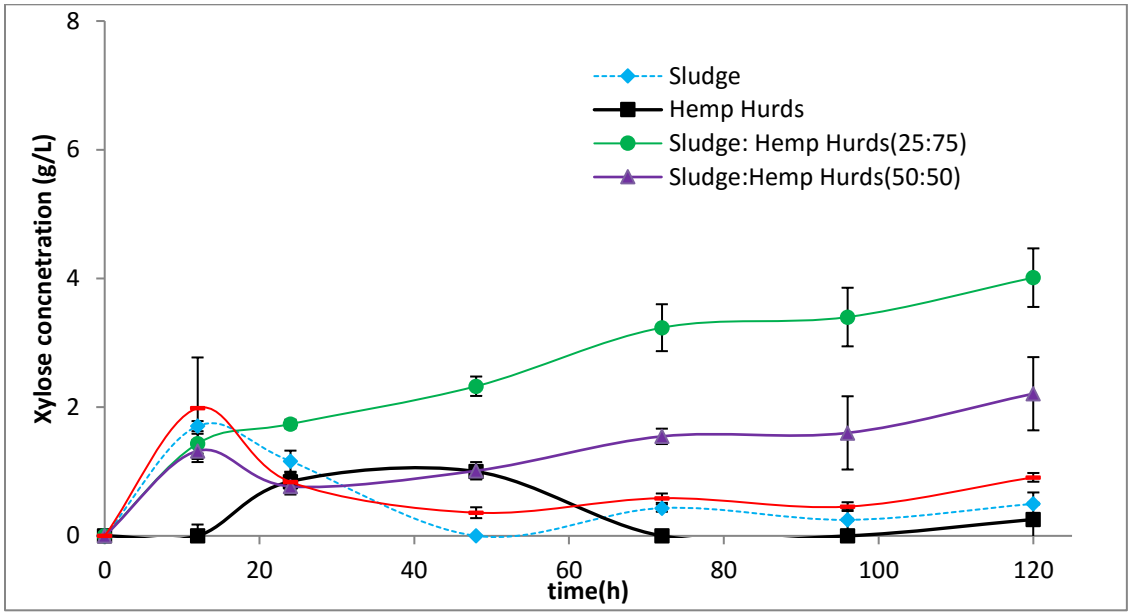

f) pH profile

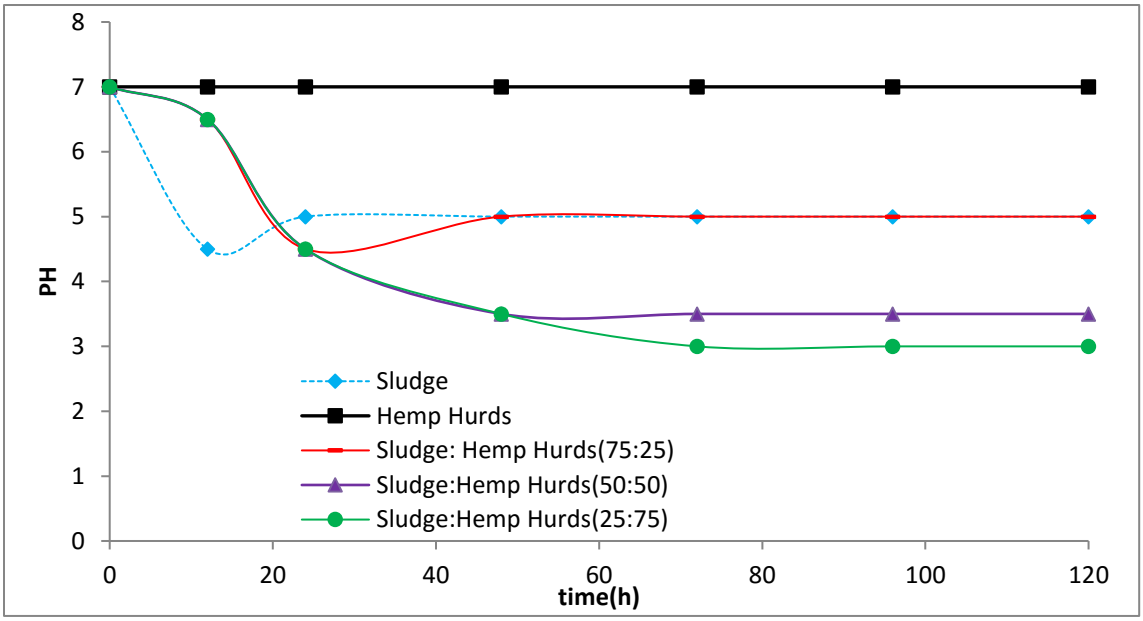

Figure 4-3 Effect of mixing ratio on simultaneous saccharification and co-fermentation (SSCF) of mixture of sludge and alkali-pretreated hemp hurd under the solid loading of 5% and enzyme loading of 15 FPU/g-glucan.

When the solid loading was raised to 10%, lactic acid concentration reached maximum 47.8 g/L (corresponding yield ≈ 69%) in sludge-rich mixture at 72 h and remained constant until 120 h (Figure 4-4a&4-4b). In equal-mixture, lactic acid increased to 38.2 g/L (yield ≈ 51 %) at 48 h and then decreased to 36.4 g/L at 120 h. The maximum lactic acid concentration was 27.6 g/L (yield ≈ 34%) for hemp hurd-rich mixture at 48 h and then decreased to 25.5 g/L at 120 h. The acetic acid concentration reached maximum at 48 h and stayed almost constant for all three mixtures. The concentrations were 4.5, 2.5 and 1.5 g/L in sludge-rich, equal and hemp hurd-rich mixture respectively (Figure 4- 4c). Glucose started to accumulate after 48 h and reached to 14.4, 10.3 and 4.1 g/L at 120 h in sludge-rich, equal and hemp hurd-rich mixtures respectively (Figure 4-4d). The xylose concentration increased to 1.5 g/L at 12 h and then stayed in the range of (1.5 – 1.9) g/L until 120 h in sludge-rich mixture (Figure 4-4e). It continued to increase 3.5 g/L in equal mixture and 3.8 g/L in hemp hurd rich mixture at 120 h.

When the 12.0% solid loading was used in SSCF with the mixture of (sludge and hemp hurd=80:20), the maximum lactic acid concentration was obtained 66.5 g/L (equivalent to 81% yield based on hexose sugar) as shown in Table 4-3.

a) Lactic acid concentration

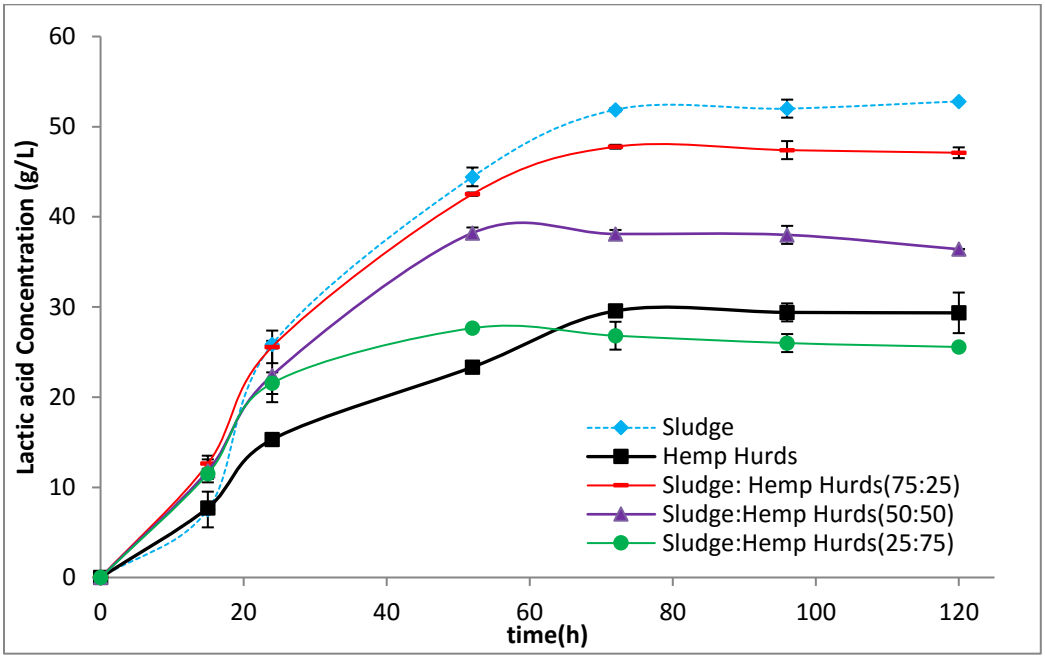

b) Lactic acid yield

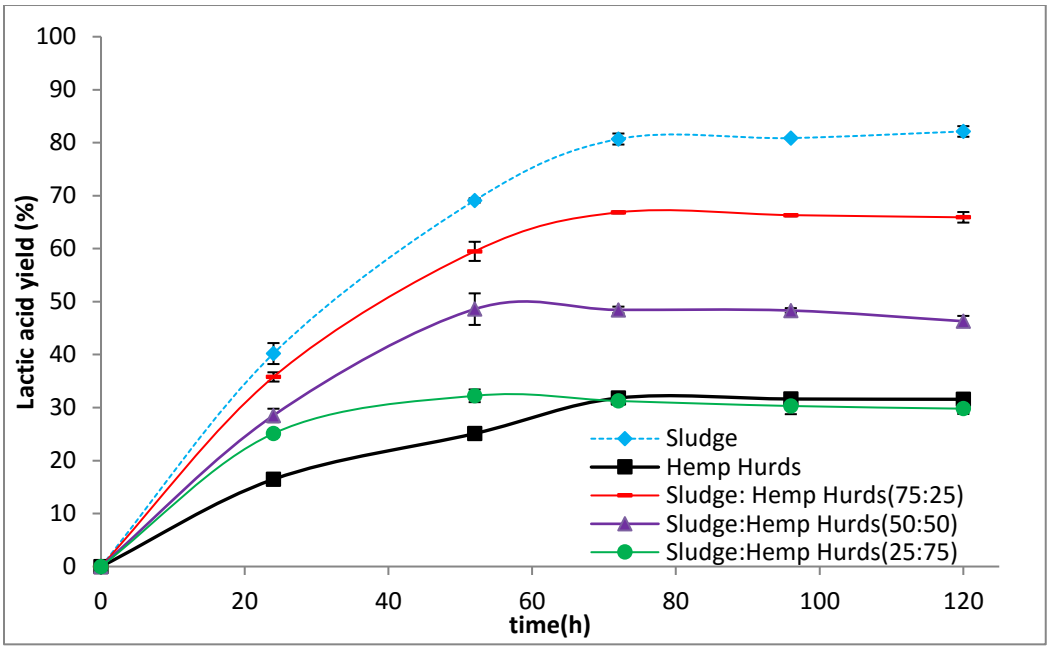

c) Acetic acid concentration

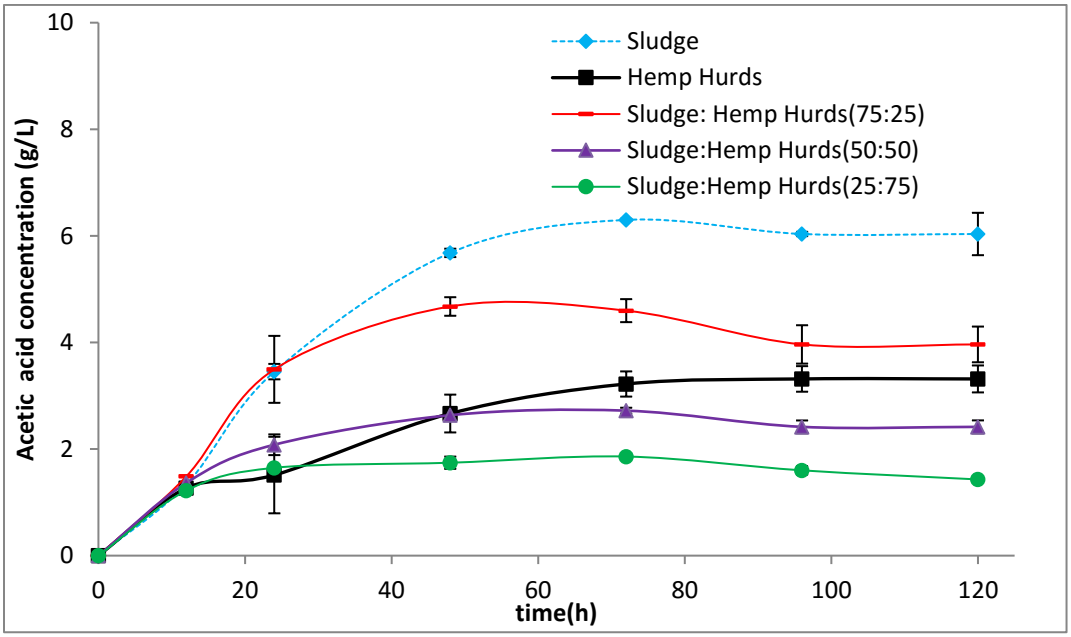

d) Glucose concentration

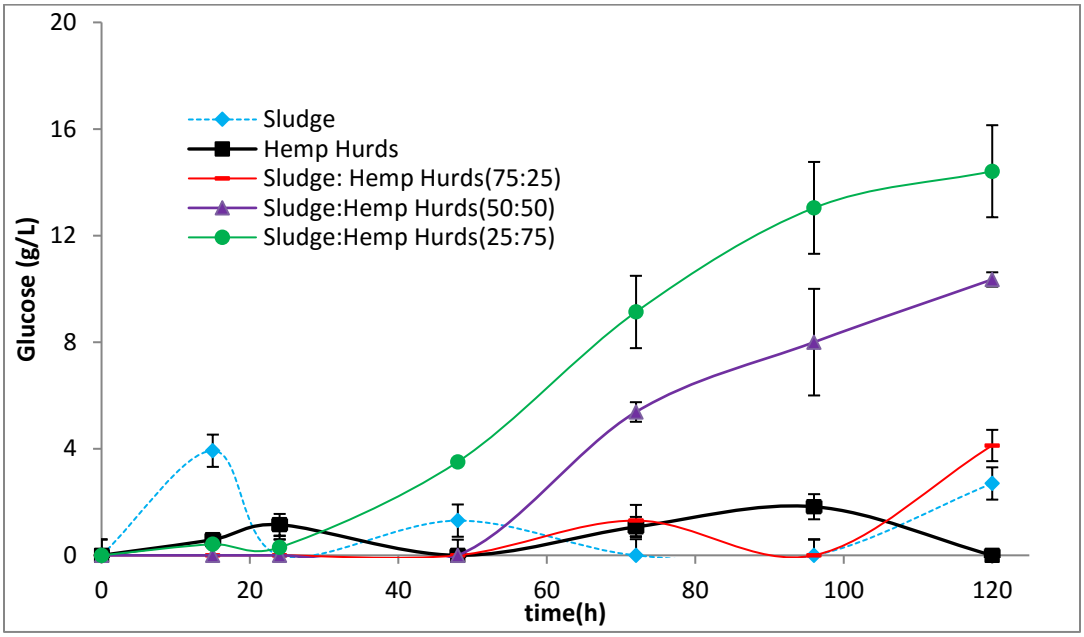

e) Xylose concentration

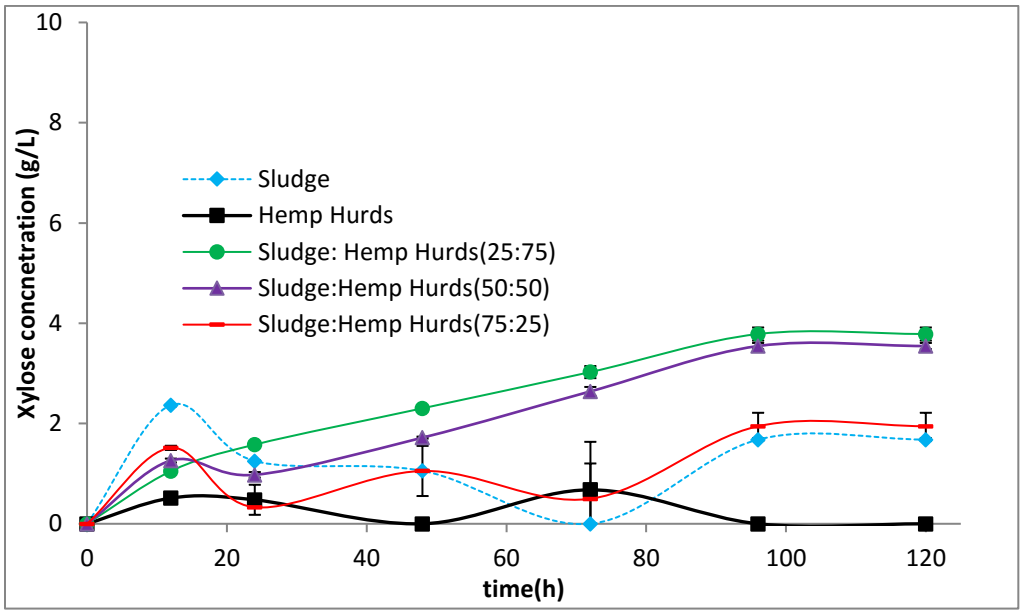

f) pH Profile

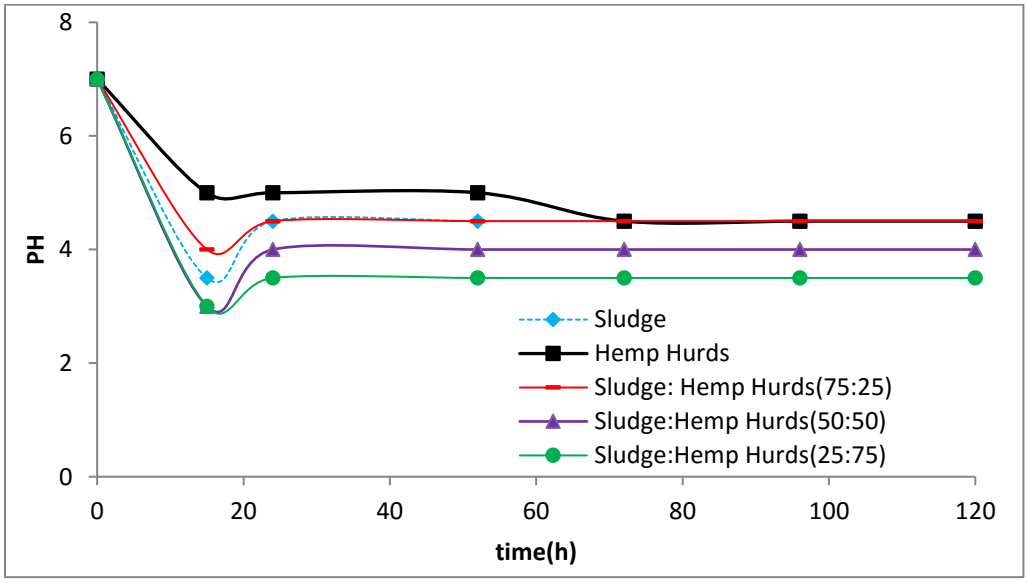

Figure 4-4 Effect of mixing ratio on simultaneous saccharification and co-fermentation (SSCF) of mixture of sludge and alkali-pretreated hemp hurd under the solid loading of 10% and enzyme loading of 15 FPU/g-glucan.

4.4.4.2 Effect of enzyme loading on SSCF

To examine the effect of enzyme loading on lactic acid production, SSCF was performed under 10% solid loading with different enzyme loading (15, 20, and 25 FPU/g-glucan) at two different mixtures (equal and sludge-rich) as demonstrated in Figure 4-5&4-6.

When the equal mixing was used in SSCF, the maximum lactic acid concentrations were found to be same (~37 g/L) at 48 h in spite of high enzyme dosage were applied (15 FPU to 25 FPU). Then these values were decreased to around 34 g/L at 120 h (Figure 4-5a). On the other hand, acetic acid has inverse association with enzyme dosage at this mixing. It shows the concentration of acetic acid is decreased with the increase of enzyme dosage. Glucose was not built up until 24 h and then with the increase of enzyme dosage, glucose concentration was increased. When enzyme dosage was increased from 15 FPU/g-glucan to 25 FPU/g-glucan, glucose concentration was enhanced from 11 to 16.3 g/L (Figure 4-5b). The xylose concentration was also doubled due to high enzyme dosage.

When the sludge-rich mixing was used in SSCF, the maximum lactic acid concentration was found to be 51.4 g/ L for the enzyme loading of 15 & 20 FPU and 52.4 g/ L for 25 FPU at 72 h as shown in Figure 4-6a. Then a little decrease in lactic acid concentration was observed for 15 and 25 FPU. However, lactic acid decreased to 48.3 g/ L at 120 h for the enzyme loading of 20 FPU which is even lower than that of 15 FPU. The acetic acid concentration was kept around 3.8-4.3 g/ L for the enzyme loading 15 FPU and these values decreased to in the range of 3.7-3.3 g/L for 20 and 25 FPU. Glucose was not built up until 48 h and then concentrations were increased to 4.1, 9.7 and 6.7 g/ L at 120 h for the enzyme loading of 15, 20 and 05 FPU. The xylose concentration increased linearly to 2.1, 4.2 and 3.5 g/ L for these enzyme dosages respectively.

a) Products (lactic acid and acetic acid) concertation

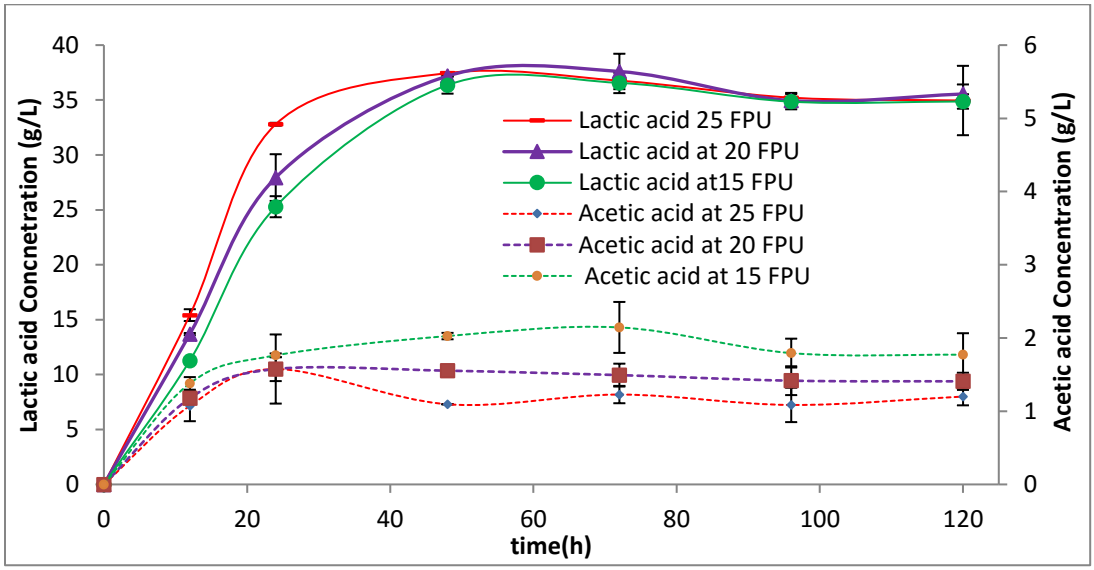

b) Substrate (glucose and xylose) concentration

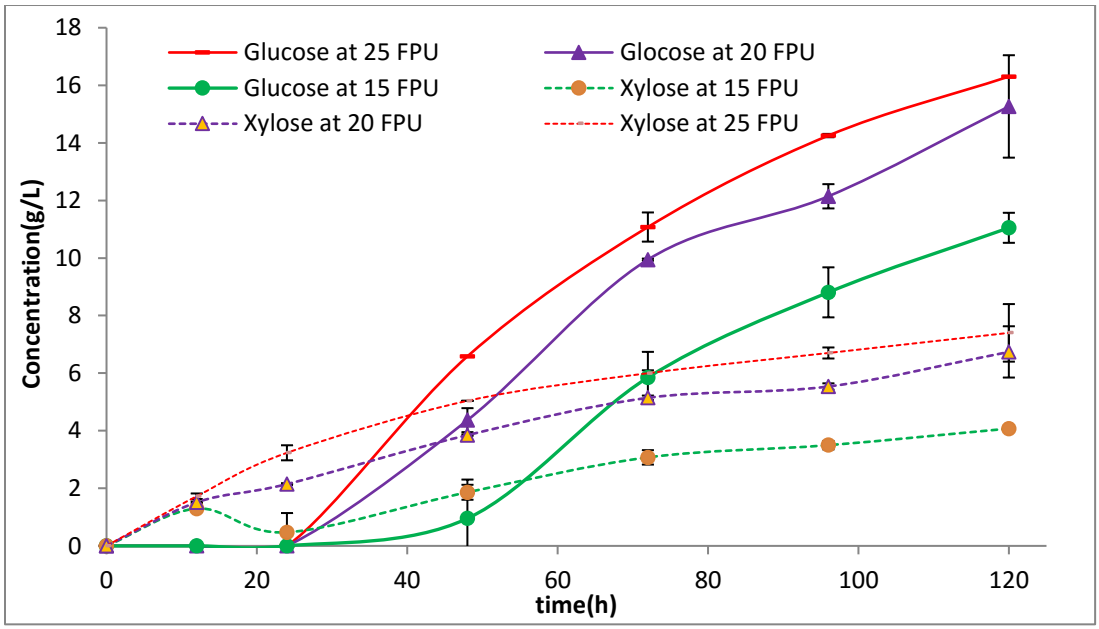

Figure 4-5 Effect of enzyme loading on simultaneous saccharification and co-fermentation (SSCF) of the mixture of sludge and hemp hurd under 10% of solid loading at equal mixture (sludge: hemp hurd =50:50).

a) Products (lactic acid and acetic acid) concertation

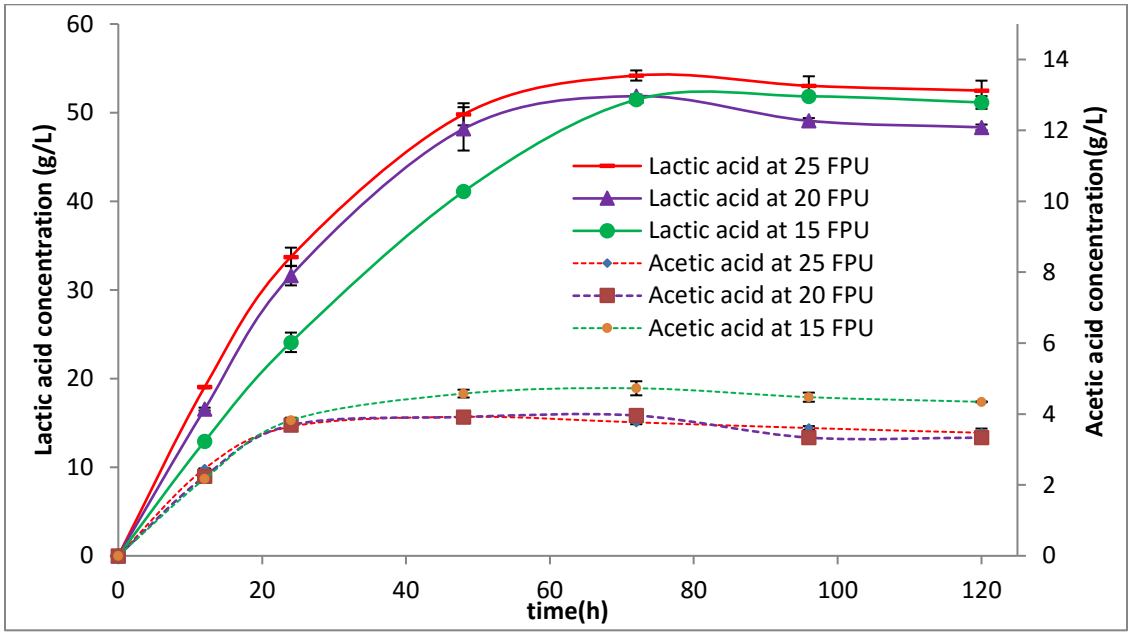

b) Substrate (glucose and xylose) concentration

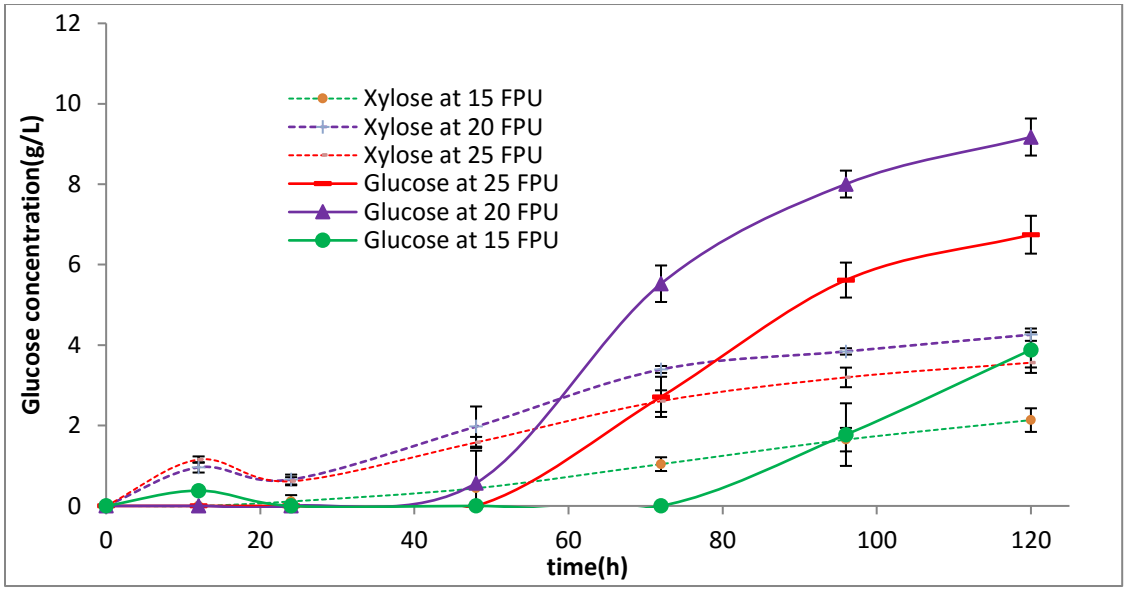

Figure 4-6 Effect of enzyme loading on simultaneous saccharification and co-fermentation (SSCF) of the mixture of sludge and hemp hurd under 10% of solid loading at sludge-rich mixture (sludge: hemp hurd =75:25).

4.5 Discussions

Hemp hurd were utilized directly as complementary feedstocks to paper mill sludge for lactic acid production via SSCF. Under the solid loading of 10-12% and enzyme loading of 15 FPU/g-glucan, a total of 52-66 g/L of lactic acid was produced with the mixture of sludge and hemp hurd (Table 4-3).

Table 4-3 Net amount of lactic acid generated from sludge, hemp hurd and mixture

Solid loading	Feedstocks	Total Glucan (g/L)	Total Xylan (g/L)	Total sugar (g/L)	Sugar from sludge (g/L)	Sugar from Hemp Hurds (g/L)	Maximum Lactic acid (g/L)	Lactic acid Yield (%)
5%	**Sludge**	25.88	6.28	32.16	32.16	-	21.32	66.29
	Hemp Hurds	42.44	0.76	42.44	-	43.94	15.16	35.72
	Mix (S:H=25:75)	38.30	1.56	39.86	8.04	31.84	22.40	52.89
	Mix (S:H=50:50)	34.16	3.14	37.30	16.09	21.23	19.25	60.05
	Mix (S:H=75:25)	30.02	4.70	34.72	24.13	10.61	19.21	55.33
10%	**Sludge**	51.76	12.56	64.32	64.32	-	51.88	80.66
	Hemp Hurds	84.88	1.50	84.88	-	86.38	29.56	34.83
	Mix (S:H=25:75)	76.60	3.14	79.74	16.09	63.68	26.81	33.62
	Mix (S:H=50:50)	68.32	6.28	74.60	32.18	42.45	38.09	51.06
	Mix (S:H=75:25)	60.04	9.42	69.46	48.27	21.23	47.77	68.77
12%	**Mix (S:H=80:20)**	68.72	12.56	81.28	64.36	16.98	66.57	81.90

4.5.1 Effect of process variables on lactic acid production

When 5% solid loading was used in SSCF, the pH of the sludge quickly dropped to 4.5 from the initial value of 7 and then stayed at 5 throughout the SSCF (Figure 4-3f). With high solid loading (10 %), this drop went further down to 3.5 and then stayed at 4.5 (near optimum for the SSF) (Figure 4-4f). The initial quick drop of pH is due to production of lactic acid, which eventually turns into calcium lactate. The presence of calcium lactate and calcium acetate along with sludge-ash collectively acts as a buffer, maintaining a steady pH afterwards (Shi et al., 2015).

The pH profile of sludge-rich mixtures resembles that of sludge alone due to little difference in ash content between the two. The same applies to the lactic acid profile, only the level of lactic acid is slightly higher for sludge than the mixture (Figure 3a& 4a). The lower lactic acid concentration of sludge-rich mixture than that of sludge is attributed to initial glucan loading. Although experiments were conducted at same solid loading and the same enzyme-to-substrate

ratio, the lactic acid production decreased linearly with increased total carbohydrate loading specifically "initial glucan" as xylan has less impact on lactic acid production. This is well-documented, often reported as "solids effect" in bioconversion of biomass (Kristensen et al., 2009; Wang et al., 2012). For example at 10 % solid loading, the total amount of initial glucan (60 g/L) in sludge-rich mixture is higher than that of sludge (52 g/L) (Table 4-3). Hence, relatively low amount of glucose is released by the suppressed activity of cellulase enzyme (solids effect) and eventually, less amount of lactic acid is produced in sludge-rich mixture (Figure 4-3a &4-3b; Figure 4-4a &4-4b).

Another point is that feedstock type also plays an important role in enzymatic hydrolysis. Literature information confirms that ash contained in the sludge interferes with the enzymatic reaction. Specifically, $CaCO_3$ in ash acts as a buffer, which maintains the pH two units above the optimum for the cellulose enzymes. However, this pH problem was resolved when SSCF end-product lactic acid reacts with $CaCO_3$ forming calcium lactate, thus bringing the pH toward the optimum. The calcium carbonate in the sludge essentially served as a pH control reagent in the hydrolysis as well as fermentation process; hence eliminating the requirement of external alkali. At optimum pH, the short fibers found in most Kraft mill sludges are readily hydrolyzed by enzymes into fermentable sugars (Marques et al., 2008) . The enzymatic digestibility data of sludge suggest that glucose might be easily released from sludge than hemp hurd (Table 4-2).

At 10 % solid loading, the maximum available sludge-sugar for lactic acid production was 48 g/L in sludge-rich mixture and rest of 21 g/L became available from hemp hurd-sugar (Table 4-3). Since hemp herd has lower digestibility than sludge, the overall digestibility is lower for the mixture than the sludge. This combined with the "solids effect" led to lower lactic acid production for the mixture than sludge.

On the other hand, for the equal and hemp hurd-rich mixtures, the pH steadily declined and stayed at 3-4 due to low total amount of ash in the mixture, not enough to totally neutralize the lactic acid. Thus, the overall acidity of the lactic acid supersede the $CaCO_3$ in the sludge driving the pH to the range of 3–4 (Figure 4-3f& 4-4f), which is below the optimum of the SSCF. This eventually led to low lactic acid yield in the SSCF (Figure 4-3b&4-4b) (Shi et al., 2015). Moreover, "solid effects" and type of feedstocks also played their role as described earlier. Consequently, with the increase of both initial glucan content and the amount of hemp hurd in the mixture, the yield of lactic acid decreased. Another point should be noted here that lactic acid concentration was reduced after certain point in some cases. This might be explained by the fact that under anoxic conditions in the presence of alternative electron acceptors, lactic acid starts to degrade into acetic acid by *Lactobacillus pentosus* especially at acidic conditions i.e. at low pH (Elferink et al., 2001). It is also possible that some lactic acid is converted to volatile fatty acids (Zhu et al., 2007).

4.5.2 Effect of process variables on glucose release and consumption

The glucose profiles of sludge and sludge-rich mixture, in Figure 3d &4d resemble the most simultaneous saccharification and fermentation (SSF) or SSCF processes, wherein consumption of glucose are much more rapid than hydrolysis, the latter being the controlling step throughout the process. However, glucose is started to accumulate after 48 or 72 h in equal and hemp hurd-rich mixture. According to literature, weak acids, e.g., lactic acid inhibit bacterial growth because as the external pH declines, the acid is protonized as soon as it is exported out of the bacteria. Uncharged, it diffuses back into the cell and dissociates due to the higher intracellular pH. The cell then has to use ATP to pump out protons, and energy eventually is depleted causing growth stop and the bacteria die (Mussatto et al., 2008).

In addition to pH, both initial glucan content and feedstock type also play an important role in glucose accumulation (Kristensen et al., 2009). Hence, with the increase of initial glucan content from equal (68 g/L) to hemp hurd-rich mixture (77 g/L), the accumulation is increased from 10.3 g/ L to 14.4 g/L at 10 % solid loading (Table 4-3). However, at 5 % solid loading, the glucose concentration increased from 2 g/ L to 3 g/L even with the decrease of initial glucan content from hemp hurd-rich mixture (24 g/L) to equal mixture (16 g/L). This difference might be explained by the fact that the pH of the hemp hurd-rich mixture at 5 % solid loading was far from optimum level than that of 10 % solid loading (Figure 4-3f&4-4f). The pH of 3 was observed at 5% solid loading, and pH of 3.5 at 10% solid loading after 72 h. It appears that at pH 3 the cells die out or their activity becomes extremely low. Thus, from this point on sugars accumulate since they are not consumed but still produced by enzyme that is still active at this pH. The same applies at pH 3.5 (10% solid). But at this pH the cell activity may still exist, which explains higher sugar buildup than that of 5% solid. This also explain why glucose concentration increased in hemp hurd-rich mixture compared to equal mixture at 5% solid loading.

4.5.3 Effect of process variables on xylose release and consumption

The assimilation of xylose was rather slow compared to glucose. As the curve indicates, the xylose concentration increased almost linearly before 12 h. After that point, xylose variation takes two different patterns (Figure 4-3e&4-4e). Xylose in sludge and sludge-rich mixture feeds started to decrease and its consumption occurred shortly after depletion of glucose. This is a classic example of diauxic consumption of substrates wherein glucose is preferred to xylose (Zhu et al., 2007). On the contrary, xylose concentration in equal and hemp hurd-rich mixture continued to build up. Since microbial actions are not the rate-controlling step, the main

difference between the two groups is that the latter has a buildup of xylose. The same explanation given for glucose buildup applies here.

4.5.4 Effect of process variables on acetic acid generation

Glucose assimilation under anaerobic conditions gave only lactic acid whereas xylose was converted into acetic acid in addition to lactic acid. Two different pathways, the PK and PP/glycolic pathways are proposed as the metabolic pathways of pentoses in LAB (Tanaka et al., 2002). At low xylose concentrations, xylose is metabolized predominantly by the PK pathway, due to the increase in the specific activities of phosphoketolase and PFL and the decreased activities of transaldolase and transketolase. As a result, the yield coefficient of L-lactate decreases and those of the other products increase i.e. acetic acid increase (Tanaka et al., 2002). Another source of the excess acetic acid production was because of difficulty of tightly controlling the anaerobic condition. Under anoxic conditions in the presence of alternative electron acceptors, lactic acid starts to degrade into acetic acid especially at acidic conditions i.e. at low pH (Elferink et al., 2001; Zhu et al., 2007). The pH profile and lactic acid data collectively support this explanation as enhancement of acetic acid concentration was more visible after certain period of time when pH went below 4 (Figure 4-3e& Figure 4-4e). This also divert part of the glucose to take PK pathway, leading to the production of acetic acid in addition to lactic acid (Zhu et al., 2007).

4.5.5 Effect of enzyme loading on SSCF

The effect of enzyme loading on SSCF depends on the mixing ratio. In equal mixture, the maximum lactic acid concentrations remain same even with the higher dosage of enzyme due to low pH (Figure 4-5a). Thus more glucose and xylose is released by the action of enzyme yet to convert lactic acid (Figure 4-5b). The concentration of acetic acid is decreased with the increase

of enzyme dosage. The possible explanation is, at high concentration, glucose is metabolized predominantly by the EMP pathway giving lactic acid as sole product and this process is accelerated by high pH. At lower concentration, glucose is converted to lactic acid and acetic acid via PK pathways and this process is accelerated by low pH. Thus the acetic acid concentration is increased with low enzyme loading. When sludge-rich mixture was used in SSCF, the maximum lactic acid concentrations were almost same for the applied dosages. Interestingly, the degradation of lactic acid is more prominent after 72 h and relatively high concentration of glucose and xylose is observed in SSCF for the enzyme loading of 20 FPU. We don't have any explanation for this. This may be due to microbes turn into spores,

The major advantages of Hemp hurd as a complementary feedstock to paper sludge for lactic acid production for lactic acid production are that no further pretreatment is needed and no pH control is required. By comparing sludge data at 10 % solid loading and sludge rich mixture at 12% solid loading, one can conclude that 14.6 g/L lactic acid was obtained from hemp hurd without more feedstock cost (Table 4.3).

4.6 Conclusions

Pulp mill sludge is a feedstock suitable for lactic acid production. The buffering effect of CaCO3 existing in sludge can be effectively used in lactic acid production by SSCF as it keeps the pH near optimum level resulting calcium lactate as the end-product. The ash content in pulp mill sludges is 30-40%, which gives higher than required neutralizing capacity when it is used as a sole feed, especially at high solid loading. The SSCF of sludge can thus accommodate additional common cellulosic feedstocks. As a proof, it was demonstrated that a mixed feed of pulp mill sludge and hemp hurd can effectively processed by SSCF. In addition to pH, both initial glucan content and feedstock type also play an important role in lactic acid production process.

Applying proper operating conditions, lactic acid concentration of 67 g/L corresponding to the yield of 0.82 g/g-sugar were achieved. It was attained under the condition of: sludge/hemp hurd ratio= 4, total solid loading of 12 wt%, and enzyme loading of 15 FPU/g-glucan. The maximum lactic acid concentrations remain same even with the higher dosage of enzyme whereas the acetic acid concentration is increased with low enzyme loading in this experimental range. This study suggests that combination of sludge and other cellulosic feedstock can be used to produce lactic acid, eliminating the need of external neutralizing reagent.

.

Chapter 5

Chlorine dioxide as a secondary pretreatment reagent for herbaceous biomass

5.1 Abstract

Chlorine dioxide (ClO_2) is a bleaching reagent used in paper industry. Two different types of pretreatment methods were investigated incorporating ClO_2 as a secondary reagent: (a) alkaline followed by ClO_2 treatment; (b) dilute-sulfuric acid followed ClO_2 treatment. In these methods, ClO_2 treatment has shown little effect on delignification. Scheme-a has shown a significant improvement in enzymatic digestibility of glucan far above that treated by ammonia alone. On the contrary, dilute-acid followed by ClO_2 treatment has shown negative effect on the enzymatic hydrolysis. The main factors affecting the enzymatic hydrolysis are the changes of the chemical structure of lignin and its distribution on the biomass surface. ClO_2 treatment significantly increases the carboxylic acid content and reduces phenolic groups of lignin, affecting hydrophobicity of lignin and the H-bond induced association between the enzyme and lignin. This collectively led to reduction of unproductive binding of enzyme with lignin, consequently increasing the digestibility.

5.2 Introduction

The cell wall of lignocellulosic biomass is a composite material of crystalline cellulose fibrils bound by non-crystalline cellulose fibrils and hemicellulose and surrounded by a matrix of hemicellulose and lignin (Rubin, 2008). Among them, lignin is believed to be a major hindrance to bioconversion as it surrounds carbohydrates (cellulose and hemicellulose) making it highly recalcitrant to enzymes, pathogens and microorganisms (Studer et al., 2011). Delignification is therefore an important step for successful enzymatic hydrolysis and subsequent microbial fermentation of lignocellulosic biomass. A wealth of research has been conducted to improve enzymatic hydrolysis through a specific delignification. For example, hydrogen peroxide (Gupta & Lee, 2010), chlorine dioxide (Barroca et al., 2001),aqueous liquid ammonia (Kim et al., 2003), ozone (Kaur et al., 2012) and sodium chlorite (Kumar et al., 2013) have been studied to reduce the lignin content in lignocellulosic biomass but relatively few address the effect of ClO_2 on enzymatic hydrolysis of biomass through delignification.

ClO_2 is a bleaching reagent commonly used in pulp and paper industry. Chlorine dioxide based delignification method and acid-chlorite delignification, often utilize aqueous solution of acetic acid and sodium chlorite (Kumar et al., 2013). In water solution, sodium chlorite ($NaClO_2$) becomes a strong and stable alkali, but when acidified it forms gaseous chlorine dioxide (ClO_2), which is a highly selective bleaching reagent, preferentially oxidizing lignin in the presence of carbohydrates thereby fulfilling the requirement of pretreatment (Svenson et al., 2006). Kumar et al. (2013) carried out the reaction at 70 °C for 8 h with successive addition (every two hour) of fresh sodium chlorite and acetic acid at loadings of 0.6 g/g dry biomass of $NaClO_2$ and 0.6 ml/g dry biomass of acetic acid. They removed more than 90 % lignin from all biomass they studied. In another study, Siqueira et al., (2013) employed $NaClO_2$ to increase enzymatic digestibility of

sugarcane bagasse by removing lignin. They observed that removing approximately 60% of lignin can result in a considerable increase in cellulose conversion (80%) after 72 h of hydrolysis of feed stocks. Yu et al., (2011) investigated the effect of delignification methods on enzymatic hydrolysis of forest biomass using softwood and hardwood that were pretreated at an alkaline condition followed by $NaClO_2$ or ozone delignification. They found both delignifications improved enzymatic hydrolysis especially for softwood, while pretreatment alone was found effective for hardwood. A recent laboratory investigation by Sannigrahi et al., (2012) explored the use of an aqueous solution of ethanol and ClO_2 mixture for ethanol production from sweet gum. They achieved 87% ethanol yield with sweet gum treated using 60% ethanol solution with 1.1% ClO_2, liquid/solid ratio 7, 75 °C, 3 hours.

Acid-chlorite primarily acts on lignin in biomass, but it can also affect the polysaccharides. The two most likely scenarios for cellulose degradation during acid-chlorite delignification are acidic cleavage of the glycosidic bonds and/or oxidative degradation of the polysaccharides (Hubbell & Ragauskas, 2010). However, the oxidation efficiency of acid chlorite treatment largely depends on pH as ClO_2 is generated from the acid chlorite solution at pH below 4 (Svenson et al., 2006). Usually, acetic acid is added to the delignification procedure to reduce pH.

On the other hand, aqueous ammonia (NH_3) is widely used in various pretreatment processes including ammonia recycle percolation (ARP), ammonia fiber explosion (AFEX) and soaking in aqueous ammonia (SAA) (Gupta & Lee, 2010; Gupta & Lee, 2009; Kim et al., 2016; Kim et al., 2003). Under normal pretreatment conditions, ammonia in aqueous solution reacts primarily with lignin showing little effects on carbohydrates in biomass (Gupta & Lee, 2010). The ammonia based processes have been proven to be effective in improving the glucan digestibility (Kim et al., 2003).

In this study, a two-step pretreatment was performed to enhance the overall efficiency of enzymatic deconstruction of agricultural residue to monomeric sugars feedstocks. In the 1st stages called as primary stage, feedstocks were treated with either alkali or acid. Then the washed sample was treated with ClO_2 at 2nd stage (secondary stage) before performing enzymatic hydrolysis. The objective of this study is to determine the effectiveness of ClO_2 as a secondary reagent, and to identify the underlying cause of its effectiveness.

5.3 Materials and Methods

5.3.1 Feedstock and reagents

Corn stover and poplar were dried, milled and the fraction between 20-80 mesh was used as standard laboratory feedstocks. All chemicals except ClO_2 used in this study purchased from VWR (Radnor, PA) were of analytical grade and used without purification. ClO_2 was synthesis in our lab according to procedure described in AkzoNobel Pulp and Performance Chemicals brochure (personal communication).

5.3.2 Experimental procedure for pretreatment

Primary pretreatment (Stage-1): Primary pretreatment reactions were carried out in stainless steel reactors (ID: 1.375 inch and Length: 6 inch). The reactors were loaded with appropriate amount of feedstocks with required amount of pretreatment reagent (mostly aqueous ammonia) with solid/ liquid (S: L) ratio of 1:10. The sealed reactors were placed in constant-temperature oven. The reactor was preheated for 15–30 min to reach the set temperature and maintained at the level for desired period of time. The reaction time in this report is defined as the duration after it reached the set temperature. Once pretreatment was done, the reactors were removed from the oven and quenched in cold water to room temperature to stop the reaction. After the reactor reached room temperature, the contents in the reactor was filtered out by vacuum filtration. The pH of the liquid

was measured before washing and the solid part was washed for subsequent analysis until it achieved a pH of 7.

Secondary pretreatment (Stage-2): Secondary pretreatment were carried out in screw-capped laboratory tubular glass reactors following the same procedure as primary treatment other than that water bath was used for heating. The washed solid samples obtained from 1st stage were mixed with required amount of specified concentration of ClO_2 with a S: L ratio of 1:10 to maintain consistency of chemical usage per gram of dry biomass. The reactors were filled to 50 % of the total volume to allow for volume expansion due to heating. After the pretreatment reaction, the content in the reactor was filtered out by vacuum filtration.

5.3.3 Enzymatic hydrolysis

The cellulase enzyme (Cellic C-Tec 2) was a generous gift from Novozymes (North America, Franklinton, NC). Its specific enzyme activity was 119 FPU/mL and total protein number was 255 mg/mL was applied to pretreated feedstocks. The enzymatic digestibility tests were carried out in screw capped 125 mL Erlenmeyer flasks at 50°C, and pH 4.8 using 0.05 M sodium citrate buffer in an incubator shaker (New Brunswick Scientific, Innova-4080) agitated at 150 rpm. Antibiotics sodium nitride was added into the reaction media to maintain sterile conditions. The digestibility tests for treated biomass were done with 1 g dry biomass loading/50 mL of total reactant volume. The hydrolysate samples taken at different time period (12, 24, 48, and 72 h) were analyzed in HPLC to measure the level of glucose and xylose. The glucose content released at different time period of hydrolysis was used to calculate the enzymatic digestibility (Kothari & Lee, 2011).

5.3.4 Composition analysis

The composition of the feedstocks was analyzed by the NREL standard protocols to determine sugar components in carbohydrates, lignin, and ash. Each sample was analyzed duplicate. The

moisture content was measured by infrared moisture balance (Denver Instrument, IR-30). Sugars were determined using an HPLC system consisting of a AcuFlow Series III pump (LabX, Midland, ON, Canada), Alcott 708 auto sampler (LabX, Midland, ON, Canada), a Bio-Rad HPX-87P or a Bio-Rad HPX-87H column (Hercules, CA) , a refractive index detector (Shodex, NY) and PeakSimple Chromatography Data Systems(Torrance, CA). Ultrapure DI water was used as carriers at a flow rate of 0.55 ml/min for the Bio-Rad HPX-87P. The aqueous solution of 0.005 M sulfuric acid with a flow rate of 0.55 ml/min was selected as mobile phase for Bio-Rad HPX-87H column. In both cases, the columns were operated at 85 °C. The analysis for a sample was completed within 40 minutes.

5.3.5 FTIR and SEM analysis

The infrared spectra of biomass were recorded in the range of 650–4000 cm^{-1} on a PerkinElmer (Waltham, MA, USA) 400 FT-NIR spectrometer using 32 scans, a resolution of 4 cm^{-1} and interval of 1 cm^{-1}. The SEM pictures of the biomass samples were taken by a ZEISS DSM940 scanning electron microscope.

5.3.6 Biomass crystallinity

The XRD patterns were obtained using a Bruker D8 Discover diffractometer. The spectra were acquired at a scan rate of 1.6 degrees/min between $2\theta = 5$ to 35. An accelerating voltage of 40 kV was used at 40 mA. The crystallinity index (CI) was calculated according to the equation: $CI= (I_{002} – I_{18})/I_{002}$, where, I_{002} is the diffraction intensity of peaks corresponding to lattice plane of 002 ($2\theta=22.6°$) and I_{18} is the intensity of the amorphous background, which has a minimum value between lattice planes of 101 and 002 ($2\theta=18°$) (Kim et al., 2003).

5.3.7 Nitrogen porosimetry

The surface areas, pore volumes and size distribution of biomass were determined by nitrogen adsorption at 77 K using a Quantachrome automated gas sorption system Nova 2200e surface area and pore volume analyzer (Boynton Beach, Florida). Initially, the biomass samples were degassed in vacuum for 12 h at 40 °C (Dougherty et al., 2014). The method of Brunauer, Emmett, and Teller (BET) is used to determine the total surface area of biomass and the micro pore volume.

5.4 Results

5.4.1 Effect of ClO_2 on aqueous ammonia treated corn stover

The efficacy of ClO_2 as a secondary pretreatment reagent was investigated on aqueous ammonia treated corn stover. Experiments were carried out with 15% NH_3 at stage-1 at 60 °C followed by two different charges (0.9 & 2.2 wt. % on solid basis) at two different temperatures (30 °C & 60 °C) at satge-2 with a S: L ratio of 1:10. Approximately 60 % lignin was removed in the 1st stage while preserving most of the cellulose and hemicellulose. Less than 10% of the remaining lignin was removed by ClO_2 during the 2nd stage (Figure 5-1).

The effect of ClO_2 on enzymatic hydrolysis of aqueous ammonia followed by ClO_2 (NH_3+ClO_2) treated corn stover is presented in Figure 5-2. These five runs affirmed that treating with small amount of ClO_2 (0.9-2.2 wt. % on solid basis) leads drastic improvement of enzymatic digestibility, from 84% to 100%. It is to be noted that treatment at 30 °C was equally effective as treatment at 60 °C. Since the experiments of ClO_2 treatment were all done at either 30 °C or 60 °C, a question arose whether the improvement of digestibility was partly due to exposure to hot water (30 °C& 60°C). In order to verify this, corn stover was treated with aqueous ammonia followed by water (NH_3+H_2O) at 60 °C. The results clearly indicate that hot-water treatment has no effect on either the digestibility or the composition as shown in Figure 5-1& 5-2.

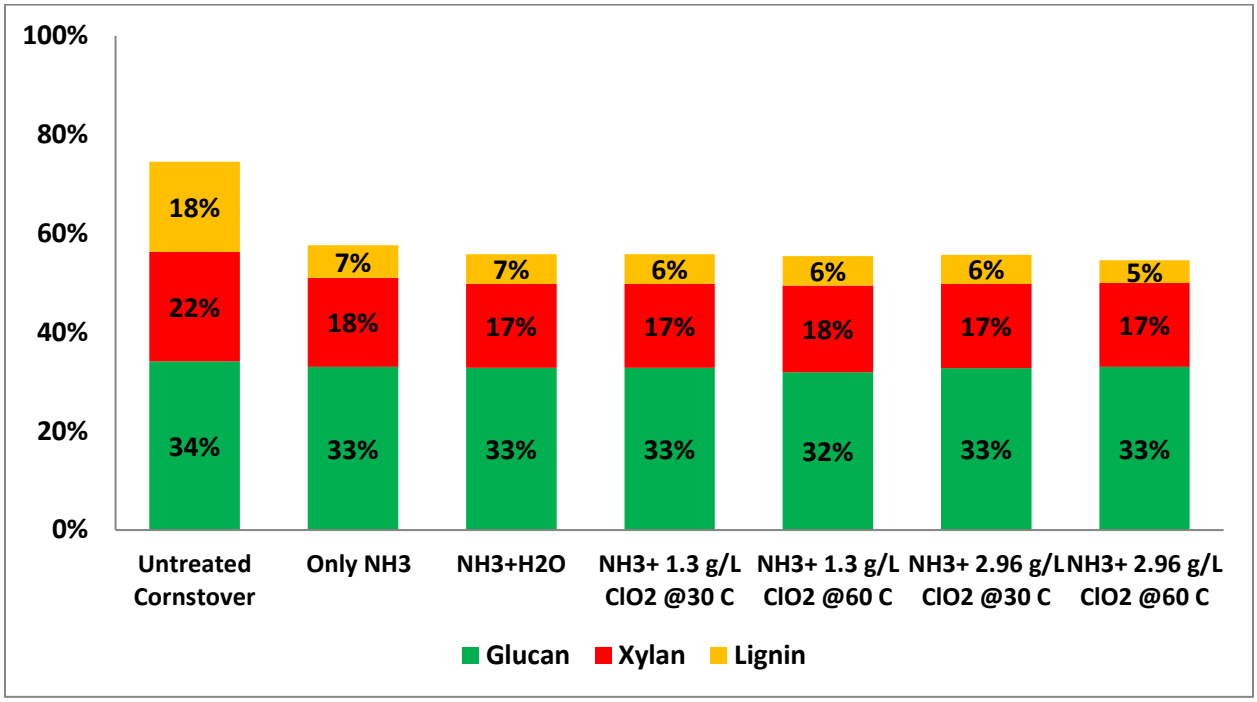

Figure 5-1 Effect of ClO_2 as a secondary pretreatment reagent on corn stover composition. Pretreatment conditions: Stage 1 - 15% aqueous NH_3 & (60 ° C+24 h), solid/liquid ratio =1:10. Stage 2 -Concentration of ClO_2= (1.3 g/L & 2.96 g/L) equivalent to (0. 93 & 2.2) % on untreated dry solid basis & 60 °C, 2 h, pH = 3.3-3.4

To assess the effect of ClO_2 on enzyme loading of NH_3+ClO_2 treated corn stover, enzymatic hydrolysis was performed with different enzyme loadings. Addition of ClO_2 significantly improved not only final glucan digestibility but also initial hydrolysis rate as shown in Figure 5-3. For example, under 15 FPU, it took 72 hours of enzymatic hydrolysis to generate maximum glucan digestibility 84%; whereas with addition of ClO_2, it took only 14 hours to reach the same level of glucan digestibility; after 72hours of hydrolysis, glucan digestibility rose to 100%.

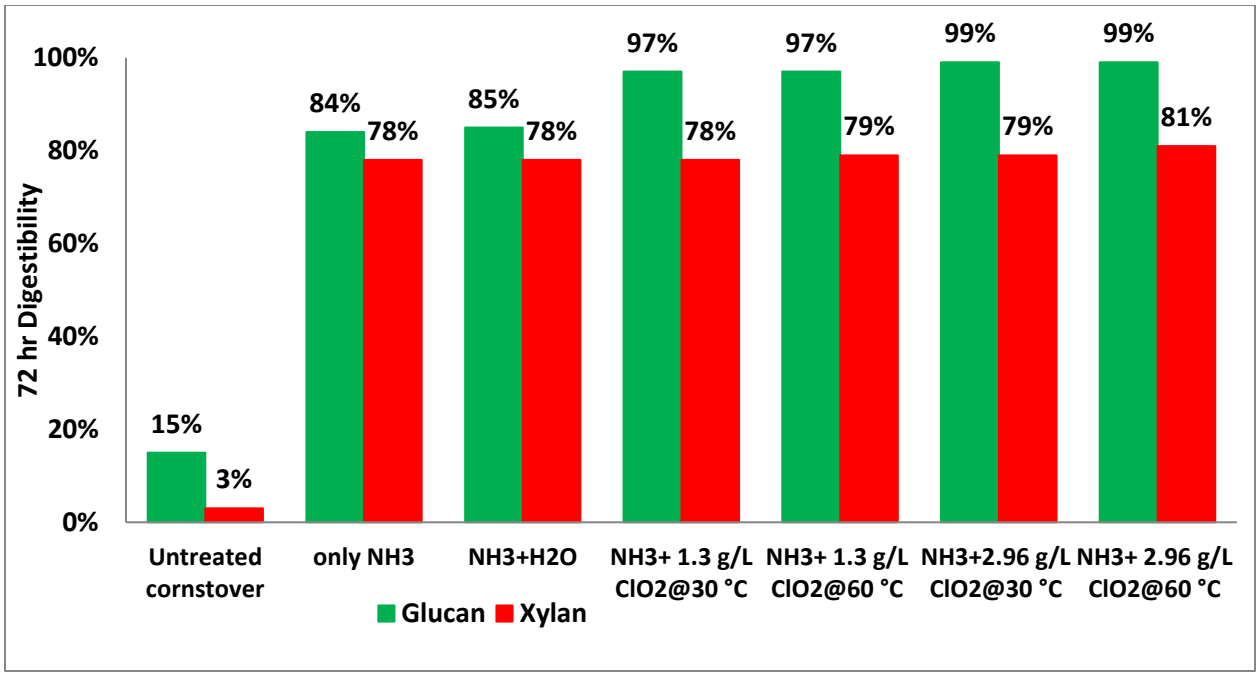

Figure 5-2 Effect of ClO_2 as a secondary pretreatment reagent on digestibility of corn stover. Pretreatment conditions: Stage 1 - 15% aqueous NH_3 & (60 ° C+24 h), solid/liquid ratio =1:10. Stage 2 -Concentration of ClO_2= (1.3 g/L & 2.96 g/L) equivalent to (0. 93 & 2.2) % on untreated dry solid basis & 60 °C, 2 h, pH = 3.3-3.4. Stage -2 (in the case of H_2O) - Amount of distilled water remains same as the amount of ClO_2 & 60 ° C, 2 h. Enzyme loading: 15 FPU (Ctech-2)/g glucan & solid loading 2%.

Tests on the positive effect of ClO_2 were further carried out applying low enzyme loadings (5 and 10 FPU/g-glucan). When the enzyme loading was reduced to 10 FPU, the maximum glucan digestibility still remains almost 100 % for (NH_3+ClO_2) treated corn stover while it decreased to 79% for NH_3 treated corn stover. However, at 5 FPU, the glucan digestibility went lower still maintaining 20 % higher digestibility for combined treatment over the single treatment. By tripling the enzyme dosage from 5 FPU/g glucan to 15 FPU/g glucan without ClO_2 treatment, the 72-hr glucan digestibility was improved from 40 % to 86%. With ClO_2 treatment, the same digestibility

can be obtained with enzyme dosage less than 10 FPU /g glucan. These data prove that it can be an effective tool to reduce enzyme cost in the enzymatic saccharification of corn stover. We also note that digestibility in the range of 70-80% is acceptable from a process viewpoint. However, ClO_2 treatment did not show any effect on the xylan digestibility in all three different enzymes loading as shown in Figure 5-4.

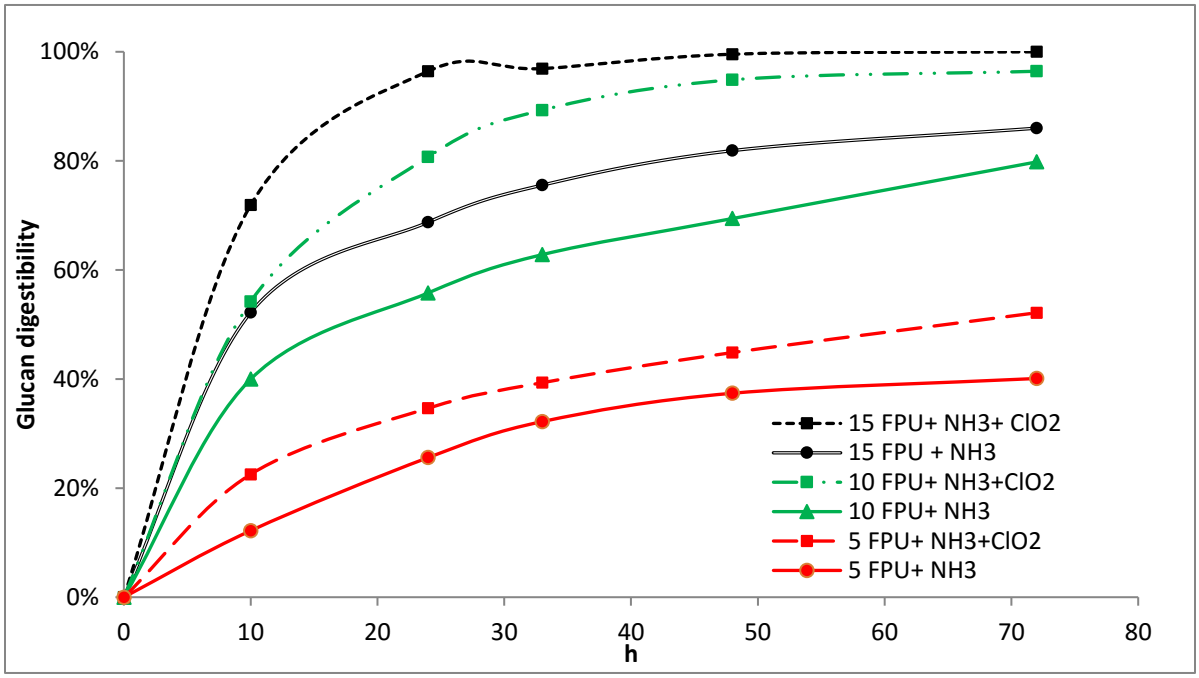

Figure 5-3 Effect of enzyme loading on glucan digestibility of aqueous NH_3 followed by ClO_2 (NH_3+ ClO_2) treated corn stover. Pretreatment conditions: Stage 1 - 15% NH_3 & (60 ° C+24 h), solid/liquid ratio= 1:10. Stage 2 - Concentration of ClO_2= (2.96 g/L) equivalent to (2.2) % on untreated dry solid basis & 60 ° C, 2 h, pH = 3.3-3.4. Enzyme loading: 15 FPU (Ctech-2)/g glucan & solid loading 2%.

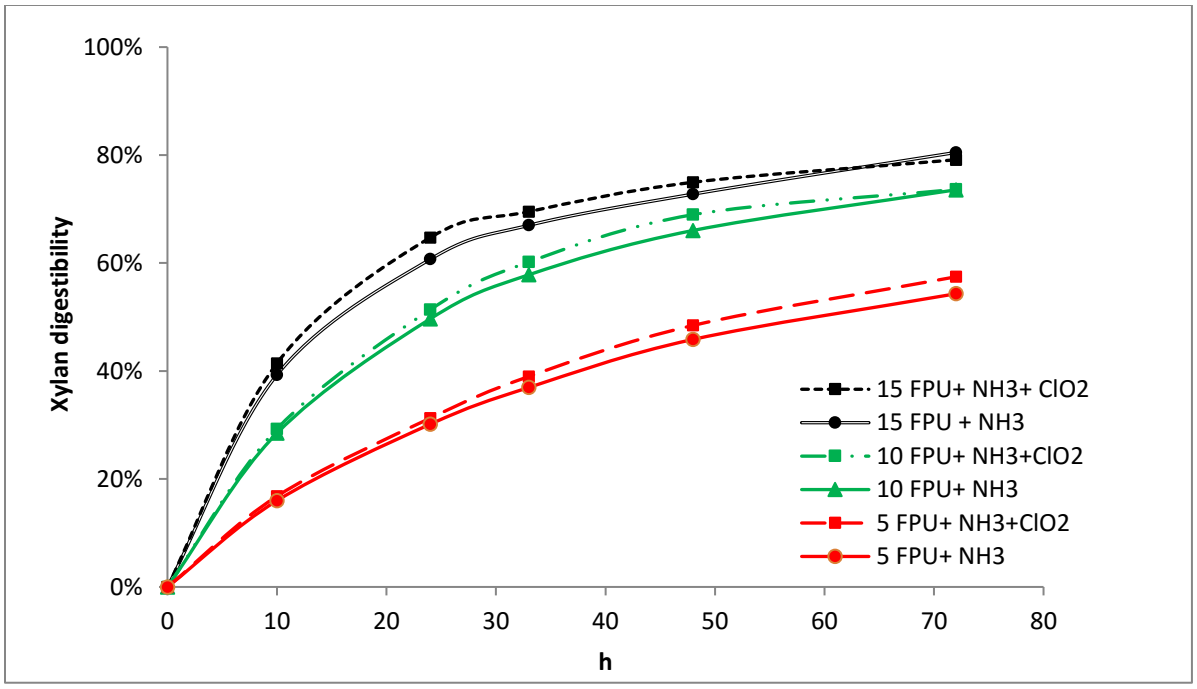

Figure 5-4 Effect of enzyme loading on xylan digestibility of aqueous NH_3 followed by ClO_2 (NH_3+ ClO_2) treated corn stover. Pretreatment conditions: Stage 1 - 15% NH_3 & (60 ° C+24 h), solid/liquid ratio= 1:10. Stage 2 - Concentration of ClO_2= (2.96 g/L) equivalent to (2.2) % on untreated dry solid basis & 60 ° C, 2 h, pH = 3.3-3.4. Enzyme loading: 15 FPU (Ctech-2)/g glucan & solid loading 2%.

Primary treatment conditions were extended to very low concentration of NH_3 (3.3%) and relatively high temperature (140 °C), low reaction time (30 minutes) with high solid loading (S: L=45:55) while secondary stage conditions remain same as previous experiments. The results are presented in Table 5-1. Approximately 33% lignin is removed in 1st stage and addition of ClO_2 doesn't improve delignification. However, with the addition of ClO_2, the enzymatic digestibilities were improved from 57% to 64 % for glucan and from 50% to 60 % for xylan. This differs from the previous observation where xylan digestibility was unaffected by the ClO_2.

Table 5-1 Effect of ClO_2 as a secondary pretreatment reagent on corn stover treated by aqueous ammonia. Pretreatment conditions: Stage1 – 3.3% NH_3 & (140° C+0.5 h), solid/liquid ratio =45:55. Stage 2 - Concentration of ClO_2= (2.96 g/L) equivalent to (2.2) % on untreated dry solid basis & 60 ° C, 2 h. pH = 3.3-3.4. Enzyme loading: 15 FPU (Ctech-2)/g glucan & solid loading 2%. Time for enzymatic digestibility is 72 h. pH during ClO_2 experiment = 3.4-3.5.

Pretreatment Conditions	Solid composition (%)			Digestibility	
	Glucan	Xylan	Lignin	Glucan	Xylan
Untreated	34.1	22.2	18.2	15.0	3.0
NH_3 treated Corn stover	33.3	17.4	12.3	57.3	46.9
NH_3 +ClO_2 treated Corn stover	32.4	16.4	12.2	64.1	50.7

Additional experiments were carried out using corn stover as feedstock which underwent either low-moisture anhydrous ammonia (LMAA) or extremely low-liquid ammonia (ELLA) followed by ClO_2 treatment. These primary pretreatments were done elsewhere (Bioenergy Laboratory, Gongjoo University, Korea by Professor T. H. Kim and his associates) and sent to us for this work. The details procedure is described by Nghiem et al. (2016). The data showing the effect of ClO_2 on LMMA and ELLA treated corn stover are presented in Table 5-2. The carbohydrate and lignin content are unaffected by the ClO_2 treatment. Addition of ClO_2 increased the 72-hr glucan digestibility from 27 % to 51% for LMAA and from 30 % to 40 % for ELLA treated corn stover at enzyme loading 5 FPU/g glucan. It also increases the 72-hr xylan digestibility from 13% to 46 % for LMAA and from 18 % to 38 % for ELLA. In a parallel test, it was found that by doubling the enzyme dosage from 5 FPU/g glucan to 10 FPU/g glucan, the 72-hr enzyme digestibility of LMMA corn stover was improved from 27% to 45% for glucan and 13% to 35% for xylan. With ELLA, these values were increased from 30 % to 49% for glucan and 18 % to 38% for xylan. It indicates that, applying a small charge of ClO_2 (22 mg/ g dry) has similar effects on enhancement of enzymatic hydrolysis, the net effect is equivalent to doubling the enzyme dosage.

Table 5-2 Effect of ClO_2 as a secondary pretreatment reagent in which feedstocks were treated with either low-moisture anhydrous ammonia (LMAA) or extremely low-liquid ammonia (ELLA). Pretreatment conditions: Stage1 – For LMAA- 0.1g NH_3/g dry biomass & (90° C+120 h), For ELLA- 0.1g NH3/g dry biomass & (120° C+72 h). Stage 2 - Concentration of ClO_2= (2.96 g/L) equivalent to (2.2) % on untreated dry solid basis & 60 ° C, 2 h. pH = 3.3-3.4. Enzyme loading: 15 FPU (Ctech-2)/g glucan, 2% solid loading, 72 h.

Pretreatment Conditions	Solid composition (%)			Digestibility			
				5 FPU		10 FPU	
	Glucan	Xylan	Lignin	Glucan	Xylan	Glucan	Xylan
LMMA	42.5	25.9	20.4	27.1	13.4	44.8	35.0
ELLA	42.7	24.1	20.4	30.6	18.2	49.0	37.5
LMMA+ ClO_2	41.8	25.3	20.0	51.3	46.8	75.4	62.1
ELLA+ClO_2	42.5	24.1	19.0	40.0	38.3	76.2	59.0

5.4.2 Effect of ClO_2 on H_2SO_4 treated corn stover

To see the effect of ClO_2 on acidic pretreatment, corn stover was first treated with dilute H_2SO_4 at two different temperatures. Nearly 45% of initial xylan was removed from the biomass during dilute acid pretreatment at 140 °C and all of xylan was removed at 160°C as shown in Table 5-3. The delignification is about 20% and 11 % at 140 °C and 160 °C respectively. Second stage treatment ClO_2 does not show any effect on delignification of corn stover treated at 160°C and only a slight on the sample treated at 140°C. Surprisingly, ClO_2 showed negative effect on enzyme digestibility of acid pretreated corn stover. With the addition of ClO_2, the 72 h glucan digestibility decreased from 42 % to 39 % and 64 % to 57 % on the sample treated at 140°C and 160°C respectively.

Table 5-3 Effect of ClO_2 as a secondary pretreatment reagent on H_2SO_4 treated corn stover. Pretreatment conditions: Stage1 – 0.5% H_2SO_4, 0.5 h, solid/liquid ratio =1:10, at temperatures 140 °C & 160°C. Stage 2 - Concentration of ClO_2= (2.96 g/L) equivalent to (2.2) % on untreated dry solid basis & 60 ° C, 2 h, pH = 3.3-3.4. Enzyme loading: 15 FPU (Ctech-2)/g glucan , 2% solid loading, 72 h

Pretreatment Conditions		Untreated Corn stover	140 °C		160 °C	
			H_2SO_4	H_2SO_4 + ClO_2	H_2SO_4	H_2SO_4 +ClO_2
Composition	Glucan (%)	34.1	33.7	32.1	33.0	33.0
	Xylan (%)	22.2	12.5	12.0	0.0	0.0
	Lignin (%)	18.2	14.5	12.5	16.1	17.0
Digestibility	Glucan (%)	15.0	42.0	39.0	64.0	57.0
	Xylan (%)	3.0	21.0	20.0	0.0	0.0

5.4.3 Effect of ClO_2 on NaOH treated Poplar

Additional experiments were carried out using NaOH treated poplar as the feedstock. Treatment of poplar, with 1% NaOH brought about 25% of delignification and the enzymatic digestibility increased by 26% for glucan and 28 % for xylan as shown in Table 5-4. Different schemes of ClO_2 addition were applied as shown in Table 5-4, all of which were done at 60 °C. In scheme 2 (Table 5-4), ClO_2 was added with 1% NaOH at stage-1 and ClO_2 alone at stage-2. However, in scheme 3, only NaOH was applied in the first stage and ClO_2 was added only to 2nd stage. In scheme 4, NaOH, ClO_2, $CuSO_4$ and 2,2´-bipyridine (bpy) were applied altogether in a single stage. In scheme 5, these chemicals applied in the second stage after NaOH treatment. $CuSO_4$ and 2,2´-bipyridine (bpy) were reported to be effective when used with alkaline pretreatment (Bhalla et al., 2016). The most favorable scheme seems NaOH followed by ClO_2 (scheme 3) as it requires lower chemical input with reasonable digestibilities among the schemes studied. Of notable point deduced from these data is that the effectiveness of ClO_2 applies only to the alkali treated biomass.

Table 5-4 Effect of ClO_2 as a secondary pretreatment reagent on NaOH treated corn poplar. Pretreatment conditions: Stage 1 – 1% NaOH & (60 °C+24 h), solid/liquid ratio =1:10. Stage 2 Stage 2 - Concentration of ClO_2= (2.96 g/L) equivalent to (2.2) % on untreated dry solid basis & 60 ° C, 2 h, pH = 3.3-3.4. Enzyme loading: 15 FPU (Ctech-2)/g glucan & solid loading 2%. Time for enzymatic digestibility is 72 h.

Pretreatment Conditions	Solid composition (%)			Digestibility	
	Glucan	Xylan	Lignin	Glucan	Xylan
Untreated	42.2	16.5	25.9	-	-
Scheme 1	39.5	16.5	19.6	25.5	28.7
Scheme 2	41.3	16.8	17.9	33.4	32.9
Scheme 3	41.7	17.1	19.0	36.2	32.4
Scheme 4	40.9	16.0	18.2	38.2	35.5
Scheme 5	41.6	14.9	18.9	40.0	36.0

The Pretreatment schemes are described as follows:

Scheme 1: 60 °C, 24 h, 1% NaOH, solid/liquid ratio =1:10

Scheme 2: 1st stage- 60 °C, 22 h, 1% NaOH+ ClO_2(2.96 g/L) equivalent to (2.2) % on untreated dry solid basis. 2nd stage- 60 °C,2 h, ClO_2(2.96 g/L) equivalent to (2.2) % on untreated dry solid basis.

Scheme 3: 1st stage- 60 °C, 22 h, 1% NaOH, solid/liquid ratio =1:10. 2nd stage- 60 °C, 2 h, ClO_2 (2.96 g/L) equivalent to (2.2) % on untreated dry solid basis.

Scheme 4: 1st stage- 60 °C, 22 h, 1% NaOH+ ClO_2(2.96 g/L) equivalent to (2.2) % on untreated dry solid basis + 2.5 ml 40 mM $CuSO_4$ and 2.5 ml 40 mM 2,2´-bipyridine (bpy) for solid/liquid ratio =1:10.

Scheme 5: 60 °C, 22 h, 1% NaOH, solid/liquid ratio =1:10. 2nd stage- 60 °C, 2 h + ClO_2(2.96 g/L) equivalent to (2.2) % on untreated dry solid basis + 2.5 ml 40 mM $CuSO_4$ and 2.5 ml 40 mM 2,2´-bipyridine (bpy) for solid/liquid ratio =1:10.

5.5 Discussions

The pretreatment efficiency on enzymatic hydrolysis largely depends on biomass composition (Balan et al., 2009). In general, alkaline pretreatments targets on the removal of the lignin component, whereas, acidic pretreatments primarily solubilize the hemicellulose fraction of the carbohydrates. Pretreatment also affects the physical and chemical structure of lignin. Lignin physically blocks the access of cellulase enzyme to cellulose and forms unproductive binding with the cellulase enzyme, reducing the amount of active enzyme (Gupta & Lee, 2010). Hence, the amount and the characteristics of lignin are regarded as the main factors affecting the enzymatic digestion of the carbohydrates.

5.5.1 Lignin reaction under alkaline conditions at the primary stage

Under alkali conditions, in general, the carbon-carbon bonds in lignin are stable, whereas the carbon-oxygen bonds are liable to cleavage (Santos et al., 2013). The fragmentation of lignin during alkaline treatment including NH_3 pretreatment (primary stage) is mainly due to by the cleavage of both α- and β- aryl ether linkages (Santos et al., 2013). Most of the inter-unit β-O-4 ether structures are cleaved but alkali stable ether linkages between lignin and polysaccharides tend to remain intact. An increased degree of branching and /or cross-linking is also found during the treatment (Gellerstedt et al., 1995). Due to the structural changes, the residual lignin becomes less reactive. The phenolic end groups are the most abundant reactive ligands exist within the residual lignin. Low amount of non-phenolic groups such as styrene and stilbene are also observed (Gellerstedt et al., 1995).

5.5.2 Lignin reaction with ClO_2 at the secondary stage

In the secondary stage, ClO_2 reacts preferentially with phenolic lignin units and olefinic side chains through a radical reaction mechanism (Scheme 5-1). During chlorine dioxide oxidation of phenolic

lignin units, aromatic ring opening is the favored pathway, which leads to the formation of dicarboxylic acids and its derivatives (Scheme 5-1A) (Ma et al., 2015). However, another study suggest that the main oxidative products are quinones; not muconic structures (Brogdon et al., 2004). Besides, the electrophilic attack of ClO_2 on the double bond of ring-conjugated structures of lignin followed by epoxidation through elimination of the chloromonoxide radicals generate unstable epoxides which eventually transform into related phenolic aldehyde/acid structure as main products (Scheme 5-1B).

Scheme 5-1Chlorine dioxide oxidation of lignin mechanisms A) for phenolic units and B) for conjugated units (Ma et al., 2015).

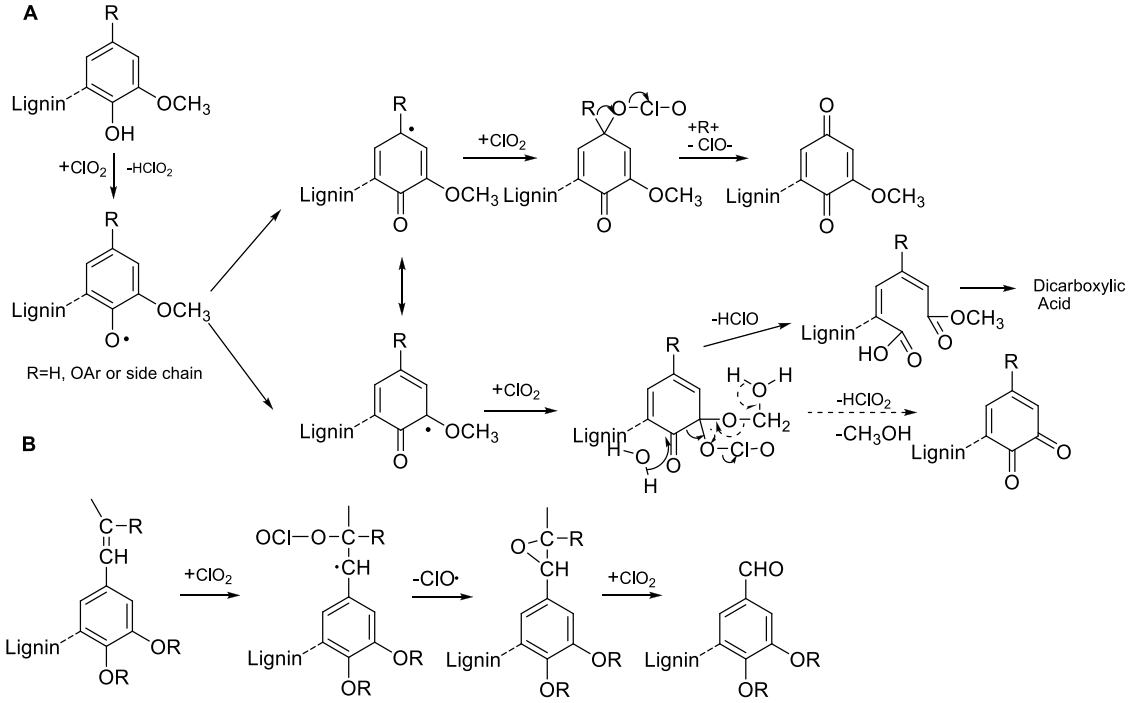

The initial reaction of ClO_2 with phenolic lignin units and olefinic side chains moieties forms both chlorite and hypochlorous acid (HOCl) (Svenson et al., 2006). Chlorite ions decompose in the acid medium to reform chlorine dioxide or they react with the hypochlorous acid to form chlorate and chloride ions. The latter reaction represents a waste of oxidation power of chlorite (Jiang et al., 2007). Lignin oxidation by ClO_2 followed by ClO_2 regeneration in the acid medium continued until all of the chlorite was consumed. As a result, at low pH, residual chlorite did not contribute to losses in ClO_2 oxidation efficiency (Svenson et al., 2006). Therefore, pH has a major effect on ClO_2 oxidation efficiency (Jiang & Berry, 2011; Svenson et al., 2006).

ClO_2 oxidation of ring-conjugated structures (Scheme 1B) leads to formation of lower molecular weight lignin fragments (Santos et al., 2013). Although ClO_2 produce lignin fragment with low molecular weight, lignin is not dissolved and removed under the acidic conditions as the pH of ClO_2 is in the range of 3.4-3.5 according to our experimental data. Therefore, Kason lignin was not removed significantly by ClO_2 from NH3 treated corn stover as shown in Figure 5-1.

5.5.3 Effect of lignin modification on enzymatic hydrolysis

Two schools of thoughts have been reported as to how lignin affect the yield of cellulose hydrolysis. According to steric theory, the soluble enzymes while acting on an insoluble substrate encounter ancillary components of lignin, which may restrict their access to cellulose due to heterogeneous system. The other theory suggest that the non-productive binding of cellulases to the lignin bonding limit the accessibility of the enzymes to the cellulose (Nakagame et al., 2010). Although hydrophobic, electrostatic, and hydrogen bonding interactions are involved in these cellulase-lignin interactions, the exact mechanisms by which cellulases interact with lignin and result in the reduction in the efficiency of hydrolysis have yet to be fully resolved (Nakagame et al., 2010).

It is well known that phenolic hydroxyl group of lignin plays a key role in lignin-induced enzyme inhibition. However, it is still unclear how phenolic hydroxyl groups affect the enzymatic hydrolysis. The hydroxyl groups in lignin may form hydrogen bonds with cellulase, which may interfere the interactions between cellulose and cellulase (Nakagame et al., 2011). Yang & Pan (2016) observed that blocking free phenolic hydroxyl groups by chemical reaction such as hydroxypropylation significantly reduced the inhibitory effect of lignin. Since ClO_2 treatment reduces phenolic hydroxyl group in lignin (Lachenal et al., 1995; Liu & Zhou, 2011;), it would lower the interaction between cellulase and lignin, consequently enhance the enzymatic hydrolysis Yang & Pan, 2016).

Hydrophobic interaction has also been considered as a driving force that governs protein adsorption. When enzyme is dissolved in water, it tends to minimize the exposure of its hydrophobic groups to the aqueous environment. Hence, if the hydrophobicity of both the enzyme and solid surface of lignin increases there is a greater tendency for adsorption to occur, and vice versa. Yang & Pan (2016) showed that the introduction of carboxyl groups reduced the hydrophobicity of the lignin, thereby reduced enzyme adsorption on the modified lignin to enhance enzymatic hydrolysis. Moreover, quinonid structure, the oxidative product of ClO_2 might have lower hydrophobicity than that of its corresponding lignin (Kim et al., 2014). These would serve as plausible explanation for our data that ClO_2 treatment significantly reduced the hydrophobicity of lignin and increased enzymatic digestibility.

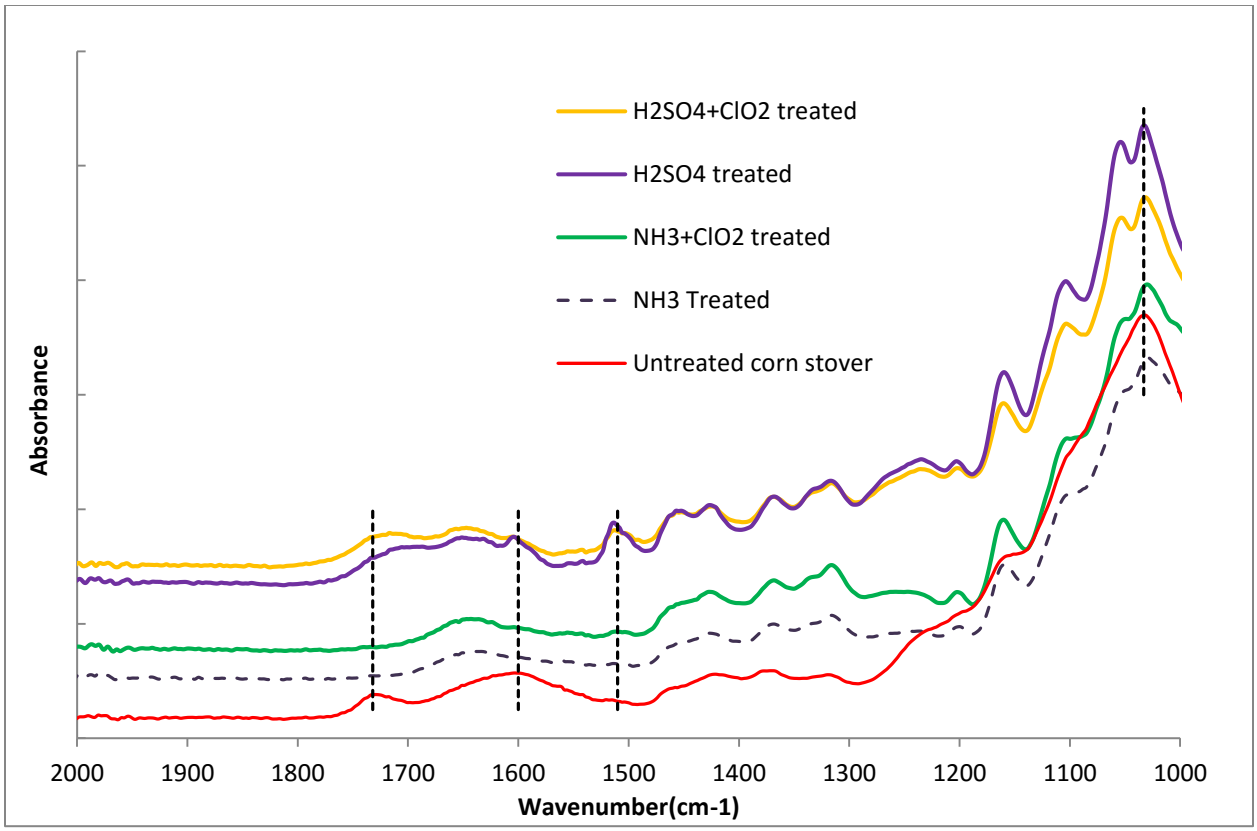

Figure 5-5 FTIR data of untreated, NH_3 treated, (NH_3+ClO_2) treated, H_2SO_4 treated, (H_2SO_4+ClO_2) treated corn stover.

5.5.4 Effect of lignin distribution on enzymatic hydrolysis

The FTIR spectra of treated and untreated corn stover representing only in the fingerprint region between 1800 and 1100 cm^{-1} are shown in Figure 5-5. The broad band located around 3400 cm^{-1} corresponded to the −OH stretching vibration and the band at about 2924 cm^{-1} was due to the asymmetric stretching vibration of the aliphatic moieties in lignin and polysaccharides (data not represented here). Literatures suggest the lignin characteristic peaks were observed at 1732 cm^{-1} corresponds to the stretching of the unconjugated carbonyl group (C=O), at 1600 cm^{-1} band position assigned to aromatic skeletal vibration, and reduction or shift in this position is attributed to condensation reactions and/ or splitting of lignin aliphatic side chains (Kumar et al., 2009; Sun

et al., 2005). The absorbance at 1510 cm^{-1} is attributed to the aromatic ring stretch. The region of 1200–1000cm^{-1} represents C–O stretch and deformation bands in cellulose, lignin and residual hemicelluloses chains (Kumar et al., 2009; Sun et al., 2005). The appreciable reduction in peak intentieis at 1510, 1600, and 1732 cm^{-1} corresponding to different kinds of bonds confirms lignin degradation during NH_3 and NH_3+ClO_2 treatment. On the contrary, lignin band at these locations particularly at 1510 cm^{-1} (aromatic ring stretch) are increased in the H_2SO_4 treated corn stover. The most important reaction during acidolysis of lignin is the autocatalytic cleavage of the β-O-4 bonds among various lignin and hemicellulosic bonds. The cleavage of this linkage leads to the formation of lower molecular weight lignin fragments as well as more phenolic hydroxyl groups. The carboxylic moieties in the lignin is also increased due to cleavage of the ester bonds of lignin–carbohydrate complexes. However, degradation reactions is more dominant at lower severities whereas condensation reactions at higher severities (Moxley et al., 2012). Therefore, at relatively high temperature (160 °C), lignin is softened and relocalized to the outer surface of the cell wall (Kristensen et al., 2008). Moreover, pseudo-lignin might be generated from carbohydrates without significant contribution from lignin during dilute acid pretreatment especially at this condition. This pseudo-lignin yields a positive klason lignin value (Sannigrahi et al., 2012). Hence, the fact that lignin band at these locations are increased indicates that essentially no lignin removed due to relocation during acidic treatment in accordance with composition data as shown in Table 5-3.

Figure 5-6 also demonstrates the fate of surface lignin. It shows both aqueous ammonia and aqueous ammonia followed by ClO_2 treatment removed surface lignin of corn stover as yellow color is the indicator of lignin-rich surface where as black color indicate lignin depleted surface. On the other hand, dilute acid treatment transformed the yellow surface to dark goldenrod surface

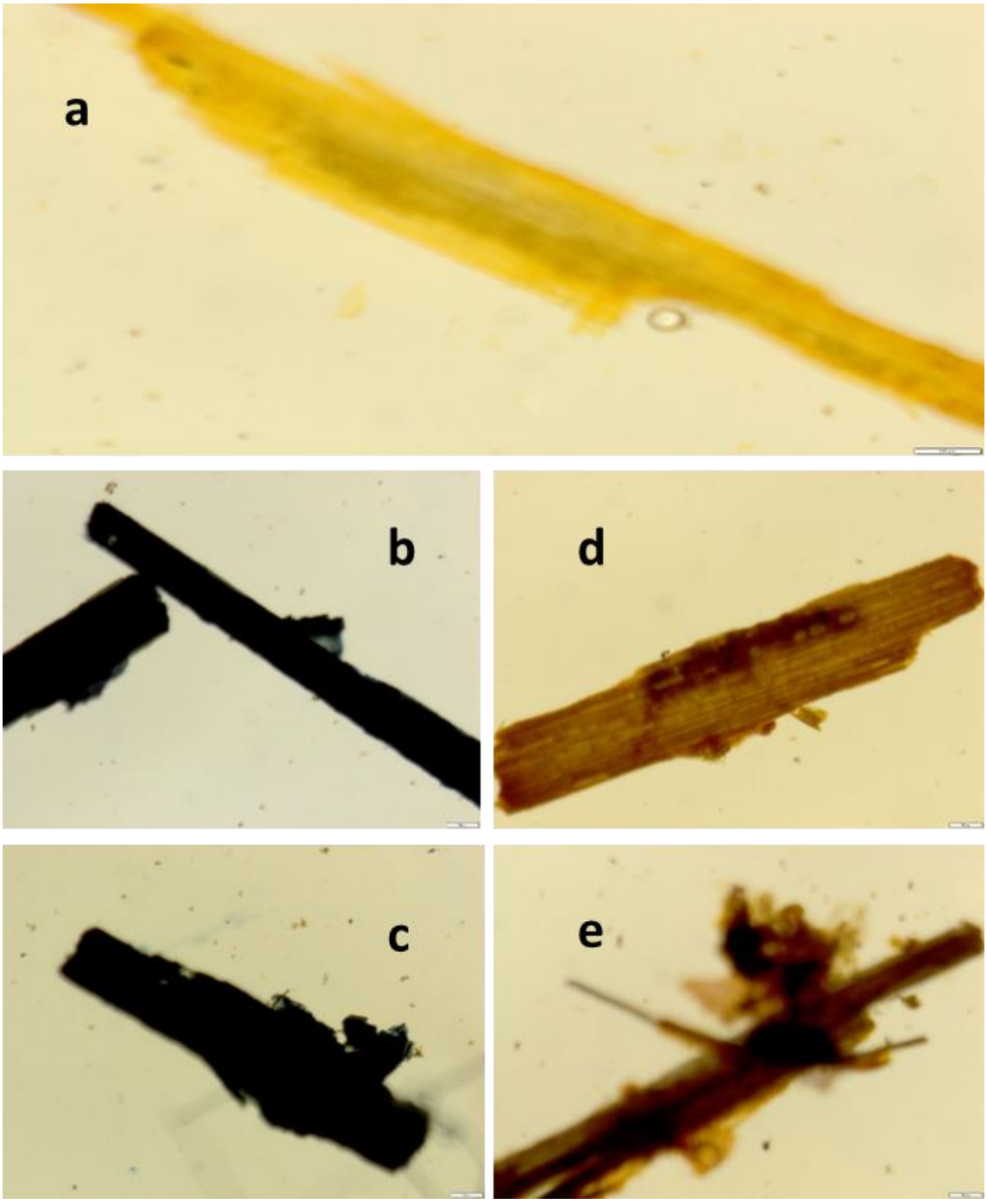

Figure 5-6 Stained microscope images of a) untreated, b) NH_3 treated, c) (NH_3+ ClO_2) treated, d) H_2SO_4 treated, e) (H_2SO_4+ClO_2) treated corn stover.

and ClO_2 introduced sporadic black color onto dark goldenrod indicating small amount of lignin is removed during ClO_2 treatment. Liu et al. (2017) showed that surface lignin concentration has a strong negative effect on glucan digestibility of poplar. Nevertheless, the glucan digestibility of H_2SO_4 treated corn stover is still high due to xylan removal.

The main difference between acidic and alkaline pretreatment is that the acidic treatment makes cellulase enzyme easily accessible to the adsorption site by xylan removal whereas alkali treatment does this by removing lignin. One possible reason for decrease of digestibility for acid treated corn stover after ClO_2 treatment is related with the fact that low molecular weight lignin is generated at the second stage. Since most of the lignin is removed during alkali treatment, low molecular weight lignin has little effect on enzyme accessibility. However, it has much greater effect on the H_2SO_4-treated corn stover as high amount of the lignin is relocated at the surface during primary stage. When acid treated corn stover is subjected to another treatment by ClO_2, low molecular weight lignin is redistributed throughout the biomass substrate, and forms a protective layer. Consequently, negative effect of ClO_2 was observed in enzymatic hydrolysis of H_2SO_4-treated corn stover. Acid treatment also enhances the number of phenolic hydroxyl groups and carboxylic moieties. The subsequent ClO_2 treatment reduce the number of phenolic group and increases the number of carboxylic moieties which is beneficial to enzymatic hydrolysis as explained earlier. However, the steric hindrance of lower molecular weight lignin surpass these effects due to larger amount of lower molecular weight lignin still retain inside treated biomass.

The BET surface area, pore volume, and pore diameter were measured for treated and untreated samples. Both acid and alkali treatment at primary stage increase external surface area of the feedstock. Contrary to this, ClO2 treatment at 2nd stage reduces the surface area as shown in Table 5-5. Virtually no change was seen in pore volume and pore diameter. Considering the extremely

low pore volume (0.001–0.003 cm^3g^{-1}) and pore size (7-9 nm) much smaller than enzyme molecules, the physical properties of the biomass have no effect on the enzymatic

Table 5-5 Changes in surface area and pore volume of corn stover

Treatment	Pore diameter (nm)	Surface area [m^2g^{-1}]	Pore volume [$cm^{-3}g^{-1}$]
Untreated corn stover	7.9	0.91	0.002
NH_3 only	9.3	1.17	0.003
NH_3 & ClO_2	8.0	0.95	0.002
H_2SO4 only	8.9	1.21	0.003
H_2SO4 + ClO_2	7.1	0.67	0.001

5.5.5 Other factors that are being altered during ClO_2 pretreatment.

In addition, crystallinity is believed to significantly affect enzymatic saccharification of glucan. Generally, low crystallinity was desirable as high crystallinity of cellulose may lead to lower enzymatic digestibility (Tian et al., 2016). The diffraction patterns show that the crystallinity index of corn stover significantly enhanced with pretreatment (Figure 5-7). The increased crystallinity index upon treatment is primarily due to removal of amorphous substances (lignin and hemicellulose), not due to changes in the basic crystalline structure of the cellulose as the alkali, treatment removed mostly lignin while acid treatment removed mostly xylan (Kim et al., 2003). Although, thermochemical pretreatments can change cellulose crystalline structure by disrupting inter/intra hydrogen bonding of cellulose chains, crystallinity index is not an accurate representation of what effect pretreatments have on just cellulose crystallinity (Kumar et al., 2009).

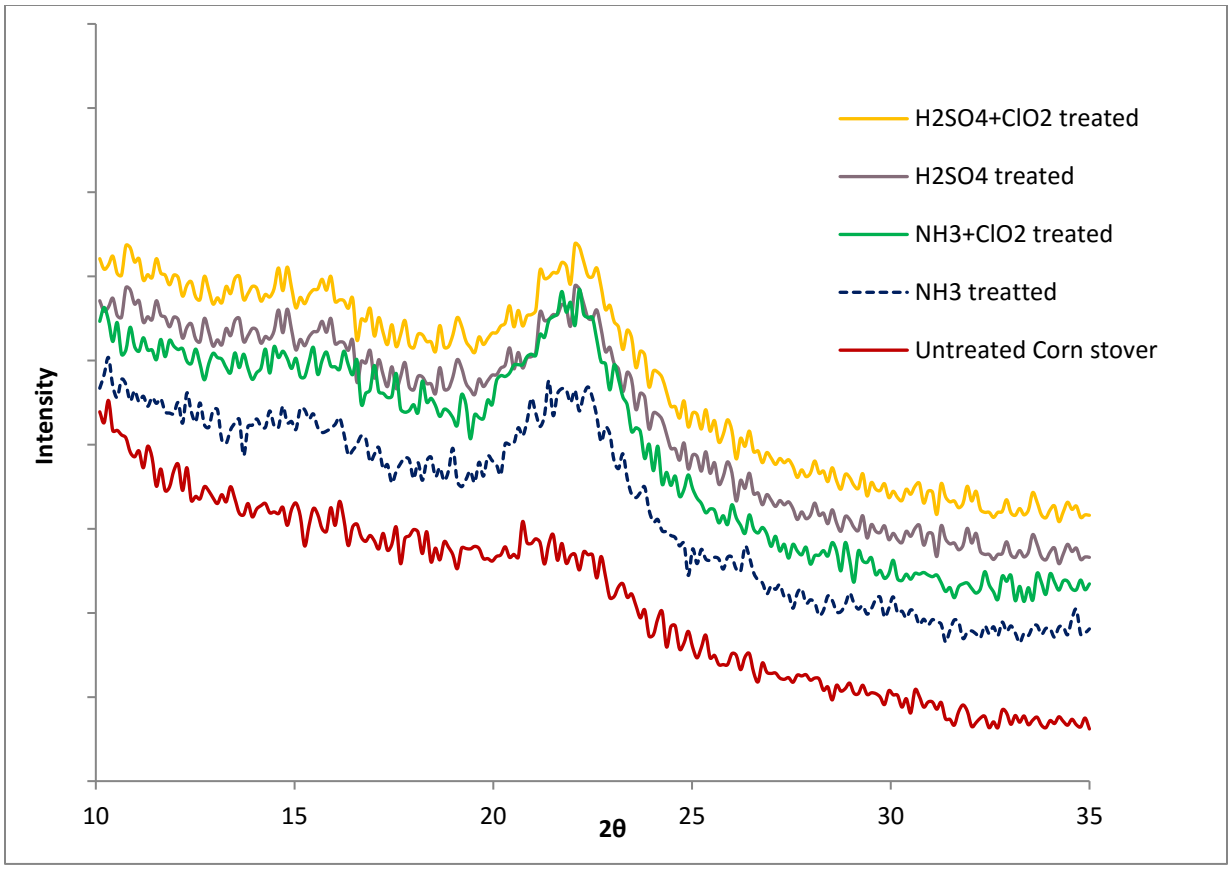

Figure 5-7 XRD data of untreated, NH_3 treated, (NH_3+ ClO_2) treated, H_2SO_4 treated, (H_2SO_4+ClO_2) treated corn stover

In their studies, Carlsson and their groups found ClO_2 always reduces the amount of surface lignin, but the extent of reduction depends on amount and reactivity of residual lignin which varies in various morphological areas of fibres (Laine, 1997; Laine et al., 1994). (Simola et al., 2000) observed that a granular surface structure was replaced by a fibrillar surface during delignification of kraft pulp. When observed in micro level, the pretreated samples exhibited a considerable change in morphology (Figure 5-8). Both the images of the corn stover taken after the primary stage (NH_3) and the images of samples from secondary stage (NH_3+ClO_2) show the disrupted structure of corn stover. Besides, H_2SO_4 and H_2SO_4 followed ClO_2 treatment reduces fiber length and totally disrupted biomass structure. Since ClO_2 reduces surface lignin, there might be some

structural change although it is difficult to distinguish the effect of ClO_2 on this change in SEM pictures. However, the surface lignin removal is obvious for acid followed by ClO_2 as shown in Figure 5-6d.

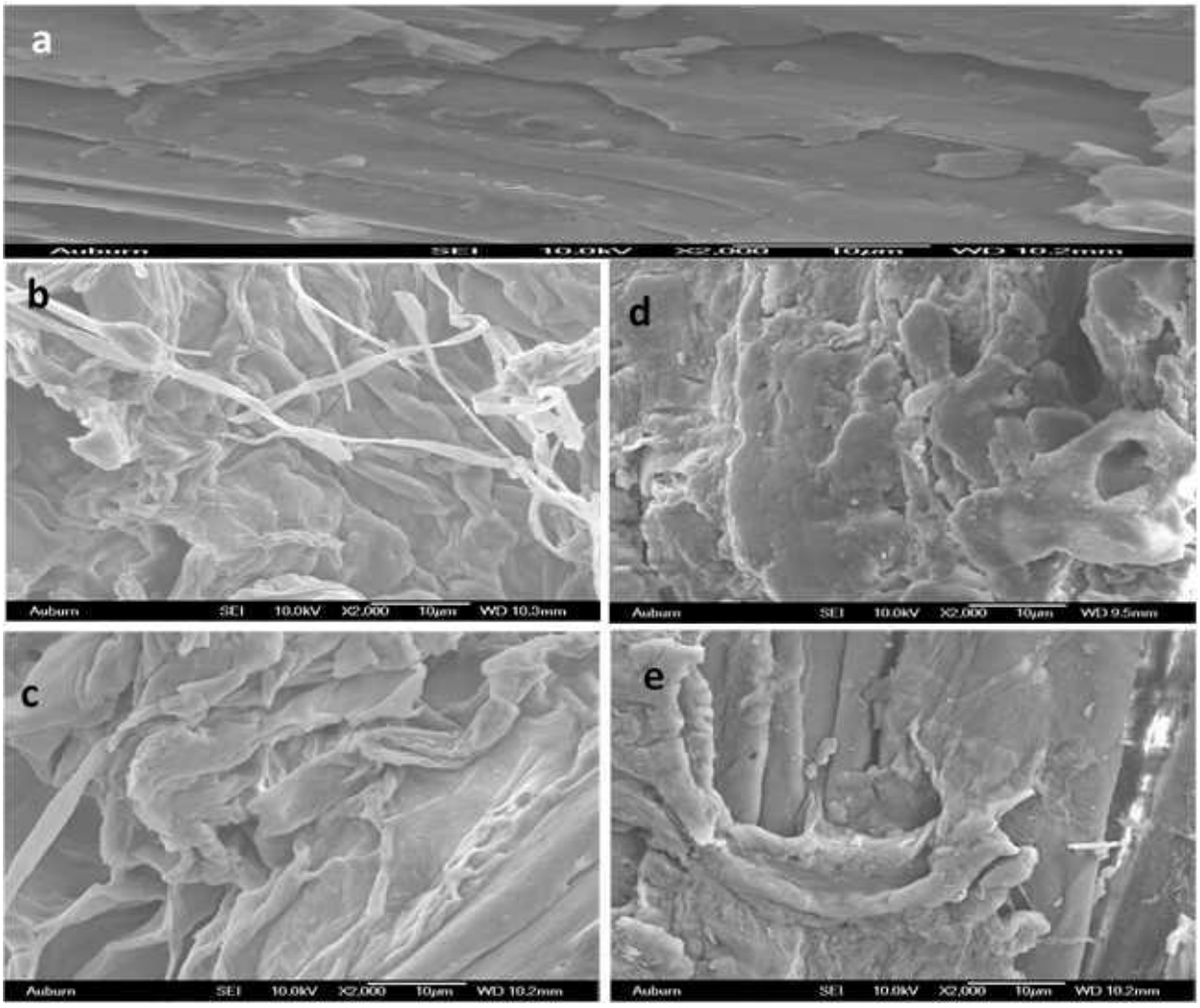

Figure 5-8. Scanning electron microscope images of a) untreated, b) NH_3 treated, c) (NH_3+ ClO_2) treated, d) H_2SO_4 treated, e) (H_2SO_4+ClO_2) treated corn stover.

5.6 Conclusion

Chlorine dioxide treatment significantly improves the efficiency of enzymatic hydrolysis of alkali-treated biomass. The main effect of ClO_2 treatment is the structural change of the lignin, not reduction of the gross lignin content. ClO_2 treatment reduces phenolic hydroxyl group and increases carboxylic acid groups and its derivatives in lignin. These two structural changes bring about reduction of the hydrophobicity of residual lignin and interfere with the H-bond between cellulase and lignin, consequently reducing the unproductive binding of cellulase and lignin, the main reason for increased enzymatic hydrolysis reaction.

Chapter 6

Conclusions and Recommendations for Further Research

The focus of this dissertation was to develop technical strategies for the aqueous phase production of several value added chemicals from carbohydrate through biochemical and thermochemical pathways. In first stage of this study, a kinetic model was developed, based on the data collected on batch reactor, to predict the optimal reactor design and operating conditions for HMF and LA production in a continuous system. Then a dual-solid acid catalyst system was introduced to achieve higher LA yield from glucose. In the 2nd part, a bioconversion strategy for lactic acid production from mixed feedstocks via simultaneous saccharification and co-fermentation (SSCF) was developed. Then a technical strategy to enhance enzymatic saccharification of lignocellulosic biomass using chlorine dioxide as a supplementary pretreatment reagent was developed. Thus, this study shows that both biochemical and thermochemical pathways can be effectively used to produce biomass derived chemical LA and lactic acid. Based on this study, we proposed few more task, which will determine the technical feasibility of these processes in a comprehensive manner. This is very important for any process to be implemented in industrial scale.

6.1.1 Develop a generalized kinetic model of sulfuric acid catalyzed LA production from hexose sugar

The aqueous phase production of LA from glucose involves isomerization, dehydration, fragmentation, reversion, and condensation steps. There are two schools of thought exists with

regard to the HMF formation from C6 carbohydrate in literature. One pathway postulates that the isomerization of glucose into fructose is the primary reaction pathway together with a small amount of mannose (Choudhary et al., 2013; Moliner et al., 2010). Then fructose is converted to HMF by dehydration and subsequently hydrolyzes to form LA and formic acids. The Other theory suggests that the dehydration of glucose does not involve the isomerization of glucose to fructose as the first step of the reaction. According to this theory, glucose can be converted into HMF through cyclization of 3-deoxyglucosone (3-DG) intermediate formed from the open-ring form of glucose (Chidambaram & Bell, 2010; Locas & Yaylayan, 2008). In chapter 2, we have developed a kinetic model for the decomposition of glucose to produce LA and formic acid assuming no fructose formation was involved in the formation of HMF. However, we have seen fructose formation is the 1st step of HMF formation when solid catalyst was used in chapter 3. The next step of this line of study is to develop a generalized kinetic model for aqueous phase production of LA from glucose, which could explain both mechanisms. Therefore, the first task will be to develop kinetic model of fructose decomposition and then incorporate fructose model into glucose decomposition. Once developed, this generalized kinetic model can be be implemented to other sugars especially mannose since it is a dominant constituent for soft wood after glucose.

6.1.2 LA production from cellulose

In chapter three, we have prepared a series of solid Lewis acid catalysts and tested them for glucose to fructose isomerization. We also tested these solid catalysts together with a commercial solid acid catalyst (Amberlyst-15) to produce LA from glucose in aqueous media, as LA is the consequence of sequential reaction of hexose – 1st isomerization and then dehydration / rehydration. In this study, we used liquid feedstocks for the production of LA. This work can be extended to cellulose, the main component of lignocelluloses, which is also a biopolymer

consisting of many glucose units connected through β-1,4-glycosidic bonds. The first step for cellulose utilization is to depolymerize it into soluble oligosaccharides and glucose. Therefore, the next step of this line of work will be to figure out the proper catalyst, suitable conditions so that all step of the reaction can be carried out in "one pot synthesis" manner.

6.1.3 Effect of alkali or acid on ClO_2 treated biomass

In this study, two different types of two-step pretreatment process, alkaline followed by ClO2 and dilute acid followed ClO_2 were evaluated as a measure of enzymatic deconstruction of biomass to monomeric sugars. Study reveals that the glucan digestibility of alkali followed by chlorine dioxide treated feedstock is higher than that of alkali-only treated feedstocks. On the other hand, dilute acid followed by chlorine dioxide has negative effect on enzymatic hydrolysis. However, we did not have any idea about if we reverse the process i.e. ClO_2 followed by alkali or acid treatment. The objective of this task is to identify the best possible sequence of chlorine dioxide in improving subsequent enzymatic hydrolysis.

6.1.4 Lactic acid production of different feedstocks

In chapter four, hemp hurd, an industrial byproduct of bast fiber that is currently disposed as a solid waste, was investigated as a complementary feedstock to paper mill sludge for lactic acid production using SSCF. The results indicate that the mixture of sludge and hemp hurd has great potential as a feedstock for lactic acid production. This study can be extended to other feedstocks, which is compatible with sludge to produce lactic acid. The specific task is to find the proper mixing ratio to maintain pH at optimum level with as high as solid loading.

References

Abdel-Rahman, M.A., Tashiro, Y., Sonomoto, K. 2011. Lactic acid production from lignocellulose-derived sugars using lactic acid bacteria: Overview and limits. *Journal of Biotechnology*, **156**(4), 286-301.

Abdel-Rahman, M.A., Tashiro, Y., Sonomoto, K. 2013. Recent advances in lactic acid production by microbial fermentation processes. *Biotechnology Advances*, **31**(6), 877-902.

Acharjee, T.C., 2010. Thermal pretreatment options for lignocellulosic biomass, M.S. Thesis, University of Nevada, Reno.

Acharjee, T.C., 2011. Exploring the Potential Use of Camelina sativa as a Biofuel crop for Nevada , M.S. Thesis, University of Nevada, Reno

Adachi, E., Torigoe, M., Sugiyama, M., Nikawa, J., Shimizu, K. 1998. Modification of metabolic pathways of Saccharomyces cerevisiae by the expression of lactate dehydrogenase and deletion of pyruvate decarboxylase genes for the lactic acid fermentation at low pH value. *Journal of Fermentation and Bioengineering*, **86**(3), 284-289.

Alonso, D.M., Wettstein, S.G., Dumesic, J.A. 2013. Gamma-valerolactone, a sustainable platform molecule derived from lignocellulosic biomass. *Green Chemistry*, **15**(3), 584-595.

Asghari, F.S., Yoshida, H. 2006. Acid-catalyzed production of 5-hydroxymethyl furfural from D-fructose in subcritical water. *Industrial & Engineering Chemistry Research*, **45**(7), 2163-2173.

Assary, R.S., Kim, T., Low, J.J., Greeley, J., Curtiss, L.A. 2012. Glucose and fructose to platform chemicals: understanding the thermodynamic landscapes of acid-catalysed reactions using high-level ab initio methods. *Physical Chemistry Chemical Physics*, **14**(48), 16603-16611.

Assary, R.S., Redfern, P.C., Greeley, J., Curtiss, L.A. 2011. Mechanistic Insights into the Decomposition of Fructose to Hydroxy Methyl Furfural in Neutral and Acidic Environments Using High-Level Quantum Chemical Methods. *Journal of Physical Chemistry B*, **115**(15), 4341-4349.

Balan, V., Sousa, L.D., Chundawat, S.P.S., Marshall, D., Sharma, L.N., Chambliss, C.K., Dale, B.E. 2009. Enzymatic Digestibility and Pretreatment Degradation Products of AFEX-Treated Hardwoods (Populus nigra). *Biotechnology Progress*, **25**(2), 365-375.

Barroca, M., Seco, I.M., Fernandes, P.M.M., Ferreira, L., Castro, J. 2001. Reduction of AOX in the bleach plant of a pulp mill. *Environmental Science & Technology*, **35**(21), 4390-4393.

Bhalla, A., Bansal, N., Stoklosa, R.J., Fountain, M., Ralph, J., Hodge, D.B., Hegg, E.L. 2016. Effective alkaline metal-catalyzed oxidative delignification of hybrid poplar. *Biotechnology for Biofuels*, **9**.

Bozell, J.J., Moens, L., Elliott, D.C., Wang, Y., Neuenscwander, G.G., Fitzpatrick, S.W., Bilski, R.J., Jarnefeld, J.L. 2000. Production of levulinic acid and use as a platform chemical for derived products. *Resources Conservation and Recycling*, **28**(3-4), 227-239.

Bozell, J.J., Petersen, G.R. 2010. Technology development for the production of biobased products from biorefinery carbohydrates-the US Department of Energy's "Top 10" revisited. *Green Chemistry*, **12**(4), 539-554.

Brogdon, B.N., Mancosky, D.G., Lucia, L.A. 2004. New insights into lignin modification during chlorine dioxide bleaching sequences (I): Chlorine dioxide delignification. *Journal of Wood Chemistry and Technology*, **24**(3), 201-219.

Bustos, G., Moldes, A.B., Cruz, J.M., Dominguez, J.M. 2005. Influence of the metabolism pathway on lactic acid production from hemicellulosic trimming vine shoots hydrolyzates using Lactobacillus pentosus. *Biotechnology Progress*, **21**(3), 793-798.

Capek, L., Kreibich, V., Dedecek, J., Grygar, T., Wichterlova, B., Sobalik, Z., Martens, J.A., Brosius, R., Tokarova, V. 2005. Analysis of Fe species in zeolites by UV-VIS-NIR, IR spectra and voltammetry. Effect of preparation, Fe loading and zeolite type. *Microporous and Mesoporous Materials*, **80**(1-3), 279-289.

Cha, J.Y., Hanna, M.A. 2002. Levulinic acid production based on extrusion and pressurized batch reaction. *Industrial Crops and Products*, **16**(2), 109-118.

Chambon, F., Rataboul, F., Pinel, C., Cabiac, A., Guillon, E., Essayem, N. 2011. Cellulose hydrothermal conversion promoted by heterogeneous Bronsted and Lewis acids: Remarkable efficiency of solid Lewis acids to produce lactic acid. *Applied Catalysis B-Environmental*, **105**(1-2), 171-181.

Chang, C., Ma, X.J., Cen, P.L. 2009. Kinetic Studies on Wheat Straw Hydrolysis to Levulinic Acid. *Chinese Journal of Chemical Engineering*, **17**(5), 835-839.

Chang, C., Ma, X.J., Cen, P.L. 2006. Kinetics of levulinic acid formation from glucose decomposition at high temperature. *Chinese Journal of Chemical Engineering*, **14**(5), 708-712.

Chapman, J.S. 2003. Biocide resistance mechanisms. *International Biodeterioration & Biodegradation*, **51**(2), 133-138.

Cherubini, F. 2010. The biorefinery concept: Using biomass instead of oil for producing energy and chemicals. *Energy Conversion and Management*, **51**(7), 1412-1421.

Chheda, J.N., Huber, G.W., Dumesic, J.A. 2007. Liquid-phase catalytic processing of biomass-derived oxygenated hydrocarbons to fuels and chemicals. *Angewandte Chemie-International Edition*, **46**(38), 7164-7183.

Chidambaram, M., Bell, A.T. 2010. A two-step approach for the catalytic conversion of glucose to 2,5-dimethylfuran in ionic liquids. *Green Chemistry*, **12**(7), 1253-1262.

Choudhary, V., Mushrif, S.H., Ho, C., Anderko, A., Nikolakis, V., Marinkovic, N.S., Frenkel, A.I., Sandler, S.I., Vlachos, D.G. 2013. Insights into the Interplay of Lewis and Bronsted Acid Catalysts in Glucose and Fructose Conversion to 5-(Hydroxymethyl)furfural and Levulinic Acid in Aqueous Media. *Journal of the American Chemical Society*, **135**(10), 3997-4006.

Corma, A., Iborra, S., Velty, A. 2007. Chemical routes for the transformation of biomass into chemicals. *Chemical Reviews*, **107**(6), 2411-2502.

da Costa Correia, J.A., Marques Junior, J.E., Goncalves, L.R.B., Ponte Rocha, M.V. 2013. Alkaline hydrogen peroxide pretreatment of cashew apple bagasse for ethanol production: Study of parameters. *Bioresource Technology*, **139**, 249-256.

Demirbas, A. 2007. Progress and recent trends in biofuels. *Progress in Energy and Combustion Science*, **33**(1), 1-18.

Demirbas, M.F. 2006. Current technologies for biomass conversion into chemicals and fuels. *Energy Sources Part a-Recovery Utilization and Environmental Effects*, **28**(13), 1181-1188.

Dougherty, M.J., Tran, H.M., Stavila, V., Knierim, B., George, A., Auer, M., Adams, P.D., Hadi, M.Z. 2014. Cellulosic Biomass Pretreatment and Sugar Yields as a Function of Biomass Particle Size. *Plos One*, **9**(6).

Dzwigaj, S., Peltre, M.J., Massiani, P., Davidson, A., Che, M., Sen, T., Sivasanker, S. 1998. Incorporation of vanadium species in a dealuminated beta zeolite. *Chemical Communications*(1), 87-88.

Efremov, A.A., Pervyshina, G.G., Kuznetsov, B.N. 1997. Thermocatalytic transforms of wood pulp and cellulose in the presence of HCl, HBr and H2SO4. *Khimiya Prirodnykh Soedinenii*(1), 107-112.

Elferink, S., Krooneman, J., Gottschal, J.C., Spoelstra, S.F., Faber, F., Driehuis, F. 2001. Anaerobic conversion of lactic acid to acetic acid and 1,2-propanediol by Lactobacillus buchneri. *Applied and Environmental Microbiology*, **67**(1), 125-132.

Fang, Q., Hanna, M.A. 2002. Experimental studies for levulinic acid production from whole kernel grain sorghum. *Bioresource Technology*, **81**(3), 187-192.

Ferchichi, M., Crabbe, E., Gil, G.H., Hintz, W., Almadidy, A. 2005. Influence of initial pH on hydrogen production from cheese whey. *Journal of Biotechnology*, **120**(4), 402-409.

FitzPatrick, M., Champagne, P., Cunningham, M.F., Whitney, R.A. 2010. A biorefinery processing perspective: Treatment of lignocellulosic materials for the production of value-added products. *Bioresource Technology*, **101**(23), 8915-8922.

Fitzpatrick, S. W. 1997. Production of levulinic acid from carbohydrate-containing materials: U.S. Patent 5,608,105

Fitzpatrick, S.W. 2006. The Biofine technology A "bio-refinery" concept based on thermochemical conversion of cellulosic biomass. *Feedstocks for the Future: Renewables for the Production of Chemicals and Materials*, **921**, 271-287.

Fu, C.X., Mielenz, J.R., Xiao, X.R., Ge, Y.X., Hamilton, C.Y., Rodriguez, M., Chen, F., Foston, M., Ragauskas, A., Bouton, J., Dixon, R.A., Wang, Z.Y. 2011. Genetic manipulation of

lignin reduces recalcitrance and improves ethanol production from switchgrass. *Proceedings of the National Academy of Sciences of the United States of America*, **108**(9), 3803-3808.

Gallezot, P. 2012. Conversion of biomass to selected chemical products. *Chemical Society Reviews*, **41**(4), 1538-1558.

Gandolfi, S., Ottolina, G., Riva, S., Fantoni, G.P., Patel, I. 2013. Complete Chemical Analysis of Carmagnola Hemp Hurd and Structural Features of Its Components. *Bioresources*, **8**(2), 2641-2656.

Gandolfi, S., Pistone, L., Ottolina, G., Xu, P., Riva, S. 2015. Hemp hurd biorefining: A path to green L-(+)-lactic acid production. *Bioresource Technology*, **191**, 59-65.

Garde, A., Jonsson, G., Schmidt, A.S., Ahring, B.K. 2002. Lactic acid production from wheat straw hemicellulose hydrolysate by Lactobacillus pentosus and Lactobacillus brevis. *Bioresource Technology*, **81**(3), 217-223.

Gauss, W., Suzuki, S., Takagi, M. 1976. Manufacture of alcohol from cellulosic materials using plural ferments

Gellerstedt, G., Lindfors, E.L., Pettersson, M., Robert, D. 1995. Reaction of lignin in chlorine dioxide bleaching of kraft pupls. *Research on Chemical Intermediates*, **21**(3-5), 441-456.

Girisuta, B., Danon, B., Manurung, R., Janssen, L., Heeres, H.J. 2008. Experimental and kinetic modelling studies on the acid-catalysed hydrolysis of the water hyacinth plant to levulinic acid. *Bioresource Technology*, **99**(17), 8367-8375.

Girisuta, B., Dussan, K., Haverty, D., Leahy, J.J., Hayes, M.H.B. 2013. A kinetic study of acid catalysed hydrolysis of sugar cane bagasse to levulinic acid. *Chemical Engineering Journal*, **217**, 61-70.

Girisuta, B., Janssen, L., Heeres, H.J. 2006a. A kinetic study on the conversion of glucose to levulinic acid. *Chemical Engineering Research & Design*, **84**(A5), 339-349.

Girisuta, B., Janssen, L., Heeres, H.J. 2006b. A kinetic study on the conversion of glucose to levulinic acid. *Chemical Engineering Research & Design*, **84**(A5), 339-349.

Girisuta, B., Janssen, L., Heeres, H.J. 2007a. Kinetic study on the acid-catalyzed hydrolysis of cellulose to levulinic acid. *Industrial & Engineering Chemistry Research*, **46**(6), 1696-1708.

Girisuta, B., Janssen, L., Heeres, H.J. 2007b. Kinetic study on the acid-catalyzed hydrolysis of cellulose to levulinic acid. Industrial & Engineering Chemistry Research, 46(6), 1696-1708.

Guan, Wenjian., 2016. Bioconversion of lignocellulose into acetone-butanol-ethanol (ABE): pretreatment, enzymatic hydrolysis and fermentation, Ph.D. Dissertation, Auburn University, Auburn

Guan, W.J., Shi, S.A., Tu, M.B., Lee, Y.Y. 2016. Acetone-butanol-ethanol production from Kraft paper mill sludge by simultaneous saccharification and fermentation. Bioresource Technology, 200, 713-721.

Gupta, R., 2008. Alkaline pretreatment of biomass for ethanol production and understanding the factors influencing the cellulose hydrolysis, *Ph.D. Dissertation*, Auburn University, Auburn

Gupta, R., Lee, Y.Y. 2010. Pretreatment of Corn Stover and Hybrid Poplar by Sodium Hydroxide and Hydrogen Peroxide. *Biotechnology Progress*, **26**(4), 1180-1186.

Gupta, R., Lee, Y.Y. 2009. Pretreatment of Hybrid Poplar by Aqueous Ammonia. *Biotechnology Progress*, **25**(2), 357-364.

Hammond, C., Conrad, S., Hermans, I. 2012. Simple and Scalable Preparation of Highly Active Lewis Acidic Sn-beta. *Angewandte Chemie-International Edition*, **51**(47), 11736-11739.

Hayes D. J., Ross J., Hayes M. H. B., Fitzpatrick S. 2008. The Biofine Process: Production of Levulinic Acid, Furfural and Formic Acid from Lignocellulosic Feedstocks , Biorefinery (8b)

Hegner, J., Pereira, K.C., DeBoef, B., Lucht, B.L. 2010. Conversion of cellulose to glucose and levulinic acid via solid-supported acid catalysis. *Tetrahedron Letters*, **51**(17), 2356-2358.

Helmerius, J., von Walter, J.V., Rova, U., Berglund, K.A., Hodge, D.B. 2010. Impact of hemicellulose pre-extraction for bioconversion on birch Kraft pulp properties. *Bioresource Technology*, **101**(15), 5996-6005.

Hofvendahl, K., Hahn-Hagerdal, B. 2000. Factors affecting the fermentative lactic acid production from renewable resources. *Enzyme and Microbial Technology*, **26**(2-4), 87-107.

Horn, S.J., Vaaje-Kolstad, G., Westereng, B., Eijsink, V.G.H. 2012. Novel enzymes for the degradation of cellulose. *Biotechnology for Biofuels*, **5**.

Horvat, J., Klaic, B., Metelko, B., Sunjic, V. 1985. MECHANISM OF LEVULINIC ACID FORMATION. *Tetrahedron Letters*, **26**(17), 2111-2114

http://www.worldenergyoutlook.org/. Date of retrieval-May 16, 2015..

Huang, R., Qi, W., Su, R., He, Z. 2010. Integrating enzymatic and acid catalysis to convert glucose into 5-hydroxymethylfurfural. *Chemical Communications*, **46**(7), 1115-1117.

Hubbell, C.A., Ragauskas, A.J. 2010. Effect of acid-chlorite delignification on cellulose degree of polymerization. *Bioresource Technology*, **101**(19), 7410-7415.

Huber, G.W., Iborra, S., Corma, A. 2006. Synthesis of transportation fuels from biomass: Chemistry, catalysts, and engineering. *Chemical Reviews*, **106**(9), 4044-4098.

Jia, C.J., Beaunier, P., Massiani, P. 1998. Comparison of conventional and solid-state ion exchange procedures for the incorporation of lanthanum in H-beta zeolite. *Microporous and Mesoporous Materials*, **24**(1-3), 69-82.

Jiang, Z.H., Berry, R. 2011. Near-Neutral final chlorine dioxide brightening:theory and practice *J-for-Journal of Science & Technology for Forest Products and Processes*, **1**(1), 14-20.

Jiang, Z.H., Van Lierop, B., Berry, R. 2007. Improving chlorine dioxide bleaching with aldehydes. *Journal of Pulp and Paper Science*, **33**(2), 89-94.

John, R.P., Nampoothiri, K.M., Pandey, A. 2007. Fermentative production of lactic acid from biomass: an overview on process developments and future perspectives. *Applied Microbiology and Biotechnology*, **74**(3), 524-534.

Jow, J., Rorrer, G.L., Hawley, M.C., Lamport, D.T.A. 1987. Dehydration of fructose to levulininic acid over LZY zeolite catalyst. *Biomass*, **14**(3), 185-194.

Kamm, B., Kamm, M. 2004. Principles of biorefineries. *Applied Microbiology and Biotechnology*, **64**(2), 137-145.

Kang, L., Wang, W., Lee, Y.Y. 2010. Bioconversion of Kraft Paper Mill Sludges to Ethanol by SSF and SSCF. *Applied Biochemistry and Biotechnology*, **161**(1-8), 53-66.

Kaur, U., Oberoi, H.S., Bhargav, V.K., Sharma-Shivappa, R., Dhaliwal, S.S. 2012. Ethanol production from alkali- and ozone-treated cotton stalks using thermotolerant Pichia kudriavzevii HOP-1. *Industrial Crops and Products*, **37**(1), 219-226.

Kim, J.S., Lee, Y.Y., Kim, T.H. 2016. A review on alkaline pretreatment technology for bioconversion of lignocellulosic biomass. *Bioresource Technology*, **199**, 42-48.

Kim, R.S., Park, W., Hong, H., Chung, T.D., Kim, S. 2014. Quinone electrochemistry altered by local hydrophobic environment and hydrogen bonding interactions. *Electrochemistry Communications*, **41**, 39-43.

Kim, T.H., Kim, J.S., Sunwoo, C., Lee, Y.Y. 2003. Pretreatment of corn stover by aqueous ammonia. *Bioresource Technology*, **90**(1), 39-47.

Kolar, J.J., Lindgren, B.O., Pettersson, B. 1983. Chemical reactions in chlorine dioxide stages of pulp bleaching-intermediately formed hypochlorous acid. *Wood Science and Technology*, **17**(2), 117-128.

Kothari, U. D., 2012. Ethanol from Lignocellulosic Biomass: Deacetylation, Pretreatment, and Enzymatic , *Ph.D. Dissertation*, Auburn University, Auburn

Kothari, U.D., Lee, Y.Y. 2011. Inhibition Effects of Dilute-Acid Prehydrolysate of Corn Stover on Enzymatic Hydrolysis of Solka Floc. *Applied Biochemistry and Biotechnology*, **165**(5-6), 1391-1405.

Kristensen, J.B., Felby, C., Jorgensen, H. 2009. Yield-determining factors in high-solids enzymatic hydrolysis of lignocellulose. *Biotechnology for Biofuels*, **2**.

Kristensen, J.B., Thygesen, L.G., Felby, C., Jorgensen, H., Elder, T. 2008. Cell-wall structural changes in wheat straw pretreated for bioethanol production. *Biotechnology for Biofuels*, **1**.

Kumar, R., Hu, F., Hubbell, C.A., Ragauskas, A.J., Wyman, C.E. 2013. Comparison of laboratory delignification methods, their selectivity, and impacts on physiochemical characteristics of cellulosic biomass. *Bioresource Technology*, **130**, 372-381.

Kumar, R., Mago, G., Balan, V., Wyman, C.E. 2009. Physical and chemical characterizations of corn stover and poplar solids resulting from leading pretreatment technologies. *Bioresource Technology*, **100**(17), 3948-3962.

Kuster, B.F.M., Vanderbaan, H.S. 1977. Dehydration of D-fructose(formation of 5-hydroxymethyl-2-furfuraldehyde and levulinic acid). 2. Influence of initial and catalyst concentrations of dehydration of D-fructose. *Carbohydrate Research*, **54**(2), 165-176.

Lachenal, D., Fernandes, J.C., Froment, P. 1995. Behavior of residual lignin in kraft pulp during bleaching. *Journal of Pulp and Paper Science*, **21**(5), J173-J177.

Lai. L. X., 2010. Bioproducts from sulfite pulping: Bioconversion of sugar streams from pulp, sludge, and spent sulfite liquor. MS thesis, University of Washington

Laine, J. 1997. Effect of ECF and TCF bleaching on the charge properties of kraft pulp. *Paperi Ja Puu-Paper and Timber*, **79**(8), 551-559.

Laine, J., Stenius, P., Carlsson, G., Strom, G. 1994. Surface Characterization of unbleached kraft puls by means of ESCA . *Cellulose*, **1**(2), 145-160.

Lamminpaa, K., Ahola, J., Tanskanen, J. 2012. Kinetics of Xylose Dehydration into Furfural in Formic Acid. *Industrial & Engineering Chemistry Research*, **51**(18), 6297-6303.

Liua W.; Chena W.; Houa Q.; Zhanga J.; Wang B., 2017. Surface lignin change pertaining to the integrated process of dilute acid pre-extraction and mechanical refining of poplar wood chips and its impact on enzymatic hydrolysis. Bioresource Technology, 228, 125-132

Liu, F., Audemar, M., Vigier, K.D.O., Cartigny, D., Clacens, J.-M., Gomes, M.F.C., Padua, A.A.H., De Campo, F., Jerome, F. 2013. Selectivity enhancement in the aqueous acid-catalyzed conversion of glucose to 5-hydroxymethylfurfural induced by choline chloride. *Green Chemistry*, **15**(11), 3205-3213.

Liu, J., Zhou, X.F. 2011. Structural changes in residual lignin of Eucalyptus urophylla x Eucalyptus grandis LH 107 oxygen delignified kraft pulp upon chlorine dioxide bleaching. *Scientia Iranica*, **18**(3), 486-490.

Liu, X.J., Lu, M.Z., Ai, N., Yu, F.W., Ji, J.B. 2012. Kinetic model analysis of dilute sulfuric acid-catalyzed hemicellulose hydrolysis in sweet sorghum bagasse for xylose production. *Industrial Crops and Products*, **38**, 81-86.

Locas, C.P., Yaylayan, V.A. 2008. Isotope labeling studies on the formation of 5-(hydroxymethyl)-2-furaldehyde (HMF) from sucrose by pyrolysis-GC/MS. *Journal of Agricultural and Food Chemistry*, **56**(15), 6717-6723.

Lourvanij, K., Rorrer, G.L. 1993. Reaction of aqueous glucose solutions over solid-acid Y-zeolite catalyst at 110-160 degree C. *Industrial & Engineering Chemistry Research*, **32**(1), 11-19.

Ma, R.S., Xu, Y., Zhang, X. 2015. Catalytic Oxidation of Biorefinery Lignin to Value-added Chemicals to Support Sustainable Biofuel Production. *Chemsuschem*, **8**(1), 24-51.

Maldonado, G.M.G., Assary, R.S., Dumesic, J., Curtiss, L.A. 2012. Experimental and theoretical studies of the acid-catalyzed conversion of furfuryl alcohol to levulinic acid in aqueous solution. *Energy & Environmental Science*, **5**(5), 6981-6989.

Marcotullio, G., Cardoso, M.A.T., De Jong, W., Verkooijen, A.H.M. 2009. Bioenergy II: Furfural Destruction Kinetics during Sulphuric Acid-Catalyzed Production from Biomass. *International Journal of Chemical Reactor Engineering*, **7**, 17.

Marques, S., Alves, L., Roseiro, J.C., Girio, F.M. 2008. Conversion of recycled paper sludge to ethanol by SHF and SSF using Pichia stipitis. *Biomass & Bioenergy*, **32**(5), 400-406.

Moliner, M., Roman-Leshkov, Y., Davis, M.E. 2010. Tin-containing zeolites are highly active catalysts for the isomerization of glucose in water. *Proceedings of the National Academy of Sciences of the United States of America*, **107**(14), 6164-6168.

Monteagudo, J.M., Rodriguez, L., Rincon, J., Fuertes, J. 1997. Kinetics of lactic acid fermentation by Lactobacillus delbrueckii grown on beet molasses. *Journal of Chemical Technology and Biotechnology*, **68**(3), 271-276.

Moxley, G., Gaspar, A.R., Higgins, D., Xu, H. 2012. Structural changes of corn stover lignin during acid pretreatment. *Journal of Industrial Microbiology & Biotechnology*, **39**(9), 1289-1299.

Mussatto, S.I., Fernandes, M., Mancilha, I.M., Roberto, I.C. 2008. Effects of medium supplementation and pH control on lactic acid production from brewer's spent grain. *Biochemical Engineering Journal*, **40**(3), 437-444.

Nakagame, S., Chandra, R.P., Kadla, J.F., Saddler, J.N. 2011. Enhancing the Enzymatic Hydrolysis of Lignocellulosic Biomass by Increasing the Carboxylic Acid Content of the Associated Lignin. *Biotechnology and Bioengineering*, **108**(3), 538-548.

Nakagame, S., Chandra, R.P., Saddler, J.N. 2010. The Effect of Isolated Lignins, Obtained From a Range of Pretreated Lignocellulosic Substrates, on Enzymatic Hydrolysis. *Biotechnology and Bioengineering*, **105**(5), 871-879.

Nghiem, N.P., Senske, G.E., Kim, T.H. 2016. Pretreatment of Corn Stover by Low Moisture Anhydrous Ammonia (LMAA) in a Pilot-Scale Reactor and Bioconversion to Fuel Ethanol and Industrial Chemicals. *Applied Biochemistry and Biotechnology*, **179**(1), 111-125.

Nikolla, E., Roman-Leshkov, Y., Moliner, M., Davis, M.E. 2011. "One-Pot" Synthesis of 5-(Hydroxymethyl)furfural from Carbohydrates using Tin-Beta Zeolite. *Acs Catalysis*, **1**(4), 408-410.

Ohgren, K., Bura, R., Saddler, J., Zacchi, G. 2007. Effect of hemicellulose and lignin removal on enzymatic hydrolysis of steam pretreated corn stover. *Bioresource Technology*, **98**(13), 2503-2510.

Okano, K., Yoshida, S., Yamada, R., Tanaka, T., Ogino, C., Fukuda, H., Kondo, A. 2009. Improved Production of Homo-D-Lactic Acid via Xylose Fermentation by Introduction of Xylose Assimilation Genes and Redirection of the Phosphoketolase Pathway to the Pentose Phosphate Pathway in L-Lactate Dehydrogenase Gene-Deficient Lactobacillus plantarum. *Applied and Environmental Microbiology*, **75**(24), 7858-7861.

Pallapolu , V.R., 2016. Conversion of Lignocellulosic Biomass into Monomeric Sugars and Levulinic Acid: Pretreatment, Enzymatic Hydrolysis, Ph.D. Dissertation, Auburn University, Auburn

Parajo, J.C., Alonso, J.L., Moldes, A.B. 1997. Production of lactic acid from lignocellulose in a single stage of hydrolysis and fermentation. *Food Biotechnology*, **11**(1), 45-58.

Peng, L.C., Lin, L., Li, H., Yang, Q.L. 2011. Conversion of carbohydrates biomass into levulinate esters using heterogeneous catalysts. *Applied Energy*, **88**(12), 4590-4596.

Peng, L.C., Lin, L., Zhang, J.H., Zhuang, J.P., Zhang, B.X., Gong, Y. 2010. Catalytic Conversion of Cellulose to Levulinic Acid by Metal Chlorides. *Molecules*, **15**(8), 5258-5272.

Potvin, J., Sorlien, E., Hegner, J., DeBoef, B., Lucht, B.L. 2011. Effect of NaCl on the conversion of cellulose to glucose and levulinic acid via solid supported acid catalysis. *Tetrahedron Letters*, **52**(44), 5891-5893.

Pradeep, P., Reddy, O.V.S. 2010. High gravity fermentation of sugarcane molasses to produce ethanol: Effect of nutrients. *Indian Journal of Microbiology*, **50**, S82-S87.

Rhee, M.S., Wei, L.S., Sawhney, N., Kim, Y.S., Rice, J.D., Preston, J.F. 2016. Metabolic potential of Bacillus subtilis 168 for the direct conversion of xylans to fermentation products. *Applied Microbiology and Biotechnology*, **100**(3), 1501-1510.

Rivas, S., Gonzalez-Munoz, M.J., Vila, C., Santos, V., Parajo, J.C. 2013. Manufacture of Levulinic Acid from Pine Wood Hemicelluloses: A Kinetic Assessment. *Industrial & Engineering Chemistry Research*, **52**(11), 3951-3957.

Roman-Leshkov, Y., Moliner, M., Labinger, J.A., Davis, M.E. 2010. Mechanism of Glucose Isomerization Using a Solid Lewis Acid Catalyst in Water. *Angewandte Chemie-International Edition*, **49**(47), 8954-8957.

Rubin, E.M. 2008. Genomics of cellulosic biofuels. *Nature*, **454**(7206), 841-845.

Saeman, J.F. 1945. Kinetics of wood saccharification -hydrolysis of cellulose and decompostions of sugars in dilute acid at high temperature. *Industrial and Engineering Chemistry*, **37**(1), 43-52.

San Martin, R., Perez, C., Briones, R. 1995. Simultaneous production of ethanol and kraft pulp from pine (Pinus radiata) using steam explosion. *Bioresource Technology*, **53**(3), 217-223.

Sannigrahi, P., Hu, F., Pu, Y.Q., Ragauskas, A. 2012. A Novel Oxidative Pretreatment of Loblolly Pine, Sweetgum, and Miscanthus by Ozone. *Journal of Wood Chemistry and Technology*, **32**(4), 361-375.

Santos, R.B., Hart, P.W., Jameel, H., Chang, H.M. 2013. Wood Based Lignin Reactions Important to the Biorefinery and Pulp and Paper Industries. *Bioresources*, **8**(1), 1456-1477.

Serrano-Ruiz, J.C., Dumesic, J.A. 2011. Catalytic routes for the conversion of biomass into liquid hydrocarbon transportation fuels. *Energy & Environmental Science*, **4**(1), 83-99.

Shen, J.C., Wyman, C.E. 2012. Hydrochloric Acid-Catalyzed Levulinic Acid Formation from Cellulose: Data and Kinetic Model to Maximize Yields. *Aiche Journal*, **58**(1), 236-246.

Shen, X.L., Xia, L.M. 2006. Lactic acid production from cellulosic material by synergetic hydrolysis and fermentation. *Applied Biochemistry and Biotechnology*, **133**(3), 251-262.

Shi, S., Kang, L., Lee, Y.Y. 2015. Production of Lactic Acid from the Mixture of Softwood Pre-hydrolysate and Paper Mill Sludge by Simultaneous Saccharification and Fermentation. *Applied Biochemistry and Biotechnology*, **175**(5), 2741-2754.

Simeonov, S.P., Coelho, J.A.S., Afonso, C.A.M. 2013. Integrated Chemo-Enzymatic Production of 5-Hydroxymethylfurfural from Glucose. *Chemsuschem*, **6**(6), 997-1000.

Simola, J., Malkavaara, P., Alen, R., Peltonen, J. 2000. Scanning probe microscopy of pine and birch kraft pulp fibres. *Polymer*, **41**(6), 2121-2126.

Siqueira, G., Varnai, A., Ferraz, A., Milagres, A.M.F. 2013. Enhancement of cellulose hydrolysis in sugarcane bagasse by the selective removal of lignin with sodium chlorite. *Applied Energy*, **102**, 399-402.

Son, P.A., Nishimura, S., Ebitani, K. 2012. Synthesis of levulinic acid from fructose using Amberlyst-15 as a solid acid catalyst. *Reaction Kinetics Mechanisms and Catalysis*, **106**(1), 185-192.

Studer, M.H., DeMartini, J.D., Davis, M.F., Sykes, R.W., Davison, B., Keller, M., Tuskan, G.A., Wyman, C.E. 2011. Lignin content in natural Populus variants affects sugar release. *Proceedings of the National Academy of Sciences of the United States of America*, **108**(15), 6300-6305.

Sun, X.F., Xu, F., Sun, R.C., Fowler, P., Baird, M.S. 2005. Characteristics of degraded cellulose obtained from steam-exploded wheat straw. *Carbohydrate Research*, **340**(1), 97-106.

Sun, Y., Cheng, J.Y. 2002. Hydrolysis of lignocellulosic materials for ethanol production: a review. *Bioresource Technology*, **83**(1), 1-11.

Svenson, D.R., Jameel, H., Chang, H.-m., Kadla, J.F. 2006. Inorganic reactions in chlorine dioxide bleaching of softwood kraft pulp. *Journal of Wood Chemistry and Technology*, **26**(3), 201-213.

Takagaki, A., Ohara, M., Nishimura, S., Ebitani, K. 2009. A one-pot reaction for biorefinery: combination of solid acid and base catalysts for direct production of 5-hydroxymethylfurfural from saccharides. *Chemical Communications*(41), 6276-6278.

Tanaka, K., Komiyama, A., Sonomoto, K., Ishizaki, A., Hall, S.J., Stanbury, R. 2002. Two different pathways for D-xylose metabolism and the effect of xylose concentration on the yield coefficient of L-lactate in mixed-acid fermentation by the lactic acid bacterium Lactococcus lactis 10-1. *Applied Microbiology and Biotechnology*, **60**(1-2), 160-167.

Tian, X.F., Rebmann, L., Xu, C.C., Fang, Z. 2016. Pretreatment of Eastern White Pine (Pinus strobes L.) for Enzymatic Hydrolysis and Ethanol Production by Organic Electrolyte Solutions. *Acs Sustainable Chemistry & Engineering*, **4**(5), 2822-2829.

Tsai, S.P., Moon, S.H. 1998. An integrated bioconversion process for production of L-lactic acid from starchy potato feedstocks. *Applied Biochemistry and Biotechnology*, **70-2**, 417-428.

U.S. Department of Energy . 2008. Biomass multiyear program, Office of the Biomass Program, Energy Efficiency and Renewable Energy

van der Pol, E.C., Eggink, G., Weusthuis, R.A. 2016. Production of L(+)-lactic acid from acid pretreated sugarcane bagasse using Bacillus coagulans DSM2314 in a simultaneous saccharification and fermentation strategy. *Biotechnology for Biofuels*, **9**.

Wang, L., Templer, R., Murphy, R.J. 2012. High-solids loading enzymatic hydrolysis of waste papers for biofuel production. *Applied Energy*, **99**, 23-31.

Wang, T., Nolte, M.W., Shanks, B.H. 2014. Catalytic dehydration of C-6 carbohydrates for the production of hydroxymethylfurfural (HMF) as a versatile platform chemical. *Green Chemistry*, **16**(2), 548-572.

Watanabe, M., Aizawa, Y., Iida, T., Nishimura, R., Inomata, H. 2005. Catalytic glucose and fructose conversions with TiO2 and ZrO2 in water at 473 K: Relationship between reactivity and acid-base property determined by TPD measurement. *Applied Catalysis a-General*, **295**(2), 150-156.

Weingarten, R., Cho, J., Conner, W.C., Huber, G.W. 2010. Kinetics of furfural production by dehydration of xylose in a biphasic reactor with microwave heating. *Green Chemistry*, **12**(8), 1423-1429.

Weingarten, R., Cho, J., Xing, R., Conner, W.C., Huber, G.W. 2012. Kinetics and Reaction Engineering of Levulinic Acid Production from Aqueous Glucose Solutions. *Chemsuschem*, **5**(7), 1280-1290.

Weingarten, R., Kim, Y.T., Tompsett, G.A., Fernandez, A., Han, K.S., Hagaman, E.W., Conner, W.C., Jr., Dumesic, J.A., Huber, G.W. 2013. Conversion of glucose into levulinic acid with solid metal(IV) phosphate catalysts. *Journal of Catalysis*, **304**, 123-134

Werpy, T.; Petersen, G. 2004. NREL/TP-510-35523; National Renewable Energy Laboratory (NREL).

Wiggins, L.F. 1949. The Utilization if sucrose. *Advances in Carbohydrate Chemistry*, **4**, 293-336.

Ximenes, E., Kim, Y., Mosier, N., Dien, B., Ladisch, M. 2011. Deactivation of cellulases by phenols. *Enzyme and Microbial Technology*, **48**(1), 54-60.

Xu, G.Q., Chu, J., Wang, Y.H., Zhuang, Y.P., Zhang, S.L., Peng, H.Q. 2006. Development of a continuous cell-recycle fermentation system for production of lactic acid by Lactobacillus paracasei. *Process Biochemistry*, **41**(12), 2458-2463.

Yan, W., Acharjee, T.C., Coronella, C.J., Vasquez, V.R. 2009. Thermal Pretreatment of Lignocellulosic Biomass. *Environmental Progress & Sustainable Energy*, **28**(3), 435-440.

Yang, Q., Pan, X.J. 2016. Correlation Between Lignin Physicochemical Properties and Inhibition to Enzymatic Hydrolysis of Cellulose. *Biotechnology and Bioengineering*, **113**(6), 1213-1224.

Yu, Y., Lou, X., Wu, H.W. 2008a. Some recent advances in hydrolysis of biomass in hot-compressed, water and its comparisons with other hydrolysis methods. *Energy & Fuels*, **22**(1), 46-60.

Yu, Y., Lou, X., Wu, H.W. 2008b. Some recent advances in hydrolysis of biomass in hot-compressed, water and its comparisons with other hydrolysis methods. *Energy & Fuels*, **22**(1), 46-60.

Yu, Z., Jameel, H., Chang, H.-m., Park, S. 2011. The effect of delignification of forest biomass on enzymatic hydrolysis. *Bioresource Technology*, **102**(19), 9083-9089.

Zeng, W., Cheng, D.G., Zhang, H.H., Chen, F.Q., Zhan, X.L. 2010. Dehydration of glucose to levulinic acid over MFI-type zeolite in subcritical water at moderate conditions. *Reaction Kinetics Mechanisms and Catalysis*, **100**(2), 377-384.

Zhu, Y.M., Lee, Y.Y., Elander, R.T. 2007. Conversion of aqueous ammonia-treated corn stover to lactic acid by simultaneous saccharification and cofermentation. *Applied Biochemistry and Biotechnology*, **137**, 721-738.